GHENT UNIVERSITY

FACULTY OF PHARMACEUTICAL SCIENCES

DEVELOPMENT OF POROUS DELIVERY SYSTEMS FOR ORAL DRUG AND VACCINE ADMINISTRATION

An Cosijns

Thesis submitted to obtain the degree of Doctor in Pharmaceutical Sciences

2009

Promoters:

Prof. Dr. J.P. Remon

Prof. Dr. C. Vervaet

Laboratory of Pharmaceutical Technology

Dank je wel …

Het jarenlange onderzoek dat vooraf ging aan het schrijven van deze doctoraatsthesis, is een werk waar verschillende mensen op de een of andere manier hun steentje hebben toe bijgedragen. Daarom zou ik ook even de tijd willen nemen om deze mensen te bedanken.

Eerst en vooral wens ik Prof. Dr. J.P. Remon te bedanken omdat hij me de kans gaf te doctoreren, voor zijn aanstekelijk enthousiasme en de gedrevenheid waarmee hij het onderzoek begeleidde alsook voor de leerrijke discussies.

Prof. Dr. C. Vervaet wens ik te bedanken voor het kritisch nalezen van manuscripten en dit proefschrift, voor zijn nuchtere kijk op de zaken en voor de verrijkende discussies met betrekking tot dit werk.

Ook de mensen van het VITO, Jan, Steven, Jos, Ivo en Mathieu wil ik speciaal bedanken. Jullie inbreng kwam als een geschenk uit de hemel op het moment dat het onderzoek dreigde vast te lopen. Bedankt voor jullie bijdrage en voor de technische info.

Dhr. Daniel Tensy wil ik bedanken voor het deskundig uitvoeren van de dierenproeven. Voor de staalnames in de vroege en late uurtjes alsook in de weekends.

Dhr. I. Nikolakakis, thank you for all the help with the development of the porous pellets.

Prof. J. Siepmann and F. Siepmann (College of Pharmacy, Universitè de Lille 2) for the modelling experiments, their encouragement and enthusiasm.

Prof. Dr. E. Cox en Philippe Bellot (Faculteit Diergeneeskunde) bedankt voor de samenwerking omtrent orale vaccinatie. Het was voor mij een leuke ervaring om te kunnen

meewerken aan een toepassing in een ander vakgebied. Dr. Frank Verdonck wens ik te bedanken voor zijn hulp bij het opstarten van dit project.

Ik wil volgende mensen bedanken voor de goede samenwerking: Dominique Nizet (Université de Liége, Laboratoire de Technologie Pharmaceutique) for the SCF experiments, Bart De Pauw (Faculteit Diergeneeskunde) voor de SEM foto's, Olivier Janssens (Faculteit Wetenschappen) voor de SEM foto's en de XRD opnames, Thomas De Beer (Faculteit Farmaceutische Wetenschappen) voor de Raman analyses, Prof. Dr. Z. Hens (Faculteit Wetenschappen) voor de oppervlakte spanning bepalingen, Prof. Dr. Cuvelier en Dorothea Van Limbergen (Faculteit Geneeskunde) voor het maken van de pellet coupes, Veerle Cnudde en Bert Masschaele (Faculteit Wetenschappen) voor de nano CT-scans.

Aan alle thesisstudenten bedankt voor jullie inzet en praktische assistentie.

Alle collega's en ex-collega's zou ik willen bedanken voor hun hulp, bereidwilligheid en leuke sfeer op het lab.
Eveline P, bedankt voor je advies, de leuke gesprekken, je relativeringsvermogen,…, ik had me geen betere bureaugenoot kunnen wensen tijdens de eerste jaren van mijn doctoraat!
Katrien H, mijn huidige bureaugenoot, bedankt en nog veel succes met je doctoraat!
Barbara, Nele en Liesbeth P, bedankt voor de toffe middagpauzes, de ontspannende niet-wetenschappelijke gesprekken, de fijne tijd op het lab en de vriendschap. Succes met al jullie toekomstplannen!
Ellen, bedankt voor jouw deskundige uitleg en nuttige tips bij het uitvoeren van dissolutie testen en HPLC analyses, Katharine en Bruno voor het oplossen van administratieve probleempjes, Christine, voor je hulp bij de stabiliteitstudie, Els A. voor de hulp bij de statistische verwerking van de data en Katrien V. voor het delen van je kennis over de F4 fimbriae.

Mijn ouders wens ik te bedanken voor alle kansen die ze mij boden, hun steun tijdens mijn doctoraat en hun hulp bij de alledaagse dingen.
Familie en vrienden wens ik te bedanken voor hun emotionele betrokkenheid.

Pieter, bij jou kan ik duizenden redenen bedenken om je te bedanken, bedankt voor de steun, voor het verjagen van de slechte spookjes die soms in mijn hoofd zaten, voor het aanhoren van mijn geklaag maar vooral ook voor de leuke momenten die me de soms moeilijke momenten heel snel deden vergeten. Bedankt voor je geduld en liefde!
Loes, mijn klein muizeke, ook al beperken jouw “woordjes” zich nog maar tot dada en lala, dit en een knuffel of glimlach van jou zijn voldoende om er weer tegenaan te kunnen!

An Gent, januari 2009

Table of contents

Aim of the study

The goal of this study is to evaluate porous carriers for oral drug delivery. The use of porous scaffolds as carriers for drug delivery is already well established in the field of bone implants, where porous bone implants are used for local drug delivery.

The first part of this research work presents the development of a porous single-unit carrier as an alternative for conventional tablets. The preferred industrial manufacturing technique for conventional tablets is direct compression, whereby a powder mixture consisting of drug and excipients is compressed into a dense structure. This technique is suitable for the incorporation of most drugs into tablets. However some drugs cannot be compressed directly into tablets because they lack the necessary flow and bonding properties required to form a useful tablet. Furthermore it is still a major challenge during the manufacturing of low-dosed drugs to ensure content uniformity of all units. To this end porous tablet-shaped hydroxyapatite scaffolds were prepared by calcination and sintering and spiked with a drug solution. Following absorption of the solution in the porous structure of the tablet and evaporation of the solvent, a tablet-shaped formulation is obtained that has the drug incorporated in its inner pores. As the drug dose per tablet only depends on the volume spiked on each tablet and small volumes of liquid can be dosed with a high accuracy, the risk of drug inhomogeneity is minimal, what makes these tablets an innovative carrier for low-dosed drugs. Furthermore, as the drug is incorporated in the porous tablets after compression, this

manufacturing technique is also promising for processing drugs with poor tabletting characteristics.

A second part of this research work presents the development of porous pellets as multiple-unit drug carriers. Therefore pellets consisting of microcrystalline cellulose and sodium chloride were manufactured by extrusion/spheronization and after removal of the sodium chloride fraction via extraction, porous pellets were obtained.

In a first section, their potential as carrier for conventional drugs was tested by loading the porous pellets with drugs whereby conventional (immersion and fluidized-bed layering) and innovative loading techniques (supercritical fluid impregnation) were evaluated.

In a second section, the use of the porous pellets in the field of oral vaccination was investigated. There still is a need for delivery systems that allow easy oral administration of antigens as well as provide protection of the antigen against the detrimental effects of the gastrointestinal tract. In this research project a veterinary model was chosen since enterotoxigenic *Escherichia coli* infections have been identified as an important causal agent of diarrhea and mortality in neonatal and post-weaning piglets. Therefore vaccination of the piglets against post-weaning infections would increase economic profit. However, attempts to induce mucosal immunity in piglets by oral vaccination have found little or no success, due to insufficient induction of the protective immune mechanisms. As oral solutions are unpractical for regular administration to suckling animals and do not protect the antigen during gastro-intestinal passage, a solid vaccine formulation that can be mixed with creep food and that protects the antigens against the detrimental effects in the gastro-intestinal tract would be more efficient. Previously, enteric coated pellets have been used for oral administration of vaccines, as they protected F4 fimbriae (antigen used as vaccine against *E. coli* infections) against the detrimental effects in stomach and duodenum. However, as incompatibility

between F4 proteins and the enteric coating polymer was noticed, the use of porous pellets for oral vaccination of suckling piglets with F4 fimbriae was evaluated in this research study.

1

Introduction

1.1. POROUS MATERIALS

Porosity in materials can be arranged in a well-defined and homogeneous manner or in a heterogeneous manner. It can be separated or interconnected, resulting in pores having a different shape, size and/or interconnectivity. The three-dimensional assemblage of a large number of pores possessing a specific shape leads to a solid monolith displaying what can be termed as a cellular structure.

Cellular materials (manufactured using polymers, metals and ceramics) are known to have many interesting combinations of physical and chemical properties. For this reason, they have widespread applications in nearly every technology sector. Many of the applications require that a medium, either liquid or gaseous, is able to pass through the cellular material. There may be a need for various degrees of interconnectivity, ranging from very open for high flow rates to completely closed for load-bearing structural applications and isolation materials. A difference can be made whether an application is functional or structural, the difference between these two notions, however, is gradual (Banhart, 2001) (Fig. 1.1).

Structural applications of cellular material can be found in various industrial sectors: automotive, aerospace, ship building, railway, building, machine construction, sporting equipment and biomedical industry. Functional applications of porous materials are filtration

and segregation, heat exchangers and cooling machines, supports of catalysts, storage and transfer of liquids, fluid flow control etc. (reviewed by Banhart, 2001).

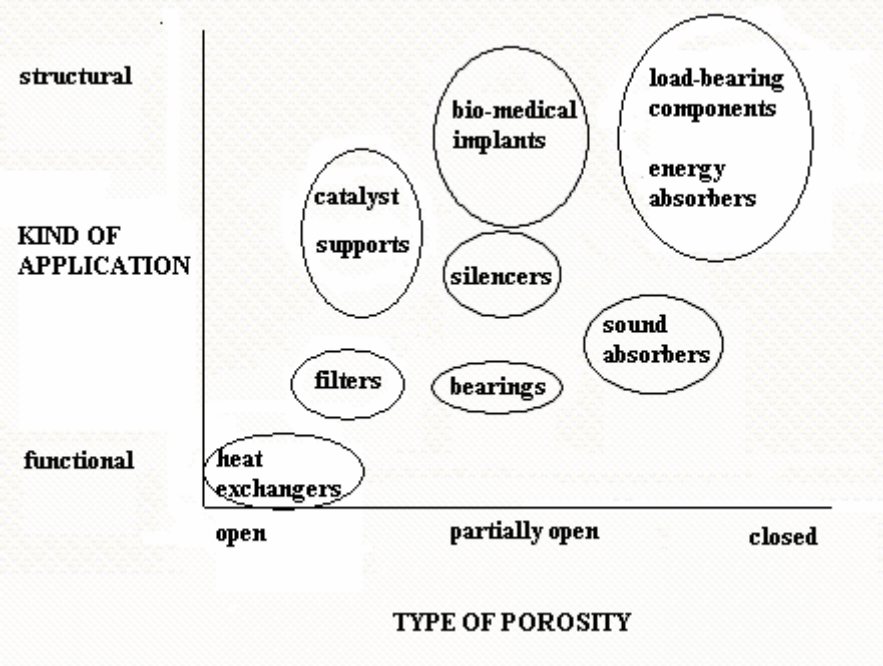

Figure 1.1.: Applications of cellular material (Banhart, 2001).

1.1.1. Porous materials for biomedical applications

The biomedical applications of cellular material are mostly found in the field of bone and dental implantation. The implant stability is not only a function of strength but also depends on the fixation established with the surrounding tissue. This was primarily achieved using screws and bone cements. However, nowadays improved fixation can be achieved by bone tissue growing into and through a porous matrix of metal or a porous layer of another biocompatible material on the prothesis. Furthermore, the presence of interconnected pores will allow extensive body fluid transport through the porous scaffolds which can trigger bone ingrowth.

Although the fabrication of porous materials has been studied as early as 1943 (Simancik, 2000), the biomedical application of porous materials has only been investigated much later, whereby the work of Weber and White (1972) is one of the earliest to describe the use of

porous materials for osteointegration. Animal studies revealed that porous ceramics, polymers and metals were potential candidates for porous implants which would enable bone ingrowth. Porous ceramics and polymers are not applied as load bearing implants due to their intrinsic brittleness and low compression strength, respectively, hence usually porous metals (eg. titanium and its alloys, stainless steel and cobalt-chrome) are used for this application.

However, porous ceramics and metallic scaffolds coated with hydroxyapatite (HA) have found large scale application as filling material for bone defects in prothesis revision surgery and dental implantology (Stigter et al., 2004). Hydroxyapatite is the preferred material for this purpose due to its biocompatibility and bioresorbability (Dubok, 2000; Jarcho, 1986) and in form of a porous body it enables one to produce cements similar to real bones (Palazzo et al., 2005). The presence of pores in the scaffolds enables bone ingrowth and in combination with the osteoinductive capacities of HA, an optimal bone replacement is obtained (Grynpas et al., 2002).

Several manufacturing techniques can be applied for the production of porous ceramics. Each technique results in porous material with different pore size distribution, density and pore structure, hence the applied technique will depend on the final application of the cellular material (Ryan et al., 2006). The manufacturing techniques can be crudely divided into three categories with a series of variations on the basic themes.

- **Replication techniques**

➢ Slurry coating of polymer foams

The replication of polymer foams is one of the first manufacturing techniques developed for producing ceramics with controlled macroporosity (Schwartzwalder and Somers, 1963), and despite its age it is still the most common and widely used technique in industry. A flexible,

open-cell polymer foam (polyurethane, polyvinylchloride, polystyrene or cellulose) is coated with ceramic slurries (Padilla et al., 2002), followed by removal of the redundant ceramic slurry. Afterwards, the polymer and any other organic additive are removed at elevated temperature (350-800°C) followed by sintering to achieve the required density and strength. Generally, any fine ceramic powder that can be made into a suspension can be used.

This approach generally yields an open reticulated structure with high permeability. The main disadvantage is attributed to the hollow struts and large number of flaws that result from burning out the polymer foam. Furthermore, during removal of the organic phase toxic gases can be released, which makes extensive scrubbing of the waste gases necessary (Binner, 2005).

➢ Electrophoretic deposition

Electrophoretic deposition is an electrochemical method that involves two steps. First, an electric field is applied between two electrodes and charged particles suspended in a suitable liquid move toward the oppositely charged electrode. In a second step, the particles accumulate at the deposition electrode and create a compact. Deposition of ceramics on carbon fibers and carbon rods (cathodic substrate) whereby the latter is removed via heat treatment results in porous material (Wang et al., 2002; Ma et al., 2003).

• Foaming techniques

➢ Incorporation of an external gas phase and gelation

One of the earliest techniques, patented by Du Pont (1967), involved the production of foams from aqueous suspension of very fine (< 200 nm), negatively charged colloidal silica particles, a cationic surfactant and binding agents such as water-soluble polymers, sugars, gums, starches and resins. The slurries were converted into foams via mechanical agitation by

using different types of mixers, by injection of gas or by introduction of an aerosol propellant. Once formed into the desired shape by casting the slurry into a mould, the foam is dried followed by sintering during which the additives are burned out.

Nowadays, the manufacturing of a ceramic foam via this procedure begins with the selection of an appropriate ceramic powder. The most important step in the process is the creation of a stable ceramic slurry. The ceramic powder is mixed with water containing dispersants, initiators, catalyst and a premixed solution containing organic monomers. High-shear mixing is used to destroy any agglomerates. The organic monomer solution can be readily polymerized to form a cross-linked polymer-water gel, whereby both the ceramic powder and water are trapped in the foamed structure. A foaming agent (surfactant) is added to the slurry, prior to transfer to the foaming unit. The onset of polymerization is controlled in order to have sufficient time for the foam to exit the foaming unit and to be cast into an appropriate mould. When polymerization is completed, the structure is strong enough to be demoulded and transferred to the oven for drying. The polymeric binder is removed followed by sintering at elevated temperature, hence a strong highly porous ceramic is obtained. The gel-foaming method is able to produce - even before sintering - parts with excellent mechanical properties, allowing green machining (Sepulveda et al., 2000). When bioceramic hydroxyapatite is processed via this technology, this resulted in foams with excellent properties for encouraging bone ingrowth.

Several variations on this manufacturing method are developed. Other additives were incorporated in the slurry e.g. gelling agents such as cellulose derivates (Moreno, 1992), alginates (Katsuki et al., 1992), compositions that intrinsically from a gel (Bagwell and Messing, 1996) and the use of in situ polymerization of an organic monomer (Young et al., 1991).

- In situ gas production

In this approach the common theme is the presence of a foaming agent that decomposes due to heat or a chemical reaction to generate a gas within the ceramic slurry (Almirall et al, 2004). A patent by A.C.I. Operations (1973) described a method of producing a ceramic foam as a result of chemical reactions to liberate hydrogen during processing. After gel formation whereby the components were bound together, hydrogen gas was formed in situ via a chemical reaction. The surfactant present in the composition served to break up the gas bubbles into smaller bubbles as well as to stabilize them, thus ensuring a porous structure with an open celled nature.

More recently, Colombo and Bernardo (2003) produced porous open-cell ceramic foams by in situ gas formation in solutions of preceramic polymers. Methyl polysiloxane resin was mixed with precursors of polyurethane (polyols and isocyanates) in dichloromethane, together with appropriate surfactants and catalysts. Blowing (expansion of gases) started by a combination of vigorously stirring and heating the mixture. The expansion and foam formation was a result of physical blowing (solvent evaporation) and chemical blowing (reaction between water generated by condensation of SiOH groups in the silicone resin with isocyanate to form carbon dioxide gas) (Takahashi et al., 2001) .

• Other techniques

The powder can be mixed with space holding material (pore forming agents) and after compression, the space holder material is removed by heat treatment or leaching with an appropriate solvent. A final sintering step can be applied to further densify the porous network (Bram et al., 2000).

Three-dimensional printing is a rapid prototyping technology used to create complex three-dimensional parts directly from a computer model, via a layered printing process the structure

is built layer-by-layer based on the computer model. The layering process is repeated until the part is completed, followed by a heat treatment in order to consolidate the bound material (Gbureck et al., 2007; Habibovic et al., 2008).

1.1.2. Calcination and sintering

- Calcination

During the calcination process the organic components are removed, resulting in pores whereby pore shape and pore size are related to the original organic material. It requires careful control of temperature, pressure, atmosphere (air or any other type of atmosphere as appropriate) and time in order to achieve a non-destructive and reproducible removal of the additives from the green body (matrix before sintering). After calcination, the structure of the green body is only held together by weak cohesive forces and requires particularly careful handling during the following process steps. For this reason, calcination is often combined with a (pre)sintering step wherever possible.

- Sintering

Sintering is broadly defined as the consolidation upon heating of a loose mass of particles, which are in contact with each other, to a denser mass. It results in a decrease of specific surface area and porosity and in an increase of density. The thermal behavior of hydroxyapatite ($Ca_5(PO_4)_3OH$) (HA) during sintering is determined by the Ca/P ratio. Usually the sinter temperature for HA powder is chosen in the range of 1150-1350°C. When stoichiometric HA (Ca/P ratio= 1.67) is sintered below 1350°C no other phases than HA are present in the end product. At 1400°C HA starts to decompose whereby α-tricalcium phosphate (TCP) is formed. Further increasing the temperature results in further decomposition of HA forming β-TCP, tertracalcium phosphate (TTCP) and calciumoxide

(CaO). Any deviation from the stoichiometric value of the non-sintered HA results in the formation of β-TCP when samples are sintered below 1350°C (Muralithran and Ramesh, 2000; Tampieri et al., 1997).

The driving force of the sinter process is a reduction of the surface free energy of the system (ΔG_T)

$$\Delta G_T = \Delta G_v + \Delta G_b + \Delta G_s \qquad \text{(Eq. 1.1.)}$$

whereby ΔG_v, ΔG_b and ΔG_s corresponds with the change in free energy associated with the grain volume, grain boundaries and grain surface, respectively.

During the sintering process mass transport occurs via different diffusion mechanisms (Fig. 1.2 . and Table 1.1.)

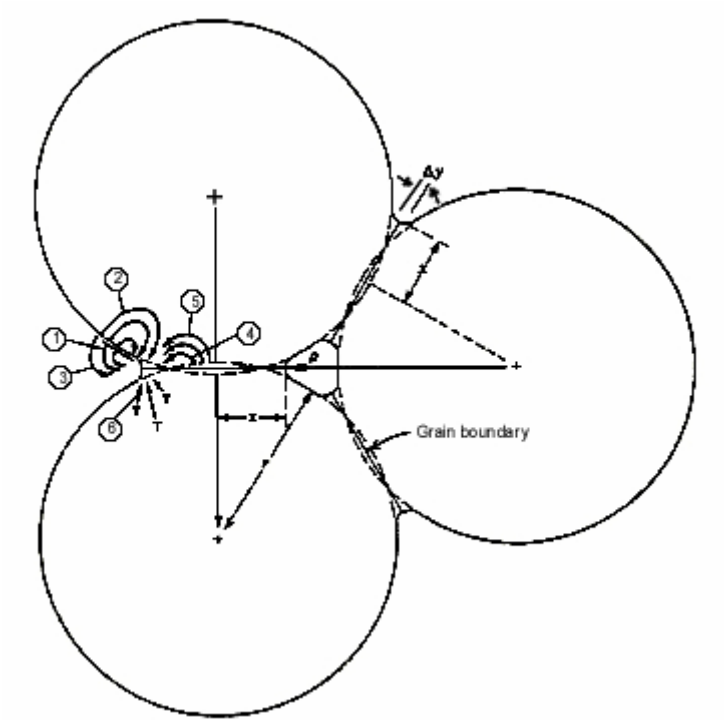

Figure 1.2.: Different diffusion mechanisms during sintering (Kingery et al., 1976).

Table 1.1.: Overview of the different diffusion mechanisms during sintering.

Nr in Fig. 1.2.	transport	transport mechanism
1	surface diffusion	from surface to neck via surface
2	lattice diffusion	from surface to neck via lattice
3	evaporation transport	from surface to neck via surface
4	grain boundary diffusion	from grain boundary to neck via lattice
5	lattice diffusion	from grain boundary to neck via lattice
6	lattice diffusion	from dislocation in the lattice to neck via lattice

The amount of material that diffuses in function of time can be described by Fick's first law of diffusion

$$J = -D \frac{\partial c}{\partial x} \qquad \text{(Eq. 1.2.)}$$

where c is the concentration per volume, x represents the diffusion path, J denote the flux and D is the diffusion coefficient (depending on the type of transport mechanism).

The diffusion coefficient is directly proportional with the atom mobility as described by

$$D = kTB_i \qquad \text{(Eq. 1.3.)}$$

where k is the Boltzmann constant, T the temperature and B_i the absolute mobility.

As the diffusion process is thermally activated, a temperature increase will result in a higher number of atoms that contain sufficient energy to exceed the energy barrier between two lattice places, resulting in a chemical potential gradient. Material transfer during sintering will occur in order to reduce the chemical potential gradient. As the amount of atoms with sufficient energy to overcome the energy barrier between two lattice places will increase at higher temperature, the temperature is a dominant factor in the sintering process whereas the influence of sinter duration is less pronounced.

Generally, sintering occurs in three stages as presented in Fig. 1.3.

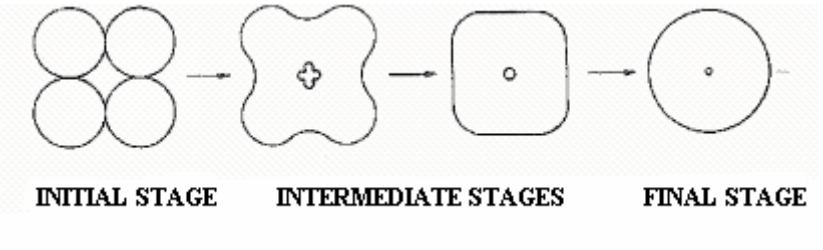

Figure 1.3.: Different stages of sintering (Kingery et al., 1976).

During the initial stage, contact areas between the individual particles are formed. Two different processes are involved: contact sintering and densification sintering. During contact sintering, material transfer from the grain surface to the grain neck occurs via surface or lattice diffusion and evaporation-condensation without a decrease in distance between the grain centers, hence no shrinkage occurs. During densification sintering, material is transferred to the neck via the lattice whereby shrinkage occurs due to the fact that the material transport occurs via the lattice.

In the intermediate stage, neck growth occurs and the large number of small particles are replaced by a smaller number of large grains. Intensive shrinkage of open pores occurs between the grain boundaries. This is associated with a change in pore geometry. The highest densification is obtained during this stage.

In the final stage of sintering, grain boundary and lattice diffusion are the dominant mass transport mechanisms. Isolated closed pores are formed which shrink in size as densification proceeds (Bailliez and Nzihou, 2004).

During the sinter process, grain growth occurs, whereby large particles grow at the expense of the smaller particles, resulting in an increased mean grain size and a decrease in the total grain surface area. The driving force for grain growth is inversely proportional with the grain size. If all grain boundaries are equal in energy, they meet to form angles of 120°. If we consider a two-dimensional example, angles of 120° between grain size can occur only for six-sided

grains. Grains with fewer side have boundaries that are concave when observed from the center of the grain. Since grain boundaries migrate toward their center of curvature, grains with less than six sides tends to grow smaller and grains with more than six sides tends to grow larger (Fig. 1.4.).

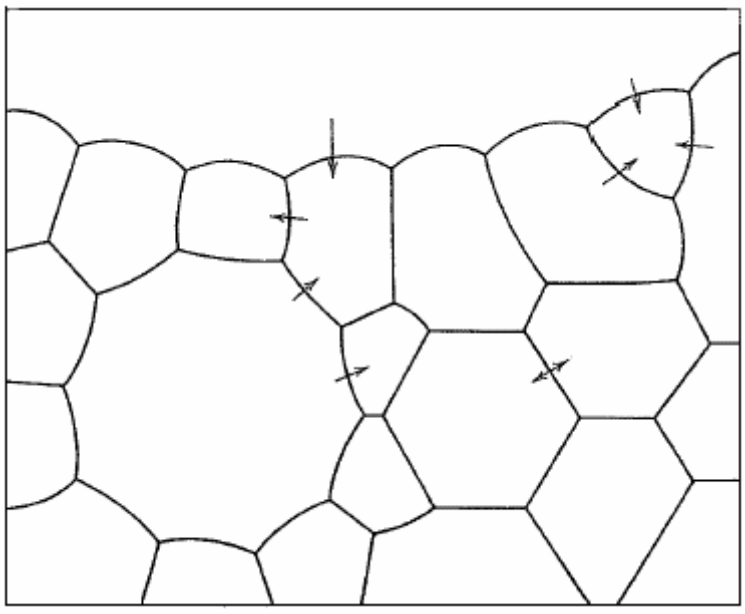

Figure 1.4.: Schematic drawing of polycrystalline specimen. Arrows indicate the directions in which boundaries migrate (Kingery et al., 1976)

Two factors are able to inhibit the grain growth: the boundary of the specimen and the presences of inclusions. When the grains obtained a size comparable with the specimen size, the grain grown will stop. The presence of inclusions (impurity) can increase the energy, necessary for movement of a grain boundary, hence no further grain growth will occur.

1.1.3. Porous materials as drug delivery systems.

The presence of pores in ceramic foams offers the possibility to use these porous ceramics not only as bone substitutes but also as carriers for local and controlled delivery of drugs. This application is useful in the treatment of different skeletal diseases which normally require a

long and painful therapy. The incorporation of antibiotics (Hasegawa et al., 2003; Sivakumar and Rao, 2002), chemotherapeutica (Burgos et al., 2002, Itokazu et al., 1999; Lebugle et al., 2002), NSAIDs and growth factors (Arm et al., 1996) in porous bone scaffolds is already well established.

Drug release from these drug delivery devices depends on different factors such as microstructure, drug solubility, possible bonding between drug and matrix. Generally in case of porous calcium phosphate devices, the drug release is diffusion-controlled as the rate of matrix degradation is much lower than the rate of drug liberation (Ginebra et al., 2006).

1.2. CONVENTIONAL ORAL SOLID DOSAGE FORMS

1.2.1. Introduction

In this research project, the possible applications of porous drug delivery systems for oral drug delivery were investigated. Porous structures were manufactured of two major groups of oral solid dosage forms: single unit and multiple unit systems. Tablets and pellets are the most popular examples of a single unit and multiple unit dosage form, respectively.

Two manufacturing techniques were selected to prepare the porous dosage forms during this research project:

(1) Of all the manufacturing techniques for porous ceramics described in section 1.1.1., the simplest method consist of preparing a mixture of ceramic powder and space holding material (pore forming agents) whereby after compression, the space holder material is removed by heat treatment or via extraction with an appropriate solvent. The resulting porous structure can be sintered to increase the mechanical strength.

(2) To obtain porous structures with well defined pores, gelation can be used. In this study, agar (a natural occurring polysaccharide) is used as gelling agent.

After gelation and drying the green body is demouled, followed by calcination and sintering in order to burn out the gelling agent and other additives and to optimize the strength of the material, respectively.

1.2.2. Tablets

Tablets are the most widely used solid dosage form for a number of reasons: they are convenient, easy to manufacture and use, and offer accurate dosing and excellent stability. Tablets are generally defined as single-unit dosage forms made by compaction of a mixture consisting of drug and specific fillers or excipients in order to aid in the processing and to improve tablet properties (Bandelin, 1989). Tablets can be prepared without pretreatment of the powder mixture via direct compression, or after wet or dry granulation to improve the compression properties of the powder mixture (Shangraw, 1989).

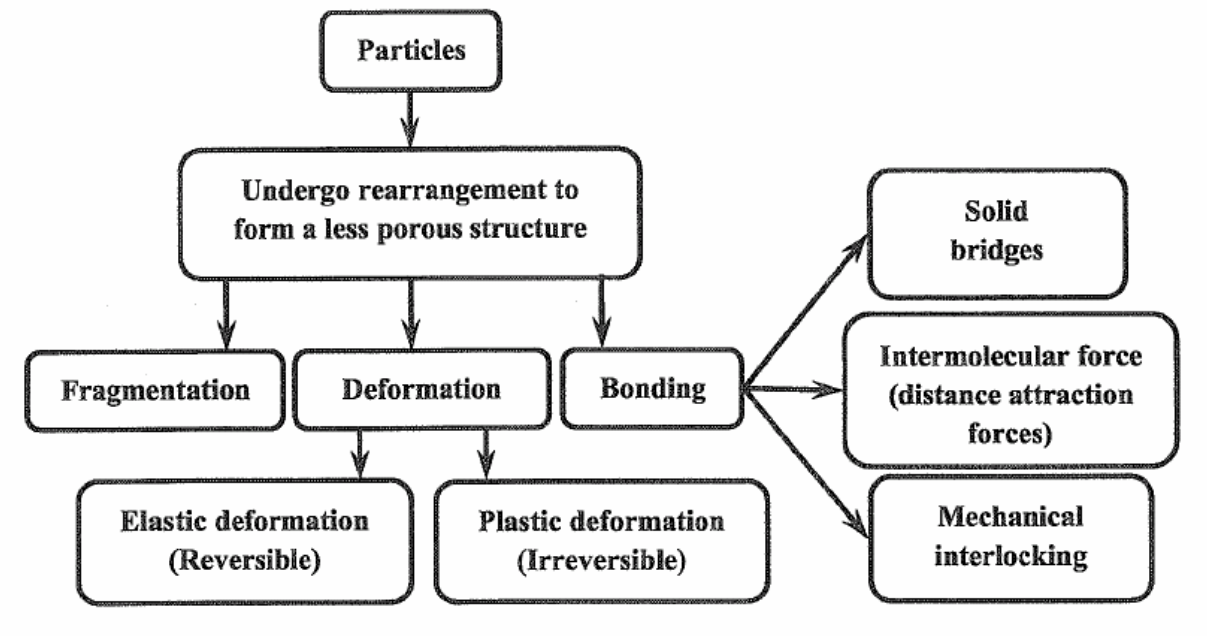

Figure 1.4.: Various steps involved in direct compression (adapted from Patel et al., 2006).

Direct compression (Fig. 1.4.) is the preferred method for manufacturing of tablets, the most obvious advantage being economy: due to the reduced processing time, lower labor costs,

limited manufacturing steps, less process validation it is a rather cost-effective technique. With regards to tablet quality, the most important advantage is the fact that there is no need for moisture or heat during the process which is beneficial for stability of the drug.

However this technique may not be suitable for the production of low-dosed tablets or for processing tablets containing drugs with poor compression characteristics. The formulator can resort to several strategies to overcome these problems: optimization of particle size and shape, selection of specific excipient grades, use of appropriate mixers, formation of ordered mixtures (Venables and Wells, 2001). When these are unsuccessful, wet/dry granulation can be used. However, these approaches cannot completely eliminate the risk of particle segregation (Vromans et al., 1999).

1.2.3. Pellets

Pellets are defined as small free-flowing, spherical or semi-spherical particles sized between 500 and 1500 μm (Ghebre-Selassie, 1989). Multiparticulate dosage forms offer important therapeutic as well as technological advantages over single unit dosage forms (Bechgaard and Hagermann, 1978; Ghebre-Selassie, 1989; Krämer and Blume, 1994):

- a predictable gastric emptying, less dependent on the nutritional state resulting in a lower inter- and intra-subject variability of drug plasma profiles
- a high degree of dispersion in the digestive tract, minimizing the risk of high local drug concentrations which could irritate the gastric mucosa
- less variance in transit time through the gastrointestinal tract
- less risk of dose dumping as every pellet acts as a single drug reservoir, a coating imperfection would only affect the release of a small drug portion
- possibility to combine several active components, incompatible drugs or drugs with different release profiles in the same dosage unit

- good flow properties, minimized dust formation and easy to coat

Extrusion/spheronization, first described by Conine and Hardely (1970) and Reynolds (1970), is the most common used manufacturing technique. It is a multi-step process involving dry mixing, wet granulation, extrusion, spheronization and drying.

- Dry mixing and wet granulation

In the first step of the process a homogeneous powder mixture must be obtained prior to wet granulation. During wet granulation, the granulation liquid is added in order to obtain a wet mass with the required plasticity or deformation characteristics. Generally, granulation is performed in the same equipment as dry mixing.

- Extrusion

During extrusion, the wet plastic mass is forced through the extrusion die in order to form cylinders or strands with a width corresponding to the die diameter. A variety of extruders is available. Based on their feed mechanism they can be divided into screw feed extruders, gravity feed extruders and piston feed extruders (Erkoboni, 2003) .

- Spheronization

Spheronization involves the rounding of extrudates into spheres or pellets due to frictional forces generated by particle-particle and particle-equipment interactions.

A spheronizer consist of a bowl with a stationary cylindrical wall and a fast-rotating bottom plate having a grooved surface (cross-hatched or radial pattern) to increase friction. When placed in the spheronizer the extrudate is broken into small pieces and within a short period of time spherical particles are formed. Due to the centrifugal forces, the pieces move

outward to the wall, climb up the wall and fall back onto the rotating disk which due to its angular motion pushes the mass again towards the wall, resulting in a rope-like formation (Fig. 1.5.).

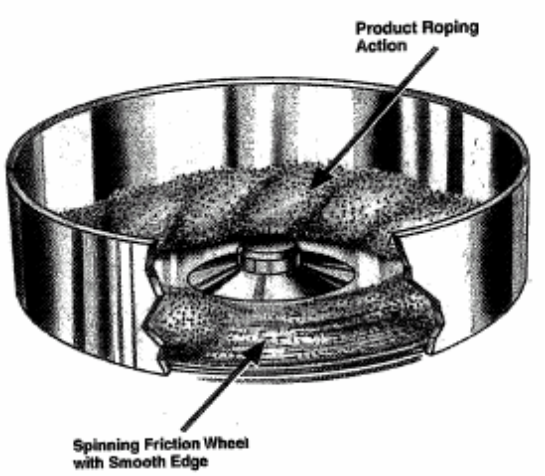

Figure 1.5.: Schematic representation of the rope-like formation during spheronization (Erkoboni, 2003).

The transformation from extrudates into pellets occurs in various stages, as proposed by two models: Rowe (1985) describes that after the initial breaking, the extrudates are rounded off into cylindrical particles with rounded edges, followed by formation of dumbbell-shaped particles, ellipsoids and finally spherical pellets (Fig. 1.6. B). The model proposed by Baert and Remon (1993) suggests that the cylinders are rounded and additionally bent, followed by twisted dumbbell formation. The twisting action eventually causes the dumb-bell to break into two parts. Due to the folding of the edges of the flat side of these parts during further spheronization, the resulting spheres often have a cavity in their internal structure (Fig. 1.6. A). The exact mechanism depends on the formulation.

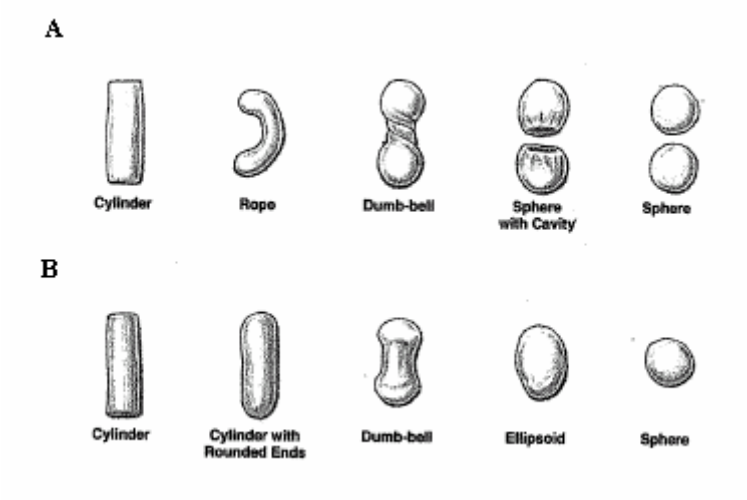

Figure 1.6.: Schematic representation of the two models to describe the mechanism of spheronization proposed by: Baert and Remon (**A**) and Rowe (**B**) (adapted from Erkoboni (2003)).

- Drying

The wet pellets are usually dried in an oven or fluidized-bed. The major difference is the rate of fluid removal. During fluidized-bed drying a more rapid drying is obtained due to the higher air volumes and the higher inlet temperatures that are used (Erkoboni, 2003).

When manufacturing conventional tablets or pellets the drug is added to the powder mixture prior to tabletting or extrusion/spheronization. In contrast, when using porous tablets/pellets the drug is only incorporated in the dosage form after manufacturing the porous carriers. Therefore appropriate loading techniques were examined to incorporate the drug into the porous tablets and pellets.

Porous tablets were loaded with a model drug (metoprolol tartrate) by spiking the tablet surface with an aliquot of the drug solution. Porous pellets were loaded with a model drug using different loading techniques: immersion the pellets in a metoprolol tartrate solution, ibuprofen impregnation via supercritical fluids and paracetamol layering via fluid-bed layering.

1.3. VACCINATION

1.3.1. Introduction

Next to conventional drug delivery, the use of porous pellets in the field of vaccination was investigated. There is an increased interest in oral vaccination due to its inherent advantages. However there is still a lot of research required to find an appropriate carrier for oral delivery of vaccines. The optimal carrier should be easy to administer and offer protection to the antigen during gastro-intestinal transit without damaging the vaccine itself.

Most of the currently available licensed vaccines are administered parenterally whereby a systemic immune response rather than a mucosal immune response is obtained. However most pathogens do not infect their host by direct inoculation into the bloodstream, rather initiate their infectious process at mucosal surfaces. A protective immune response at the site of infection is required. Hence vaccines that can induce mucosal immunization will provide a first line of defense against the many pathogens that invade via the mucosal surfaces. Furthermore mucosal administration would avoid the pain and discomfort associated with injections and would eliminate the risk of infections caused by inadequately sterilized needles or needle re-use.

Next to oral administration, nasal, pulmonary, rectal, urogenital, ocular and vaginal administration are also potential routes for mucosal immunization (O'Hagan, 1998; Walker, 1994).

1.3.2. The mucosal immune system

The intestinal, respiratory and urogenital tract are the major ports of entry for microorganisms into the host, however some barriers need to be overcome. In the gastro-intestinal tract, the gastric acidity, proteolytic enzymes, peristalsis, common microflora and mucus will have a

detrimental effect on the microorganisms. Furthermore, an immunological barrier protects the urogenital, respiratory and intestinal mucosa: mucosal-associated lymphoid tissue (MALT). The MALT comprises the gut-associated lymphoid tissue (GALT), the bronchus-associated lymphoid tissue (BALT), the nasal-associated lymphoid tissue (NALT) and the urogenital-associated lymphoid tissue, which all have similar characteristics.

- Gut-associated lymphoid tissue

The intestinal epithelial barrier is composed of a single layer of epithelial cells, mainly enterocytes interspersed by mucus-secreting goblet cells.

The gut-associated lymphoid tissue, located throughout the gastrointestinal tract, consists of clusters of lymphoid follicles (e.g. Peyer's patches) or solitary follicles which serve as the mucosal inductive sites of an immune response.

The epithelium overlaying the lymphoid follicles is called the follicle-associated epithelium (FAE) and is distinguished from intestinal epithelium at other sites by the presence of microfold cells or M-cells. M-cells lack a brush border and have a flattened apical membrane, with sparse, short, irregular microvilli (Fig. 1.7.). They have a basolateral cytoplasmic invagination which creates a pocket (infiltrates of lymphocytes/antigen presenting cells in the pocket). Furthermore, reduced quantities of sIgA and mucus are found at the apical side of the cell. Antigen sampling (and potential drug and vaccine delivery) is thought to be facilitated by these characteristics (Clark, 2001; Niedergang and Kraehenbuhl, 2000). There is low to no antigen degradation during transport through the M-cell.

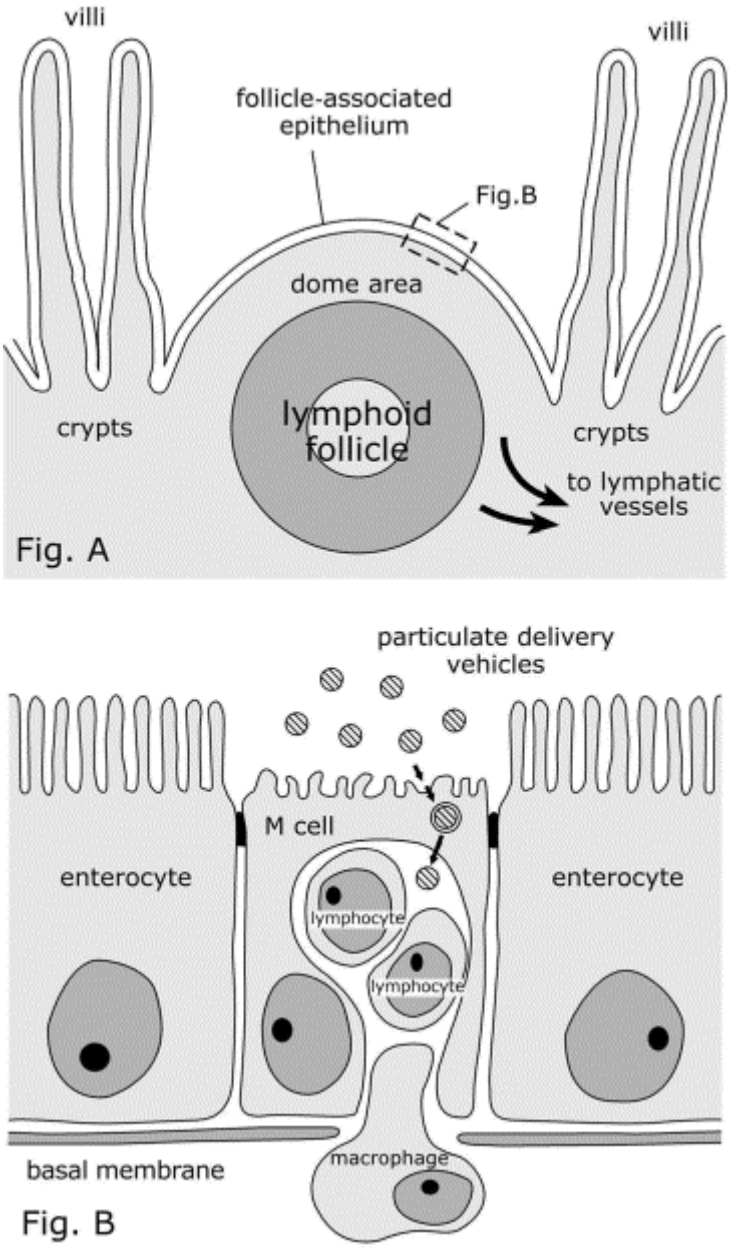

Figure 1.7.: Gut-associated lymphoid tissue (A) and a detailed structure of an M-cell (B) (adapted from Clark et al., 2001).

The possibility that delivery can be achieved by alternate routes such as dendritic cells and enterocytes should not be overlooked. Investigation in mice has been revealed that dendritic cells (DC) may directly internalize antigens from the mucosal surfaces. If this is quantitatively significant remains unclear. Enterocytes are also able to transport molecules by transcytose. Targeting and increasing the efficacy are remaining major challenges (Florence, 1997; Clark, 2001).

- The mucosal immune response

M-cells take up adherent macromolecules and small particles. The endocytosed molecules are efficiently transported through the M-cell and exocytosed inside the M-cell pocket. Transcytosed molecules do not appear to undergo major structural degradation during transport (Davis and Owen, 1997). The antigens are internalized and processed by antigen presenting cells (APC) such as dendritic cells and macrophages, present in the subepithelial dome of the Peyer's patches. In this region B-cell follicles surrounded by T-cells (next to macrophages and dendritic cells) are found. Hence all cells necessary for the induction of an adequate immune response are present. The APC will present the antigen to B- and T-lymphocytes. The APC is able to discriminate between harmful and non-harmful antigens. Harmful antigens often have specific 'pathogenic associated molecular patterns' (PAMPs) that are recognized by Toll-like receptors (TLRs) expressed by APCs. This leads to stimulation of T-cells (CD_4^+ T-helper cells and CD_8^+cytotoxic T-lymphocytes) and IgA-precursor B-cells in the Peyer's patches and the dissemination of B- and T-cells to mucosal effector tissues such as the lamina propria and mesenteric lymph nodes. Here the lymphocytes will further differentiate and maturate, and in the next phase they will migrate to the systemic circulation via the thoracic duct and to organs including the liver and the spleen (Nugent et al., 1998; Holmgren and Czerkinsky, 2005). The stimulated lymphocytes migrate preferentially to mucosal tissues, mediated by the expression of adhesion molecules on lymphocytes and on cells associated with mucosal tissue. They mainly home to the mucosal site where the infection was elicited. In plasma cells polymeric IgA is formed. The polymeric immunoglobulin receptor (pIgR) which is present on the basolateral membrane of the mucosal epithelial cells mediates the transport of polymeric IgA to the luminal side of the cell (Kaetzel et al., 1991). The complex of pIgR and polymeric IgA is endocytosed and transferred through vesicular compartments to the apical surface, where proteolysis of pIgR results in the release

of secretory IgA (sIgA). sIgA in external secretions occurs mainly in dimeric (and tetrameric) forms, with four (or eight) antigen binding sites, respectively. This isotype is usually not obtained by parenteral immunization, which is characterized by IgG and IgM. Locally produced sIgA molecules are the determinants of humoral secretory immunity at the mucosal surfaces. Next to the production of sIgA, secretion may also contain IgA (serum type), IgG, IgM, and components of cell-mediated immunity (T-cells), in varying amounts (Nugent et al., 1998).

The intestinal sIgA response to antigen exposure is relatively short. Hence memory, obtained by specific memory B-cells, is an import aspect in the mucosal immunity. By repeated exposure to the antigen it is rapidly and efficiently triggered (Holmgren, 1991).

1.3.3. Oral vaccination

Vaccines can generally be classified into cellular and acellular vaccines. Cellular vaccines consist of inactivated or attenuated organisms, whereas acellular vaccines consist of purified antigens.

As most vaccines are still administered parenterally, a lot of research efforts are focused on the development of oral vaccines. The oral vaccine against polio, Salmonella typhi and rotavirus are some examples of oral vaccines available on the Belgian market.

The development of an oral vaccine is a major challenge as the antigen has to pass through the gastro-intestinal tract where it is diluted in mucosal secretions, captured in mucus, attacked by proteases and nucleases, and excluded by epithelial barriers. Soluble antigens are taken up at low levels, whereas protection of the antigen against the detrimental GI-effects is required in order to stimulate an adequate immune response in the mucosal tissue (Neutra and

Kozlowski, 2006). Some examples of delivery systems that have potential as mucosal delivery system for antigens are:

- biodegradable particulates whereby poly(lactide-co-glycolide) (DL-PLG) particles are the most promising. The rate of degradation is influenced by the lactide-to-glycolide ratio allowing for sustained release of the antigen.
- liposomes are composed of bilayered phospholipid vesicles. The antigen may be incorporated either into the central aqueous space (water-soluble antigens) or into the phospholid layer (lipid-soluble antigens). Usually they will degrade within the gut lumen but by modifying their chemical composition their stability may increase.

However, there are some drawbacks associated to particulate delivery systems. High temperatures, high shear forces and organic solvents, all of which will inactivate the antigen, are required during the production of PLG particles and liposomes. In general, the major consideration is the poor particle uptake by the M-cells and this is mainly due to the small portion of FAE occupied by M-cells.

An increase of particle uptake by M-cells can be obtained by non-specific and specific interactions of the synthetic delivery systems with M-cells. The enhancement of M-cells' interaction using the non-specific route involves altering of the particle size, surface charge and hydrophobicity. However this is a rather unreliable method.

A more reliable method is the use of receptor–mediated M-cell targeting. To this end the surface of the particles is chemically modified in order to enhance the interactions with M-cell apical membranes. This can occur by lectin-mediated, microbial protein-mediated and immunoglobulin-mediated M-cell targeting (Clark, 2001; Gilligan and Po, 1991).

In this research work the use of porous pellets in the field of oral vaccine formulation was investigated. The porous network could offer some advantages: (a) incorporation of the vaccine only occurs after manufacturing of the porous pellet production, hence the manufacturing process has no detrimental effects on the vaccine; (b) the release from porous devices is diffusion-controlled, hence the tortuosity of the porous pellets will delay the absorption of gastric fluids and the release of vaccine, resulting in a lower loss of vaccine before reaching the target site; (c) no additional coating with an appropriate polymer is required as the vaccine is protected by the porous network.

1.4. REFERENCES

A.C.I. Operations pty; (1973). Britisch Pat. No. GB 1321093.

Almirall, A., Larrecq, G., Delgado, J.A., Martinez, S., Planell, J.A. and Ginebra, M.P. (2004). Fabrication of low temperature macroporous hydroxyapatite scaffolds by foaming and hydrolysis of an α-TCP paste. Biomaterials, 25, 3671-3680.

Arm, D.M., Tencer, A.F., Bain, S.D. and Celino, D. (1996). Effect of controlled release of platelet-derived growth factor from a porous hydroxyapatite implant on bone ingrowth. Biomaterials, 17, 703-709.

Baert, L. and Remon, J.P. (1993). Influence of amount of granulation liquid on the drug release rate from pellets made by extrusion spheronization. Int. J. Pharm., 95, 135-141.

Bagwell, R.B. and Messing, G.I. (1996). Critical factors in the production of sol-gel derived porous alumina. Key Eng. Mater., 115, 45-64.

Bailliez, S. and Nzihou, A. (2004). The kinetics of surface area reduction during isothermal sintering of hydroxyapatite adsorbent. Chem. Eng. J., 98, 141-152.

Bandelin, F.J. (1989). Compressed tablets by wet granulation. In: Pharmaceutical dosage forms: Tablets. Lieberman, H.A., Lachman, L. and Schwartz, J.B. (Eds.) Marcel Dekker, Inc. New York, USA, 131-193.

Banhart, J. (2001). Manufacture, characterization and application of cellular metals and metal foams. Prog. Mat. Sci., 46, 559-632.

Bechgaard, H. and Hagermann, N.G. (1978). Controlled-release multiple units and single unit doses. A literature review. Drug Dev. Ind. Pharm., 4, 53-67.

Binner, J. (2005). Ceramic Foams. In: Cellular ceramics: structure, manufacturing, properties and applications. Scheffler, M and Colombo, P. (Eds.), WILEY-VCH Verlag GmbH & Co. KGaA, Weinheim, Germany.

Bram, M, Stiller, C., Buchkremer, H.P., Stöver, D. and Bauer, H. (2000). High-porosity titanium, stainless steel and superalloy parts. Adv. Eng. Mat., 2, 196-1999.

Burgos, A.E., Belchior, J.C. and Sinisterra, R.D. (2002). Controlled release of rhodium (II) carboxylates and their association complexes with cyclodextrins from hydroxyapatite matrix. Biomaterials, 23, 2519-2526.

Clark, M.A., Jepson, M.A. and Hirst, B.H. (2001). Exploiting M cells for drug and vaccine delivery. Adv. Drug Del. Rev., 50, 81-106.

Colomno, P. and Bernardo, E. (2003). Macro- and micro-cellular porous ceramics from preceramic polmers. Compos. Sci. Technol., 63, 2353-2359.

Conine, J.W. and Hadely, H.R. (1970). Preparation of small solid pharmaceutical spheres. Drug Cosmet. Ind., 106, 38-41.

Davis, I.C. and Owen, R.L. (1997). The immunopathology of M cells. Springer Semin. Immunopathol., 18, 421-448.

Dubok, V.A. (2000). Bioceramics-yesterday, today, tomorrow. Powder Metall. Met. Ceram., 39, 381-394.

Du Pont de Nemours, E.I. (1967). GB Pat. No. 1 175 760.

Erkoboni, K.A. (2003). Extrusion/spheronization. In: Pharmaceutical extrusion technology. Ghebre-Sellassie, I., Martin, C. (Eds.) Marcel Dekker Inc., New York, USA, 277-322.

Florence, A.T. (1997). The oral absorption of micro- and nanoparticulates: Neither exceptional nor unusual. Pharm. Res., 14, 259-266.

Gbureck, U., Holzel, T., Doillon, C.J., Muller, F.A. and Barralet, J.E. (2007). Direct printing of bioceramic implants with spatially localized angiogenic factors. Adv. Mater., 19, 795-800.

Ghebre-Sellasie, I. (1989). Pellets: A general overview. In: Pharmaceutical pelletilization technology. Ghebre-Sellasie (Ed.), Marcel Dekker Inc., New York, USA, 1-13.

Gilligan, C.A. and Po A.L.W. (1991). Oral vaccines: Design and delivery. Int. J. Pharm., 75, 1-24.

Ginebra, M.P., Traykova, T. and Planell, J.A. (2006). Calcium phosphate cements as bone drug delivery systems: A review. J. Control. Rel., 113, 102-110.

Grynpas, M.D., Pilliar, R.M., Kandel, R.A., Renlund, R., Filiaggi, M. and Dumitriu, M. (2002). Porous calcium polyphosphate scaffolds for bone substitute applications in vivo studies. Biomaterials, 23, 2063-2070.

Habibovic, P., Gbureck, U., Dollion, C.J., Bassett, D.C., van Blitterwijk, C.A. and Barralet, J.E. (2008). Osteoconduction and osteoinduction of low-temperature 3D printed bioceramic implants. Biomaterials, 29, 944-953.

Hasegawa, M., Sudo, A., Komlev, V.S., Barinov, S.M. and Uchida, A. (2003). High release of antibiotic from a novel hydroxyapatite with bimodal pore size distribution. J. Biomed. Mater. Res. Part B: Appl. Biomater., 70, 332-339.

Holmgren, J. (1991). Mucosal immunity and vaccination. FEMS Microbiology Immunology, 89, 1-10.

Holmgren, J and Czerkinsky, C. (2005). Mucosal immunity and vaccines. Nat. Med., 11, S45-S53.

Itokazu, M., Esaki, M., Yamamoto, K., Tanemori, T. and Kasai, T. (1999). Local drug delivery system using ceramics: vacuum method for impregnating a chemotherapeutic agent into a porous hydroxyapatite block. J. Mat. Sci.: Mat. Med., 10, 249-252.

Jarcho, M. (1986). Biomaterial aspects of calcium phosphates. Poperties and applications. Dent. Clin. North. Am., 30, 25-47.

Kaetzel, C.S., Robinson, J.K., Chintalacharuvu, K.R., Vaerman J.P. and Lamm, M.E. (1991). The polymeric immunoglobulin receptor (secretory component) mediates transport of immune complexes across epithelial cells: A local defense function for IgA. Proc.Natl. Acad. Sci. USA, 88, 8796-8800.

Katsuki, H., Kawahara, A. and Ichinose, H. (1992). Preparation and some properties of porous alumina ceramics obtained by the gelatination of ammonium alginate. J. Mater. Sci., 27, 6067-6070.

Kingery, W.D., Bowen, H.K. and Uhlmann, D.R. (1976). Introduction to ceramics. (second edition).Burke, E., Chalmers, B. and Krumhansl, J.A. (Eds.) John Wiley & Sons Inc., New York, USA.

Krämer, J. and Blume H. (1994). Biopharmaceutical aspects of multiparticulats. In: Multiparticulate ral drug delivery. Ghebre-Sellassie, I. (Ed.), Marcel Dekker Inc., New York, USA, 307-332.

Lebugle, A., Rodrigues, A., Bonnevialle, P., Voigt, J.J., Canal, P. and Rodriguez F. (2002). Study of implantable calcium phosphate systems for the slow release of methotrexate. Biomaterials, 23, 3517-3522.

Ma, J., Wang, C. and Peng, K.W. (2003). Electrophoretic deposition of porous hydroxyapatite scaffold. Biomaterials,24, 3505-3510.

Moreno, R. (1992). The role of slip additives in tape casting technology. 2. Binders and plasticizers . Am. Ceram. Bull., 71, 1647-1657.

Muralithran, G. and Ramesh, S. (2000). The effects of sintering temperature on the properties of hydroxyapatite. Ceram. Int., 26, 221-230.

Neutra, M.R. and Kozlowski, P.A. (2006). Mucosal vaccines: the promise and the challenge. Nat. Rev. Immunol., 6, 148-158.

Niedergang, F. and Kraehenbuhl, J.P. (2000). Much to do about M cells. Cell Biology, 10, 137-141.

Nugent, J., Li Wan PO, A. and Scott, E.M. (1998). Design and delivery of non parenteral vaccines. J. Clin. Pharm. Therap., 23, 257-285.

O'Hagan, D.T. (1998). Microparticles and polymers for the mucosal delivery of vaccines. Adv. Drug Del. Rev., 34, 305-320.

Padilla, S., Roman, J. and Vallet-Regi, M. (2002). Synthesis of porous hydroxyapatites by combination of gelcasting and foams burn out methods. J. Mat. Sci.: Mat. Med., 13, 1193-1197.

Palazzo, B., Sidoti, M.C., Roveri, N., Tampieri, A., Sandri, M., Bertolazzi, L., Galbusera, F., Dubini, G., Vena, P. and Contro, R. (2005). Controlled drug delivery from porous hydroxiapatite grafts: An experimental and theoretical approach. Met. Sci. Eng., 25, 207-213.

Patel, S., Kaushal, A.M. and Bansal, A.K. (2006). Compression physics in the formulation development of tablets. Crit. Rev. Ther. Drug, 23, 1-65.

Reynolds, A.D. (1970). A new technique for the production of spherical particles. Mfg Chem. Aerosol News, 41, 40-43.

Rowe, R., Shesky, P.J. and Weller, P.J. (Ed.) (2003). Handbook of Pharmaceutical Excipients (Fourth Edition). Washington DC, American Pharmaceutical Association and Pharmaceutical Press.

Ryan, G., Pandit, A. and Apatsidis, D.P. (2006). Fabrication methods of porous metals for use in orthopaedic applications. Biomaterials, 27, 2651-2670.

Sepulveda, P., Ortega, F.S., Innocentini, M.D.M. and Pandolfelli, V.C. (2000). Properties of highly porous hydroxyapatite obtained by gelcasting of foams. J. Am. Ceram. Soc., 83, 3021-3024.

Schwartzwalder, K. and Somers, A.V. (1963). US Pat. No.3090094.

Shangraw R.F. (1989). Compressed tablets by direct compression. In: Pharmaceutical dosage forms: Tablets. Lieberman, H.A., Lachman, L. and Schwartz, J.B. (Eds.) Marcel Dekker, Inc. New York, USA, 195-229.

Simancik, F. (2000). Introduction: the strange world of cellular materials. In: Handbook of cellular metals. Degischer, H.P. and Kriszt, B. (Eds.). Wiley-VCHVerlag, Weinheim, pp 1-4.

Sivakumar, M. and Rao, K.P. (2002). Preparation, characterization and in vitro release of gentamicin from coralline hydroxyapatite-gelatin composite microspheres. Biomaterials, 23, 3175-3181.

Stigter, M., Bezemer, J., de Groot, K. and Layrolle,P. (2004). Incorporation of different antibiotics into carbonated hydroxyapatite coatings on titanium implants, release and antibiotic efficay. J. Control. Rel., 99, 127-137.

Takahasi, T., Münstedt, H., Colombo, P. and Modesti, M. (2001). Thermal evolution of a silicone resin/polyurethane blend from preceramic to ceramic foam. J. Mater. Sci., 36, 1627-1639.

Tampieri, M., Celotti, G., Sfontagh, F. and Landi, E. (1997). Sintering and characterization of HA and TCP bioceramics with control of their strength and phase purity. J. Mater. Sci.- Mater. M., 8, 29-37.

Venables, H.J. and Wells, J.I. (2001). Powder mixing. Drug Dev. Ind. Pharm., 27, 599-612.

Vromans, H., Poels-Janssen, H.G.M. and Egermann, H. (1999). Effects of high-shear granulation on granulate homogeneity. Pharm. Dev. Tech., 4, 297-303.

Walker, R.I. (1994). New strategies for using mucosal vaccination to achieve more effective immunization. Vaccine, 12, 387-400.

Wang, C., Ma, J., Cheng, W. and Zhang, R. (2002). Thick hydroxyapatite coatings by electrophoretic deposition. Mat. Lett., 57, 99-105.

Weber, J.N. and White, E.W. (1972). Carbon-metal graded composites for permanent osseous attachment of non-porous metals. Mat. Res. Bull., 7, 1005-1016.

Young, A.C., Omatete, O.O., Janney, M.A. and Menchhofer, P.A. (1991). Gelcasting of alumina. J. Am. Ceram. Soc., 74, 612-618.

2

Development and evaluation of porous tablets

Published in part in European Journal of Pharmaceutics and Biopharmaceutics 67 (2007) 498-506

2.1. INTRODUCTION

As described in Chapter 1, porous bone implants are already well established in the field of local drug delivery. For most type of drugs incorporated in the porous bone implants, sustained drug release is required. Generally, porous bone implants based on calcium phosphate are diffusion-controlled devices, where the drug is incorporated into a non-biodegradable matrix. Although some of the calcium phosphates are resorbable, in most cases the rate of matrix degradation is much lower than the rate of drug liberation, hence the diffusion-controlled drug release (Ginebra et al., 2006a).

The objective of the research work presented in this chapter was to explore if the applications of porous structures could be extended to oral drug delivery. Tablets are still the favorable solid dosage form for oral drug delivery attributed to their advantages for both the patient and the manufacturer. The preparation of tablets mostly occurs by direct compression due to its economic benefit. However, in some cases direct compression is not recommended, e.g. for drugs with poor compression properties or low-dosed drugs. The challenge of this project was to develop an innovative carrier, a porous tablet, that could overcome these problems.

To manufacture these tablet-shaped porous structures two techniques were evaluated: direct compression and modified gelcasting, both followed by sintering. Tablets were manufactured using calcium hydroxyapatite (HA) and an organic material, and after removal of the latter via heat treatment (calcination at 500-700°C in combination with sintering at 1250-1350°C), porous tablets were obtained. The type of pore forming agent, sinter time and sinter temperature were varied to investigate their influence on the quality of the porous matrix. After selecting an appropriate matrix, its potential as drug carrier was evaluated based on the drug loading capacity of porous HA tablets and on the release profiles of metoprolol tartrate (used as model drug) from these matrices.

2.2 MATERIALS

For tablets manufactured via direct compression followed by sintering, hydroxyapatite (HA, Ca/P-ratio:1.67) was obtained from Acros Organics (Geel, Belgium). Microcrystalline cellulose (Avicel PH 200, FMC Biopolymer, Cork, Ireland), corn starch (Amylum, Koog a/d Zaan, the Netherlands) and sorbitol (Sorbidex P 16616, Cerestar, Mechelen, Belgium) were used as pore forming agents. Magnesium stearate (Alpha Pharma, Zwevegem, Belgium) was added as lubricant.

For tablets manufactured via modified gelcasting followed by sintering, hydroxyapatite was obtained from Bekaert (Zwevegem, Belgium). Tergitol TMN 10 (polyethyleneoxyethanol) (Sigma-Aldrich, Bornem, Belgium) was used as foaming agent. Targon 1128 (ammonium polycarbonate) (BK Giulini, Ladenburg, Germany) and Benecel® (hypromellose) (Hercules, Beringen-Paal, Belgium) were used as dispersing agent and viscosity enhancer, respectively, required to stabilize the HA suspension. Agar (Fagron, Waregem, Belgium) was used as gelling agent.

Metoprolol tartrate (10 μm) (Esteve Quimica, Barcelona, Spain) was used as model drug.

2.2.1. Calcium Hydroxyapatite

Calcium hydroxyapatite ($Ca_5(PO_4)_3OH$) (HA) is an inorganic component of human hard tissues like bone and teeth.

The manufacturing routes of synthetic HA can be divided into solid-state reactions and wet methods, whereby the wet methods are the most adequate routes. The wet methods include precipitation (in the presence of phosphoric acid, urea or formamide), hydrolysis and spray pyrolysis (Ishikawa, 2000; Vallet-Régi and Gonzalez-Calbet, 2004).

In the industry, precipitation is mostly used for the preparation of HA particles since water is the only by-product of the reaction. In order to obtain stoichiometric HA (molair Ca/P ratio = 1.67), a H_3PO_4 solution (concentration: 25-80%) is added to a $Ca(OH)_2$ suspension (concentration: 2-10%) up to a Ca/P-ratio of 1.67 and a HA precipitate is formed according to the reaction:

$$5\ Ca(OH)_2 + 3\ H_3PO_4 \longrightarrow Ca_5(PO_4)_3OH + 9\ H_2O$$

The resulting precipitation is left at room temperature for more than 1 day followed by filtration and drying.

The thermostability of HA powder is influenced by the rate of addition of orthophosphoric acid, the ripening treatment, the reaction temperature and the Ca/P ratio. To obtain a thermostable HA powder, the precipitate must consist of stoichiometric HA. Therefore the rate of addition of orthophosphoric acid must be 11 ml/min, a Ca/P ratio of 1.67 is required, a ripening treatment of the HA precipitates is necessary and the precipitation must be performed at a temperature around 25°C (Osaka et al., 1991).

The crystal structure of HA is illustrated in Fig. 2.1. There are two kinds of Ca^{2+} ions in a HA crystal: Ca_I along the *c* axis (identified by the arrows) and Ca_{II} surrounding the OH^- ions. Ca_I is more easily dissolved in aqueous solutions than Ca_{II} hence Ca deficiency will occur at Ca_I sites. Since Ca^{2+}, PO_4^{3-} and OH^- of HA can be replaced by other ions, the synthesis of

stoichiometric HA is rather hard and requires particular attention. The composition of Ca-deficient HA is written as $Ca_{10-x}(HPO_4)_{6-x}(OH)_{2-x}.nH_2O$. The charge imbalance is compensated by different processes, such as protonation of PO_4^{3-} to HPO_4^{2-} or $H_2PO_4^-$, replacement of PO_4^{3-} by CO_3^{2-} and HCO_3^-, occupation of Ca^{2+} defects by other metal ions, etc. For this reason incorporation of various ions into the HA lattice leads to the formation of non-stoichiometric HA particles. When heat treatment is performed on this form, decomposition products are formed eg. tricalcium phosphate and calciumcarbonate.

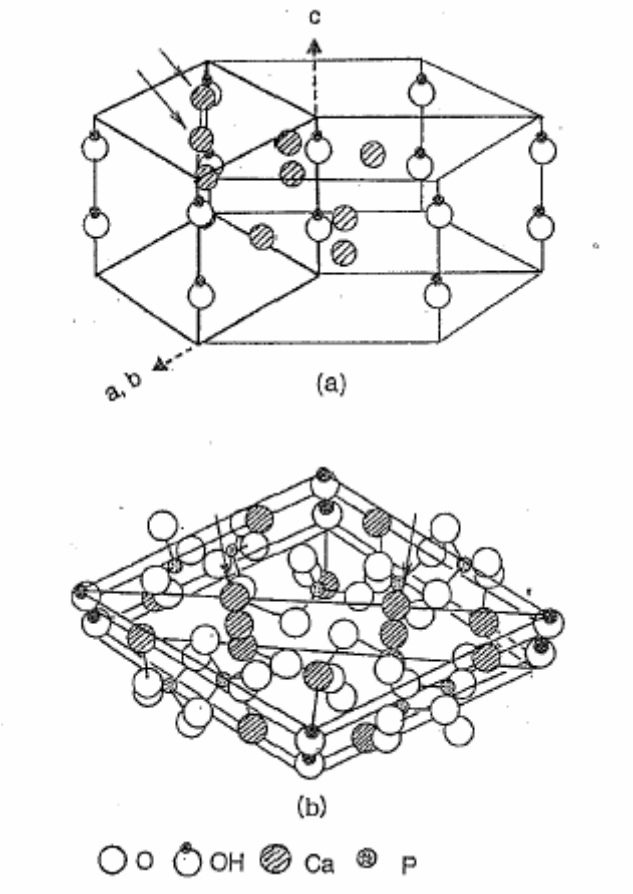

Figure 2.1.: Crystal structure of HA – adapted from Ishikawa, 2000.

Synthetic calcium hydroxyapatite can be used as tablet and capsule diluent and as described in Chapter 1, calcium hydroxyapatite is used in the manufacturing of bone implants due to its biocompatibility. Furthermore they are devoid of local or systemic toxicity, do not elicit an

inflammatory or foreign body response what indicates that calcium hydroxyapatite is a bio-safe material (Jarcho, 1986).

Calcium hydroxyapatite is practically insoluble in water and has a melting point around 1670°C (Rowe et al., 2003).

2.3. METHODS

2.3.1. Production of porous tablets

- Direct compression followed by sintering

Tablets (∅ 18 mm, flat edged, 550 mg) consisting of HA, a pore former and magnesium stearate (2%) were prepared via direct compression (14.5 kN) using an instrumented eccentric press (Korsch type EK0, Berlin, Germany). Microcrystalline cellulose, corn starch or sorbitol were added as pore formers. Prior to compression powder blends were prepared via physical mixing (using a tumbling mixer) of the materials as received from the suppliers or after a preprocessing step. During preprocessing, agglomerates of HA and pore formers were removed to ensure a homogeneous distribution of the pore former inside the tablet. Therefore, 50 g HA was suspended in 150 ml acetone and this suspension was grinded in a ball mill (containing 25 grinding balls, ∅ 10 mm) (Pulverisette 6, Fritsch, Idar-Oberstein, Germany) during 15 min (grinding speed 500 rpm). Afterwards the pore forming agent was added to the suspension and grinded for 5 min at 250 rpm. After evaporation of the acetone fraction, 2% magnesium stearate was added to the HA/pore former-mixture.

After compression the tablets were sintered in a chamber furnace (Thermoconcept, Bremen, Germany) at 800, 1000 and 1250°C (heating rate: 125 °C/h) during 1, 3 and 5 h. After cooling down (90 °C/h) to room temperature the properties of the porous tablet were evaluated.

- Modified gelcasting followed by sintering

These tablets were manufactured in cooperation with the Flemisch Instititute for Technological Research (VITO, Mol, Belgium).

Gelcasting, originally developed to manufacture dense ceramic components (Omatete et al., 1991), can be modified for the production of highly porous ceramics as a result of aeration of the ceramic suspension containing gelling and foaming agents (modified gelcasting). Conventially, the gelling of foamed suspensions resulted from in-situ polymerization of water-soluble (mostly acryl-based) monomers (Sepulveda and Binner, 1999); however due to the toxicity of the monomers, alternative gelling agents have been introduced, eg. gelatine, pectines, carrageenan and agar (Millan et al., 2001; Luyten et al., 2003; Mouazer et al., 2004).

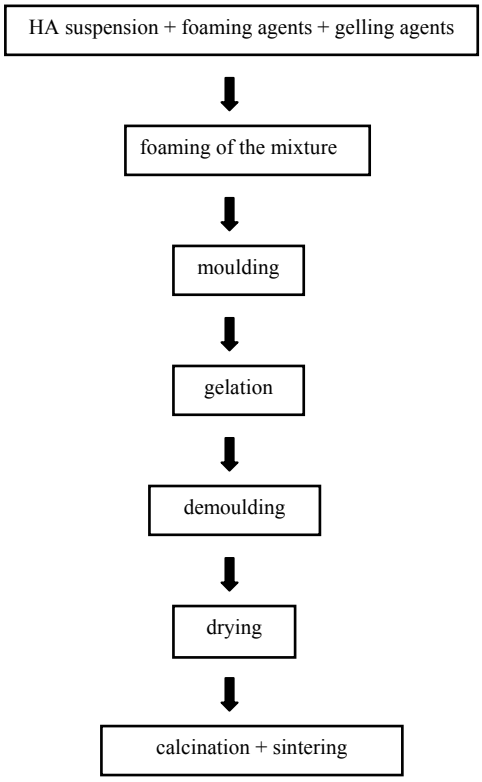

Figure 2.2.: Flowchart of the modified gelcasting procedure.

Hydroxyapatite (100 g), Tergitol TMN 10 (0.85 g) and Targon 1128 (1 g) were preheated to

80°C. Agar (2.14 g) was dissolved in water (85.6 g) at a temperature of 90°C, followed by cooling down to 70°C. Benecel® (0.17 g) was added to the agar-solution in order to increase the viscosity. The HA powder, Tergitol TMN 10 and Targon 1128 were blended with the solution and intensively mixed using a planetary Hobart N 50 mixer at 285 rpm (Hobart, Sydney, Australia) during 4 min or using a hand mixer (Philips electronics, Bruges, Belgium) during 3 and 10 min in order to form a foam. The foamed slurry was poured into a mould and was placed for 15 min at room temperature. Subsequently, the mould was placed in the refrigerator for 30 min to obtain a solid gel phase. After demoulding, the wet green component was dried during 3 days in a climate test chamber (Weiss Gallenkamp Indutrial, Leicestershire, UK) at 25°C and 70% relative humidity. The dry green mass was calcinated at 500°C whereby all organic material was burned out, followed by sintering (heating rate: 240 °C/h) at a temperature of 1350°C during 3 h. After cooling down (60 °C/h) the sintered block was cut into tablets (Ø 13 mm, height 3 mm).

2.3.2. Tablet evaluation

- Tablet strength

Based on the diametrical crushing strength of the tablets determined using a tensile strength bench (Type L1000R, Lloyd Instruments, Fareham, United Kingdom) operating at a crosshead speed of 8 mm/min, the tensile strength of the tablets (n=10) was calculated according to Fell and Newton (Fell and Newton, 1970).

- Tablet friability

The tablet friability was determined in a Pharmatest-friabilator (PTFE, Hainburg, Germany) using the method described in the European Pharmacopoeia 5 (i.e. rotating 20 tablets inside a drum for 4 min at 25 rpm).

- Tablet porosity

The tablet porosity was calculated based on the skeletal volume (V_s) and the apparent volume (V_a) of the tablets (Eq. 1). The skeletal volume was measured using helium pycnometry (Accupyc 1330, Norcross, GA, USA), while the apparent volume was calculated from the height and radius of the tablet.

$$[(V_a-V_s)/V_a] \times 100 = \text{porosity (\%)} \quad (1)$$

- Pore size distribution

The pore size distribution (0.003-360µm) of the sintered tablets was determined using mercury intrusion porosimetry (Autopore III, Norcross, GA, USA). The sample size (2 - 3 g) was adjusted in order to use between 20 and 80% of the stem volume. The sample was evacuated to 50 mm Hg, followed by low pressure mercury intrusion in a pressure range from 4.3 to 193 kPa, with a mercury filling pressure of 4.3 kPa, maximal intrusion volume of 0.03 ml/g and equilibration time of 10 s. Next high pressure intrusion was performed in a pressure range from 207 to 41.10^4 kPa, with a maximal intrusion volume of 0.03 ml/g and equilibration time of 10 s.

- Scanning electron microscopy (SEM)

SEM was used to visualize the porous structure of the tablets. Tablets were coated with a gold layer using a sputter coater (Autofine Coater, JFC-1300, JEOL, Tokyo, Japan) to assure conductivity. The SEM micrographs were obtained using a scanning electron microscope (JSM-5510, JEOL, Tokyo, Japan).

- Internal pore structure

For the determination of the 3-dimensional internal structure of the samples, the nano-computed tomography (nano-CT) scanner of the UGCT facility (www.ugct.ugent.be) was used. This scanner combines a transmission x-ray tube (Feinfocus) with a focal spot size of 900 nm and as X-ray detector, a 4008x2667 pixel CCD camera (Photonic Science). The commercially available reconstruction software "Octopus" was used for conversion of the raw images into the reconstructed cross-section. Data about the 3D structure were obtained using the 3D analysis software "μCTanalySIS (Cnudde et al., 2004) providing parameters such as total porosity, number of pores, volume of each pore together with its maximum inscribed and equivalent diameter. The maximum inscribed diameter is defined as the diameter of the largest sphere that can be enclosed in the volume and the equivalent diameter is the diameter of a spherical pore with the same volume as the (non-spherical) pore being examined. Combining the data of the maximum inscribed diameter (d_{max}) and the equivalent diameter (d_e) provides information about the structure of the pores.

- X-ray diffraction

To determine the thermostability of hydroxyapatite at high temperatures, the X-ray pattern of tablets sintered at 1250°C and 1350°C were compared with the X-ray pattern of pure unsintered hydroxyapatite powder. The X-ray patterns were obtained using a D5000 Cu Kα Diffractor (λ = 1,54 A) (Siemens, Karlsruhe, Germany) with a voltage of 40 mA in the angular range of $10°<2\theta<60°$ using a step scan mode (step width = 0.02°, counting time = 1 s/step)

2.3.3. Drug-loading of porous tablets and evaluation of drug-loaded tablets

- Drug-loading

Metoprolol tartrate was incorporated in the tablets as highly water soluble model drug. Therefore, 100 µl of an aqueous drug solution of metoprolol tartrate (1.5, 4, 15 and 40%, w/v) was spiked on one side of the tablet. After absorption of the liquid into the porous inner structure of the tablet, they were oven-dried for 8 h at 40°C. Afterwards, the same procedure was done at the other side of the tablet.

- Surface tension of the drug solutions

The surface tension of the drug solutions was determined via a dynamic 'Wilhelmy Plate' method whereby a strip of cellulose chromatography paper (Whatman Chr 1, smooth surface, 0.18 mm tick with a linear flow rate for water of 130 mm/30min) is lowered into the solution. The plate was brought in the solution during 10 s for stabilization and then slowly pulled out of the solution. The surface tension of the solution is determined from the downward force directed on the strip.

- Content uniformity of drug-loaded tablets

The content uniformity of the drug-loaded tablets was determined by soaking a tablet (n=10) during 24 h in 50 ml water, followed by stirring during 15 min. The drug concentration was measured using UV spectrophotometry (λ= 222 nm).

- Drug distribution

Riboflavin sodium phosphate was incorporated in the tablets by spiking 100 µl of an aqueous riboflavin sodium phosphate solution (3.75 %, w/v) onto one side of the tablet, after drying

the same procedure was performed on the other side. Its yellowish colour allowed a visual determination of the drug distribution in the tablet.

- Differential scanning calorimetry

In order to determine the physical state of the drug after incorporation in the porous tablet, thermograms of the raw materials, a physical mixture and the drug-loaded tablet were recorded via differential scanning calorimetry (DSC, TA 2920, T.A. Instruments, New Castle, USA). The samples (8-12 mg in a hermetically sealed Al-pan) were heated from 0 to 200°C at a rate of 10 °C/min using a refrigerated cooling system (RCS, TA Instruments, New Castle, USA).

- X-ray diffraction

To confirm the results obtained via DSC, X-ray diffraction patterns of the raw materials, a physical mixture and the drug loaded tablet were determined using a D5000 Cu Kα Diffractor (λ = 1,54 A) (Siemens, Karlsruhe, Germany) with a voltage of 40 mA in the angular range of $10°<2\theta<60°$ using a step scan mode (step width = 0.02°, counting time = 1 s/step)

- *In vitro* drug release

Drug release from the porous tablets was determined using the USP II method (VanKel VK 8000, VanKel Industries, New Jersey, USA) with a paddle speed of 50 rpm and at a temperature of 37±0.5°C. Demineralised water, phosphate buffer pH 6.8 and 0.1N hydrochloric acid were used as dissolution media. Sink conditions were maintained. Samples were collected at 5, 10, 15, 20, 30, 45, 60, 90, 120 and 180 min and analysed using an UV/VIS double beam spectrophotometer (Perkin-Elmer, Zaventem, Belgium) at 222 nm for metoprolol tartrate.

➢ Modelling of the drug release

Fick's second law of diffusion, considering axial as well as radial mass transfer in a cyclinder was used to quantitatively describe the experimentally measured drug release profiles:

$$\frac{\partial c}{\partial t} = \frac{1}{r} \cdot \left\{ \frac{\partial}{\partial r}\left(r \cdot D \cdot \frac{\partial c}{\partial r} \right) + \frac{\partial}{\partial \theta}\left(\frac{D}{r} \cdot \frac{\partial c}{\partial \theta} \right) + \frac{\partial}{\partial z}\left(r \cdot D \cdot \frac{\partial c}{\partial z} \right) \right\} \qquad (2)$$

where c is the drug concentration, t represents time; r, z denote the radial and axial coordinates and θ the angle perpendicular to the r-z-plane; D represents the apparent diffusion coefficient of the drug within the porous tablet.

Using infinite series of exponential functions this partial differential equation can be solved considering the respective initial and boundary conditions [homogeneous drug distribution before exposure to the release medium (t=0), high drug solubility and perfect sink conditions], as well as symmetries (e.g., there is no concentration gradient with respect to θ), leading to (Vergnaud, 1993):

$$\frac{M_t}{M_\infty} = 1 - \frac{32}{\pi^2} \cdot \sum_{n=1}^{\infty} \frac{1}{q_n^2} \cdot \exp\left(-\frac{q_n^2}{R^2} \cdot D \cdot t \right) \cdot \sum_{p=0}^{\infty} \frac{1}{(2 \cdot p + 1)^2} \cdot \exp\left(-\frac{(2 \cdot p + 1)^2 \cdot \pi^2}{H^2} \cdot D \cdot t \right) \qquad (3)$$

where M_t and M_∞, represent the absolute cumulative amounts of drug released at time t and infinite time, respectively; q_n are the roots of the Bessel function of the first kind of zero order [$J_0(q_n)=0$], and R and H denote the radius and height of the cylinder.

In case drug release leveled off below 100 %, the experimentally determined plateau value (amount of mobile drug) was considered as 100 % reference value for drug diffusion.

2.3.4. Stability study

Porous tablets formulated with 50% w/w Avicel PH 200 as pore forming agent and manufactured by direct compression and sintering (using the protocol previously described) were selected for stability testing, according to the USP guidelines. The porous tablets were stored at 25°C/60 ± 5 % relative humidity (RH) and at 40°C/75 ± 5 % RH and after 0, 3, 6, 9 and 12 months the drug release profile and water content of the tablets were determined.

Dissolution tests (n=3) in demineralized water were performed under the conditions described in paragraph 2.3.3. The area under the curve ($AUC_{0\text{-}3h}$) values of the dissolution profiles were statistically evaluated with a one-way ANOVA at a significance level of 0.05. The normality of the data was checked by means of a Kolmogorov-Smirnov test and the homogeneity of variances by means of the Levene test. SPSS 16.0 for Windows was used.

The water content of the porous tablets was determined using a Mettler DL35 Karl Fisher titrator (Mettler-Toledo, Beerse, Belgium) in combination with a Mettler DO337 oven operated at 150°C (n=3). The samples were placed in a Pyrex vessel inside the oven. During 10 min the moisture evaporated from the sample was carried to the titration vessel by a nitrogen stream (300 ml/min), after which the titration was started. Hydranal® Composite 5 (Riedel-de Haën, Seelze, Germany) with a theoretical titer of 2 mg H_2O/ml was used as titrant solution.

2.4. RESULTS AND DISCUSSION

2.4.1. Manufacturing and characterization of porous tablets

- Porous tablets manufactured via direct compression and sintering

In order to obtain a solid structure when the organic pore former was removed during heat treatment, the amount of pore forming agent in the tablets was limited: 50% (w/w) for Avicel

PH 200 and corn starch and 37.5% for sorbitol. Using higher concentrations adhesion between the HA particles was not sufficient to obtain strong tablets.

Physical mixing of HA and the pore former (using a tumbling mixer) resulted in a poor blending uniformity. Consequently the removal of agglomerates of pore former during heat treatment yielded a potholed surface texture of the tablets. To deagglomerate these lumps and to obtain a homogeneous distribution of the pore forming agent, a suspension of HA and the pore former in acetone was grinded in a ball mill. After evaporation of the organic solvent and production of porous tablets via direct compression and sintering, this procedure resulted in tablets with a smooth surface.

Porosity of the sintered tablets depended on the amount of pore former and on the sinter temperature (Table 2.1.). Increasing the amount of pore forming agent resulted in a higher porosity as the pore forming agent was removed during the heat treatment. Increasing the sinter temperature decreased the porosity. The lowest porosity values were recorded for tablets processed at 1250°C.

Table 2.1.: Porosity of porous calcium hydroxyapatite tablets containing different ratios of pore forming agent (Avicel PH 200, corn starch or sorbitol), sintered at 800, 1000 and 1250°C during 3h.

Pore former	% (w/w)	Sinter temperature (°C)		
		800	1000	1250
Avicel PH 200	50	79.3 ± 0.5	73.7 ± 0.4	52.5 ± 0.6
corn starch	20	64.5 ± 0.3	60.1 ± 0.9	26.0 ± 2.2
corn starch	37.5	74.6 ±0.9	70.5 ± 0.6	43.0 ± 1.1
corn starch	50	79.2 ± 0.2	76.5 ± 1.0	48.6 ± 0.9
sorbitol	37.5	71.6 ± 0.3	65.2 ± 0.7	52.7 ± 0.9

During the initial phase of heat treatment (<1000°C) the HA particles only coalesced (without densification), whereas at sinter temperatures above 1000°C densification of the material

occurred (Raynaud et al., 2002; Bernache-Assollant et al., 2003). This densification correlated with the shrinking of the tablets: after 3h sintering at 1250°C the tablet diameter and height had decreased by 24.6 and 28.0%, respectively.

For tablets sintered at 1250°C, the type of pore forming agent and a variable sinter time (range: 1 to 5 h) had no effect on tablet porosity.

The SEM micrographs of the tablet surface and the 3-dimensional images of the internal structure of the porous tablet (via nano CT-scan) are shown in Fig. 2.3. The analysis of the CT-scan images is given in Table 2.2. Within the fraction of the tablet evaluated via nano CT-scan one pore system was detected for all tablets. For each formulation the equivalent diameter was larger compared to the maximum inscribed diameter, indicating that the internal pore structure is branched. The larger pore size detected for tablets formulated with 50% Avicel PH 200 is correlated with the larger size of the microcrystalline cellulose fibres (200 µm versus 25 µm and 165 µm for corn starch and sorbitol, respectively). The pore system detected in tablets formulated with 50% Avicel PH 200 or corn starch represented more than 90% of the total porosity, indicating that an interconnecting pore network was formed. In contrast, the pore system in tablets using sorbitol as pore forming agent accounted for only 63.9% of the total porosity. As no other pore classes were detected which contributed to more than 2% of the total pore volume, the rest of the porosity is attributed to individual pores.

Table 2.2.: Nano CT-scan analysis of the 3-dimensional internal structure of the porous tablets.

Pore forming agent	% (w/w)	maximum inscribed diameter (µm)	equivalent diameter (µm)	porosity represented by pore system (%)
Avicel PH 200	50	102	322	93
corn starch	50	27	188	98
sorbitol	37.5	36	300	64

a

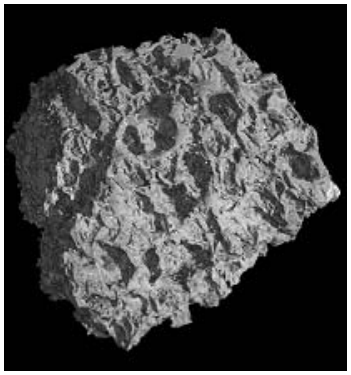

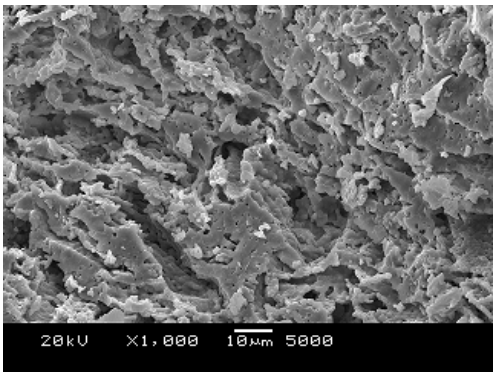

b

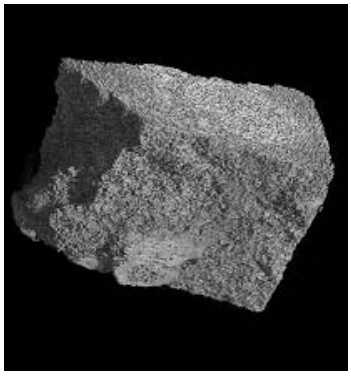

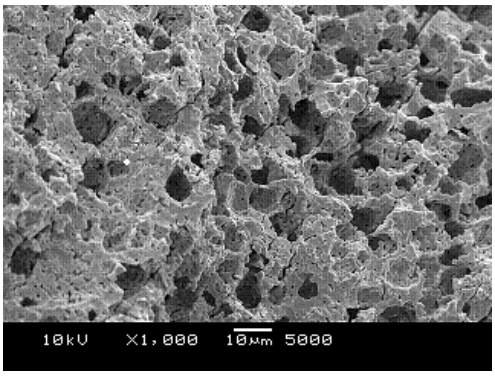

c

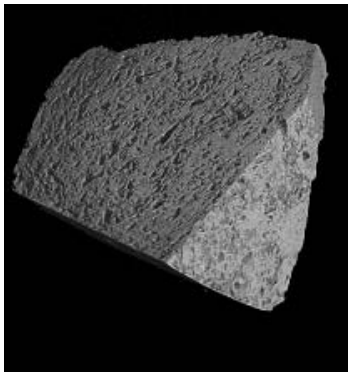

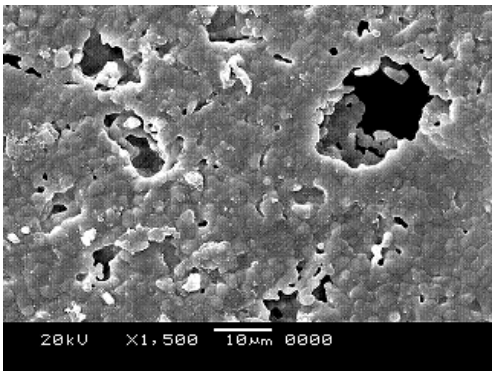

Figure 2.3.: SEM micrographs of the porous surface and 3-dimensional images of the internal structure of sintered tablets (3h, 1250°C) whereby (a) 50% (w/w) Avicel PH 200, (b) 50% (w/w) corn starch or (c) 37.5% (w/w) sorbitol was used as pore forming agent.

In contrast to the pore size detected via nano CT-scan the pore size distribution determined via mercury porosimetry was much smaller, the majority of the pores being smaller than 10 µm (Fig. 2.4.).

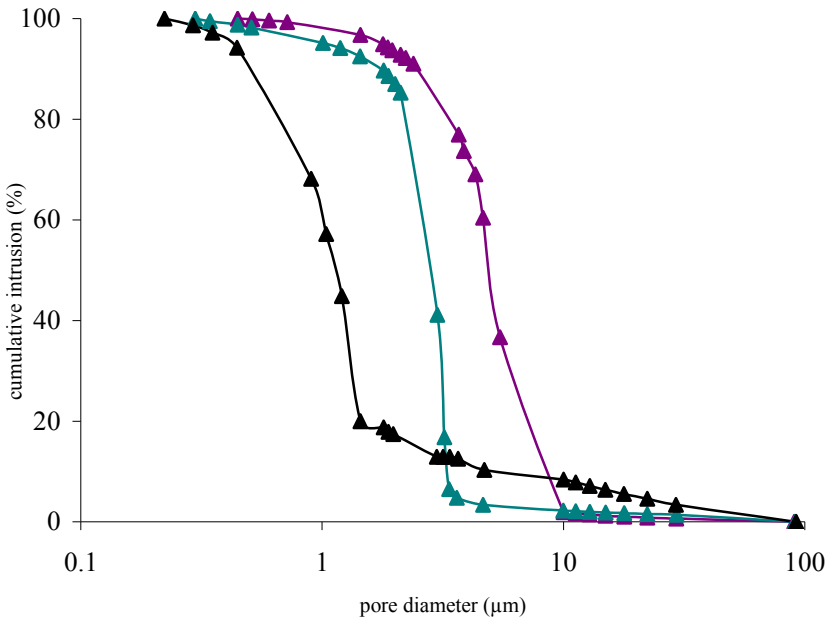

Figure 2.4.: Pore size distribution, obtained by mercury intrusion, of porous tablets with an initial diameter of 13.5mm after sintering during 3h at 1250°C whereby 50% (w/w) Avicel PH 200 (▲), 50% (w/w) corn starch (▲) or 37.5% (w/w) sorbitol (▲) was used as pore forming agent.

However, comparison between both techniques is difficult since their approach is different. Nano CT-scan analysis provides only the maximum inscribed diameter which represents the largest pore volume, whereas the entire pore size distribution is detected via mercury porosimetry. In addition, mercury porosimetry could underestimate the actual pore size due to the ink bottle effect.

Despite the porous structure of the tablets, their mechanical strength after sintering was high (tensile strength ranging between 3.9 and 7.1 MPa). However, only sintering at 1250°C resulted in tablets having a low friability.

Table 2.3.: Friability of porous calcium hydroxyapatite tablets formulated with different ratios of pore forming agent (Avicel PH 200, corn starch or sorbitol), sintered at 800, 1000 and 1250°C during 3h.

Pore former	% (w/w)	Sinter temperature (°C)		
		800	1000	1250
Avicel PH 200	50	5.5	3.9	1.2
corn starch	20	-*	0.7	0.2
corn starch	37.5	3.8	3.2	0.7
corn starch	50	-*	-*	0.5
sorbitol	37.5	1.1	0.7	0.4

* tablets fragmented during friability testing

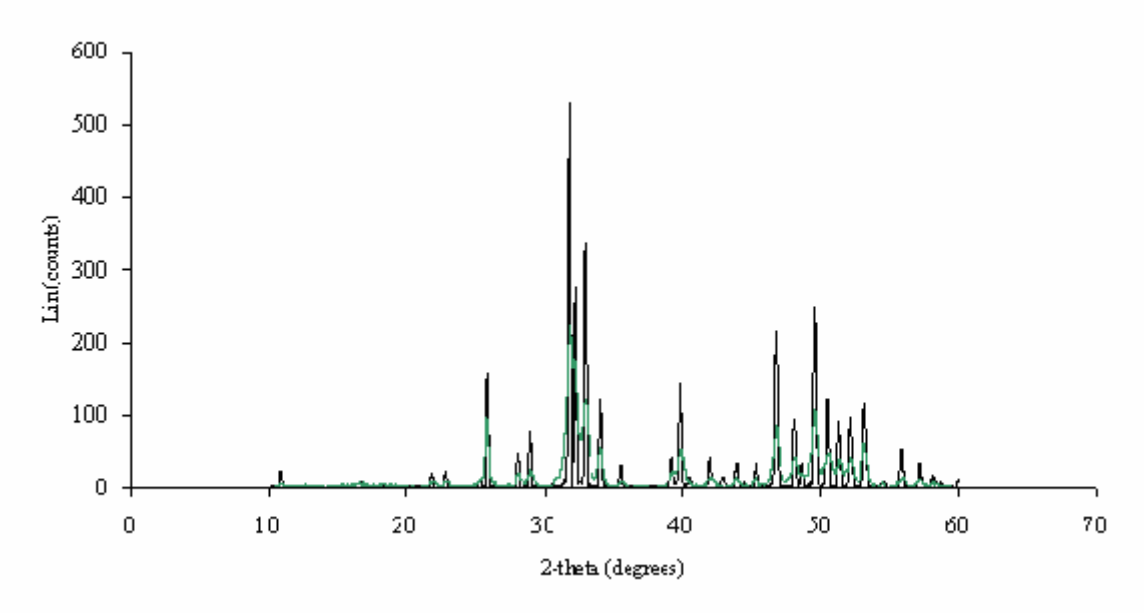

Figure 2.5.: X-ray diffraction pattern of pure calcium hydroxyapatite powder before sintering (——) and crushed porous tablets obtained by direct compression followed by sintering at 1250°C (——).

Stoichiometric (Ca/P-ratio: 1.67) hydroxyapatite (used as the main component in the tablets) is thermostable at high temperatures (Muralithran and Ramesh, 2000; Raynaud et al., 2002). The X-ray pattern of HA after sintering at 1250°C (Fig. 2.5.) showed only diffraction peaks corresponding to HA, indicating that no decomposition products and additional phases like α- and β-TCP, tetracalciumphosphate and CaO were formed during sintering and that no fraction

of the pore forming agent remained after sintering. The diffraction peaks of the sintered material were sharper and higher, indicating a higher crystallinity and the presence of larger crystals, respectively.

➢ Porous tablets manufactured via modified gelcasting and sintering

Porous carriers having larger pores were manufactured using a modified gelcasting technique resulting in tablets with a median pore size of 20, 80 and 100 µm (determined via mercury porosimetry) (Fig. 2.6.). Mixing during 3 min and 10 min with a hand mixer and 4 min with the planetary mixer resulted in a median pore size of 100, 20 and 80 µm, respectively. Mixing during 10 min resulted in a smaller pore size, due to the breaking up of larger air bubbles when a longer mixing time was applied.

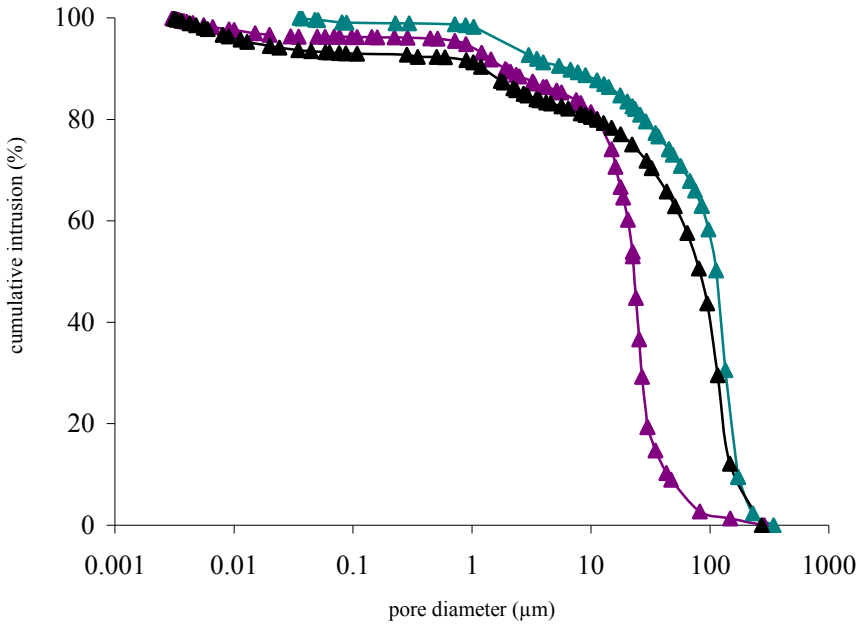

Figure 2.6.: Pore size distribution, obtained by mercury intrusion, of porous tablets manufactured via modified gelcasting. Median pore diameter: 20 µm (▲), 80 µm (▲) and 100 µm (▲).

Similar X-ray diffractograms were obtained as for the tablets prepared by direct compression. Hence the higher sinter temperature used to manufacture these porous matrices (1350°C) had no effect on the composition of the hydroxyapatite.

A porosity of 55.6 ± 0.4%, 68.8 ± 0.4% and 75.6 ± 0.5% was obtained for porous tablets with a median pore diameter of 20, 80 and 100 µm, respectively. Nano CT-scan for visualisation of the porous structure (Fig. 2.7.) detected two pore systems with a branched structure (equivalent diameter > maximum inscribed diameter) (Table 2.4.). These pore systems represented 92.5% of the total porosity volume, indicating that nearly all pores are incorporated in an interconnected network.

Table 2.4.: Nano CT-scan analysis of the 3-dimensional internal structure of a porous tablet (median pore diameter: 80 µm) obtained by modified gelcasting.

maximum inscribed diameter (µm)	equivalent diameter (µm)	porosity represented by pore system (%)
156	306	23
178	359	70

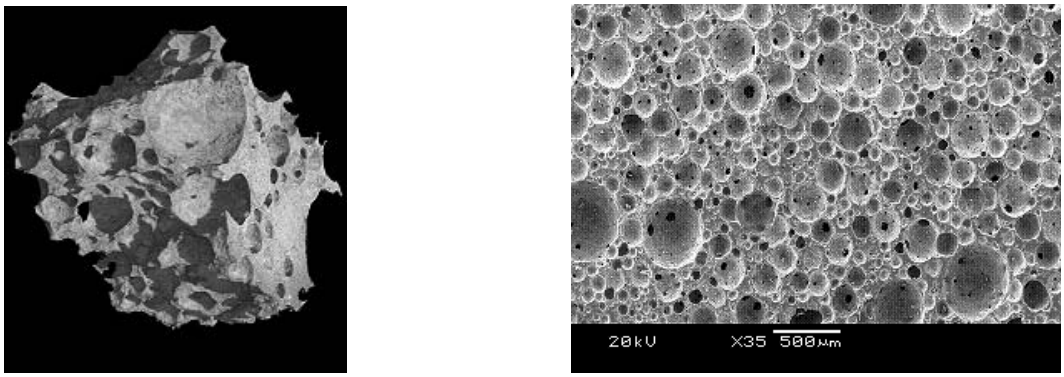

Figure 2.7.: 3-dimensional images of the internal structure and SEM micrograph of the porous surface of a tablet (median pore diameter: 80 µm) manufactured by a modified gelcasting technique.

Also for the porous tablets obtained by modified gelcasting, a high mechanical strength (6.8 ± 0.2, 5.2 ± 0.1 and 4.2 ± 0.3 MPa) in combination with a low friability (1.1 %, 1.0 % and 1.2% for tablets with a median pore diameter of 20, 80, and 100 µm, respectively) was obtained.

2.4.2. Porous tablets as drug carriers

- Drug loading

For the tablets obtained by direct compression followed by sintering, the formulations with the highest concentration of each pore forming agent (50% Avicel PH 200, 50% corn starch, 37.5% sorbitol) were selected as drug carriers as these tablets sintered at 1250°C combined a high porosity with a low friability.

For the tablets obtained by modified gelcasting followed by sintering each formulation (median pore diameter: 20, 80 or 100 µm) was evaluated as drug carrier.

Carriers formulated with Avicel PH 200 and corn starch were able to completely absorb a volume of 100 µl spiked on the surface of the tablet as the interconnected pore network allowed the drug solution to penetrate and distribute in the tablet. In contrast, the carrier formulated with sorbitol failed to completely absorb 100 µl drug solution. The results of the nano CT-scan showed that not all the pores were part of the pore network what decreased their ability to absorb the drug solution. The fastest absorption was observed for the carrier formulated with Avicel PH 200 as these tablets had the largest pores.

After spiking 100 µl of drug solution on the surface of the porous tablets obtained via gelcasting and sintering, the solution was immediately and completely absorbed by all type of tablets, no difference between the tablets was observed. The interconnected pore network in combination with large and spherical shaped pores allowed the drug solution to penetrate and distribute fast and easily in the tablets.

For all formulations, manufactured by direct compression and sintering, spiking the tablets with 150 µl drug solution to increase the drug load was unsuccessful since the porous matrix became saturated and liquid leaked through the tablet. This effectively limits the application of these carriers to the formulation of low-dosed dosage forms. Although it was possible to increase the drug load by spiking both sides of the tablet (with an intermediate drying step), the drug load in this application was limited to 30 mg metoprolol tartrate. Repetitive drug loading (up to 11 times, with intermediate drying steps) of tablets obtained by modified gelcasting and sintering was performed, hence higher drug loads were obtained (up to 165 mg metoprolol tartrate/tablet), but such a time-consuming procedure would obviously have limited application.

The content uniformity test was only performed on tablets manufactured via direct compression and sintering, using 50% (w/w) Avicel PH 200 as pore former. The result showed an average drug concentration of 100.7% (RSD 2.7%) of the theoretical concentration for metoprolol tartrate loaded tablets.

In addition to the volume spiked on the porous carriers the drug load will also be determined by the concentration of the drug solution. Therefore, porous tablets formulated with 50% (w/w) Avicel PH 200 and processed via direct compression and sintering were spiked with differently concentrated metoprolol tartrate solutions (1.5, 4, 15 and 40%). When tablets were spiked with 100 µl of a 1.5% and 4% solution (applied on each side of the tablet), immediate and complete absorption was observed, whereas for the 15% and 40% solution the drug uptake was complete but slower.

Table 2.5.: Surface tension values (n=10) of metoprolol tartrate solutions with different concentration.

(%, w/w)	Surface tension (mN/m)
1.5	59.21 ± 0.45
4	60.45 ± 0.58
15	45.58 ± 0.16
40	44.55 ± 0.12

The surface energy of all MPT solutions was lower compared to pure water (71.36 ± 0.14 mN/m), the highest drug concentration having the lowest surface tension indicating that the drug molecules have some tensio-active properties. Based on this observation an improved liquid penetration into the tablets would be expected at higher drug concentration. However, besides the surface tension (air-liquid) the uptake of the solution is also determined by the phase tension between the solid phase (tablet surface) and the liquid phase (drug solution). Due to the hydrophilic tablet surface (hydroxyl groups in hydroxyapatite) there will be competition between the tablet surface and the aqueous phase (water) to interact with the hydrophilic part of the drug molecules; a factor which increases the phase tension between liquid and solid phase. Since this competition will increase at higher drug concentrations in the solution, the increasing phase tension in function of drug concentration accounts for the slower absorption of these drug solutions (Barnes and Gentle, 2005).

Based on the yellow colour of riboflavin sodium phosphate it was visually observed that the drug was homogeneously distributed throughout the entire tablet.

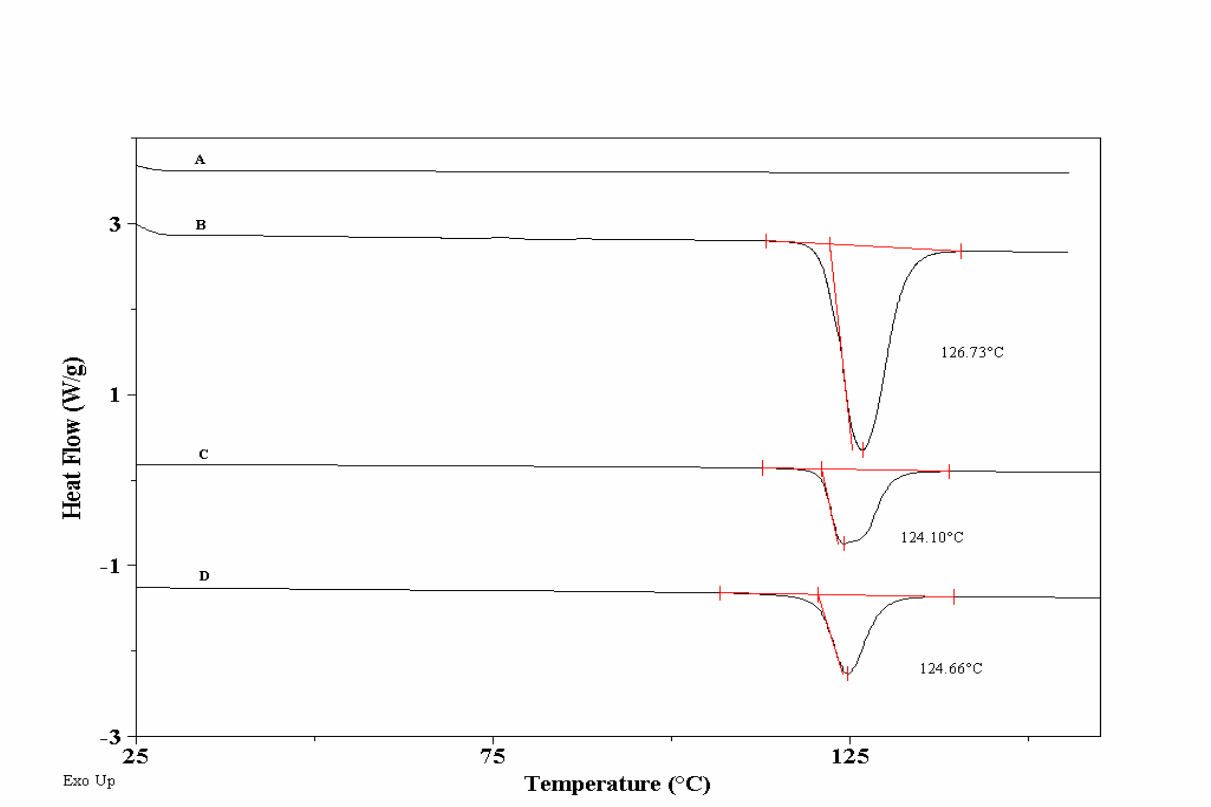

Figure 2.8.: DSC thermograms of a crushed unloaded porous tablet (A), metoprolol tartrate (B), a physical mixture of crushed porous tablet containing metoprolol tartrate (C) and of a crushed porous tablet containing metoprolol tartrate.

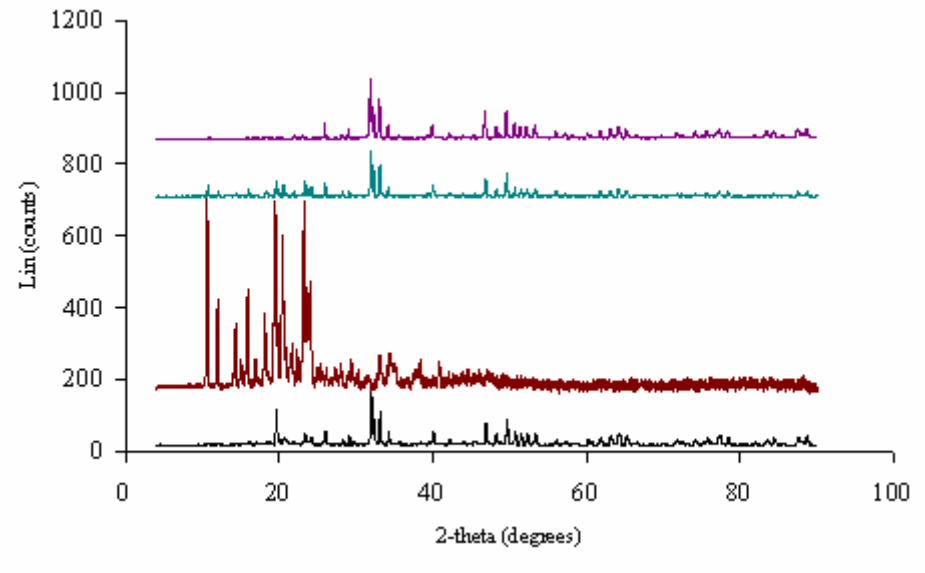

Figure 2.9.: X-ray diffraction patterns of a porous tablet loaded with metoprolol tartrate (——), metoprolol tartrate (——), a physical mixture of a crushed porous tablet containing metoprolol tartrate (——) and without metoprolol tartrate (——).

DSC thermograms (Fig. 2.8.) showed that the crystalline structure of metoprolol tartrate did not change after incorporation in the tablet. The melting peak of metoprolol tartrate in the loaded tablet (around 124°C) was identical to the melting peak of metoprolol tartrate in the physical mixture. These data were confirmed via X-ray diffraction (Fig. 2.9.).

➢ *In-vitro* drug release

Due to the fast and complete absorption of the aqueous drug solution in porous tablets formulated with 50% (w/w) Avicel PH 200 as pore forming agent and in tablets obtained by modified gelcating, these tablets were evaluated as drug carriers during dissolution experiments.

Fig. 2.10. shows the dissolution profiles of metoprolol tartrate in water, phosphate buffer pH 6.8 and 0.1N HCl.

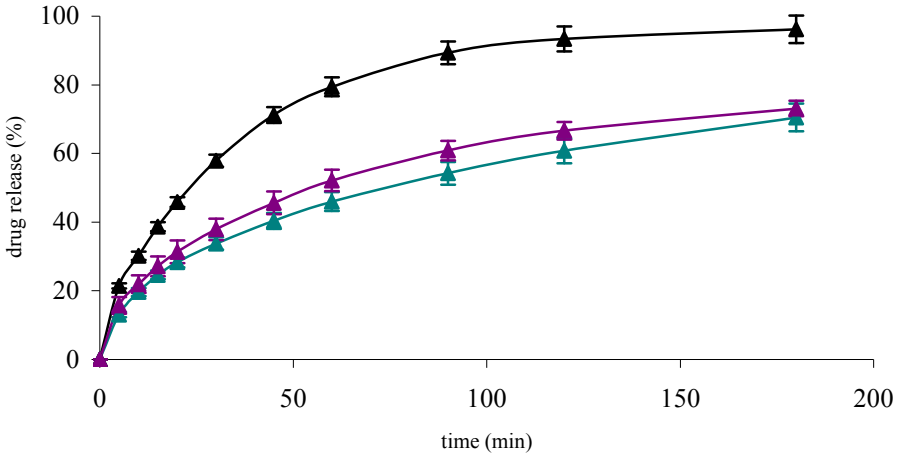

Figure 2.10.: Drug release from sintered (1250°C, 3h, using 50% (w/w) Avicel PH 200 as pore forming agent) porous tablets containing 30 mg metoprolol tartrate in 0.1N HCl (▲), water (▲) and phosphate buffer pH 6.8 (▲)

Based on the highly porous nature of these tablets an immediate drug release was anticipated. However, the burst release from these tablets was very limited in all media. Metoprolol tartrate release in 0.1N HCl was the fastest (79% within 60 min) as the HA tablets partly

dissolved in acid medium. In contrast, HA tablets remained intact in water and phosphate buffer pH 6.8, reducing drug release after 60 min to 46% and 52%, respectively.

The slower drug release from the tablets was strictly related to the porous structure of the matrices (the release rate depending on pore size, shape and connectivity) since drug dissolution of crushed samples was immediate (showing that there was no interaction between HA and drug).

The drug release from porous tablets obtained by modified gelcasting followed by sintering is shown in Fig. 2.11. The drug release was faster from tablets having a larger pore size, whereas an immediate drug release was obtained from porous tablets with a median pore diameter of 100 µm.

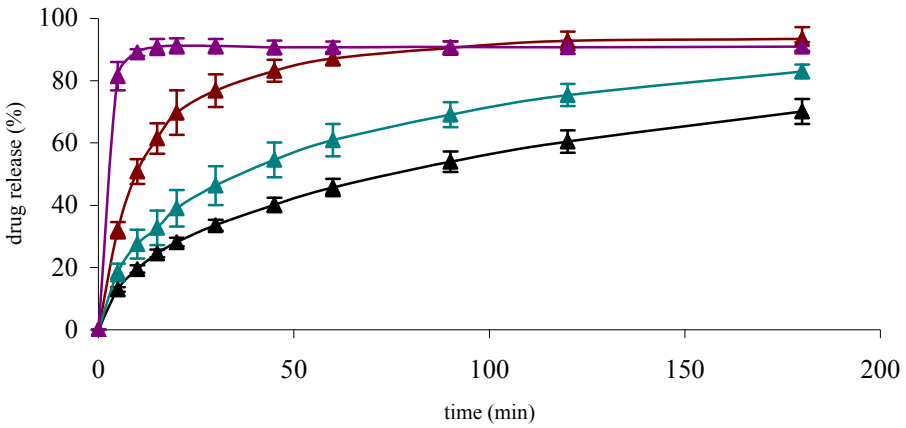

Figure 2.11.: Drug release in demineralised water from porous tablets obtained by direct compression (median pore size of 5µm (▲)) and by a modified gelcasting technique (median pore size of 20 (▲), 80 (▲) and 100 µm (▲)), containing 30 mg metorpolol tartrate.

The enhanced release rate from these gelcasted tablets was due to the larger pore size (which promoted water penetration and drug diffusion) and to the regular shape of the pore channels (which decreased the tortuosity of the matrix). The fact that the drug release was strongly influenced by these parameters was explained via drug modelling.

Fitting an appropriate analytical solution of Fick's second law of diffusion (considering axial as well as radial mass transport in cylinders, Equation 3) to the experimentally measured metoprolol tartrate release profiles obtained in water from tablets processed via direct compression (using 50% (w/w) Avicel PH 200 as pore forming agent, median pore diameter: 5 µm) and modified gelcasting (median pore diameter: 20 and 80 µm) resulted in good agreement between theory and experiment (Fig. 2.12.).

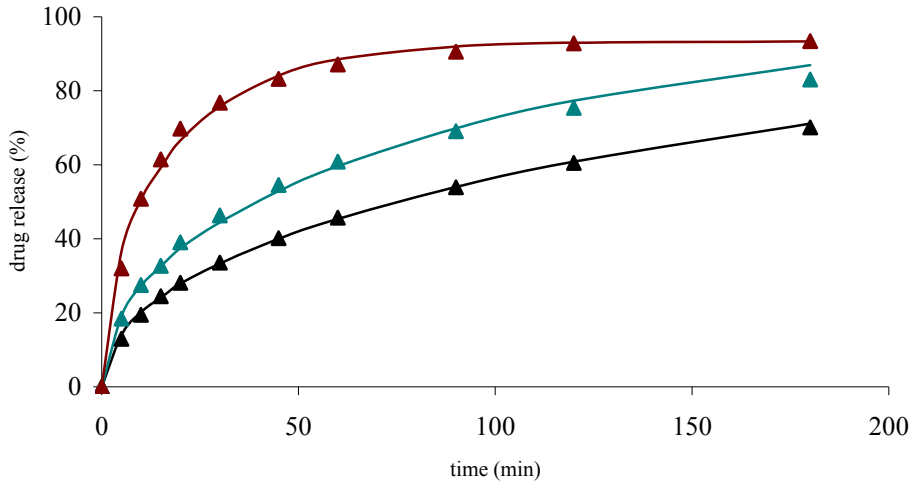

Figure 2.12.: Drug release in demineralised water from sintered porous tablets containing 30mg metoprolol tartrate. Tablets processed via direct compression and formulated with 50% Avicel PH as pore forming agent (▲). Tablets processed via gelcasting and having a pore size of 20 (▲) and 80 µm (▲). Predicted (curves, Equation 2) and experimental (symbols) dissolution profiles.

The apparent diffusion coefficients of metoprolol tartrate within the porous tablets increased with increasing pore size : 6.2×10^{-7}, 1.2×10^{-6} and 5.5×10^{-6} cm²/s for porous tablets with a median pore size of 5, 20 and 80 µm, respectively.

Fig. 2.13. shows the effect of the initial drug content (3, 8, 30 and 80 mg) on the release of metoprolol tartrate from porous tablets prepared with 50% (w/w) Avicel PH 200. Clearly, the release rate decreased with increasing drug loading.

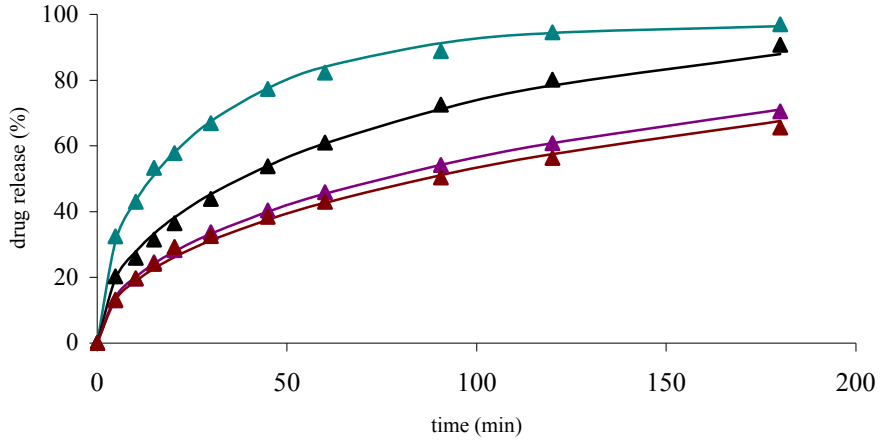

Figure 2.13.: Effects of initial drug content (3 mg (▲), 8 mg (▲), 30 mg (▲) and 80 mg (▲)) on release of metoprolol tartrate from sintered porous tablets (1250°C, 3h, pore forming agent: Avicel PH 200, 50% (w/w)) in water: Predicted (curves, Equation 2) and experimental (symbols) dissolution profiles.

Interestingly, the presented analytical solution of Fick's second law of diffusion (Equation 3) can be used to quantitatively describe the experimentally measured drug release kinetics in all case (curves and symbols in Fig. 2.13.). Based on these calculations, the following apparent diffusion coefficients of metoprolol tartrate in the porous tablets exposed to water could be determined: 3.5×10^{-6}, 1.2×10^{-6}, 5.4×10^{-7} and 6.2×10^{-7} cm²/s for tablets containing, 3, 8, 30 and 80 mg, respectively. The decrease in drug mobility with increasing drug content might be due to a concentration-dependent metoprolol tartrate diffusion coefficient in water-filled pores of the tablets and/or to limited solubility effects (Ginebra et al., 2006b).

2.4.3. Stability study

(a) 25 °C/60 % RH

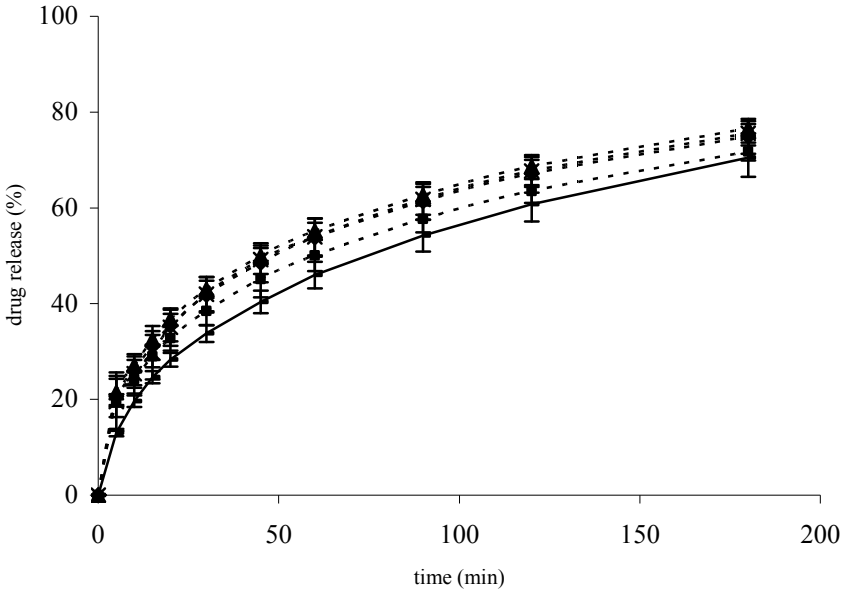

(b) 40 °C/75 % RH

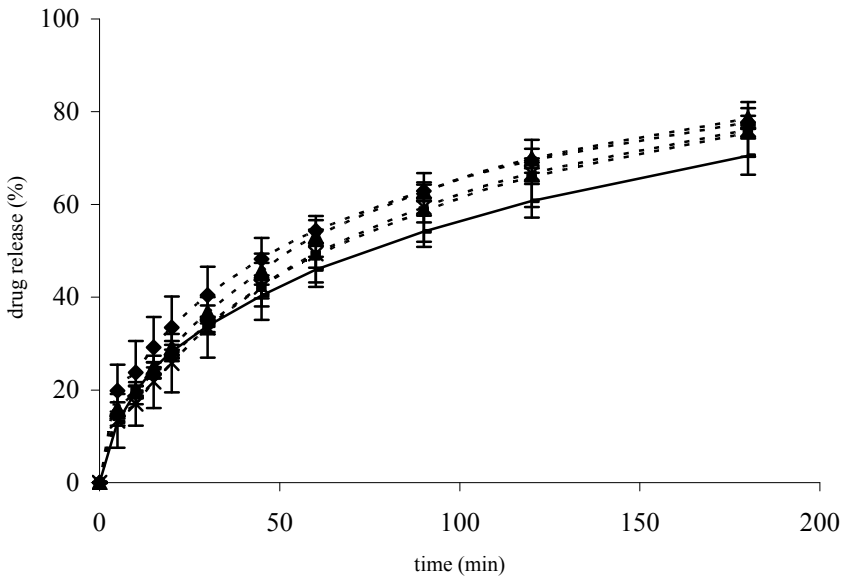

Figure 2.14.: Mean drug release profiles (± S.D.) of porous tablets obtained by direct compression followed by sintering, containing 30 mg metoprolol tartrate, stored during 0 (-), 3 (■), 6 (▲), 9 (x) and 12 (♦) months at (a) 25 °C/60 ± 5 % RH and at (b) 40 °C/ 75 ± 5 % RH

Figure 2.14. shows that the porous tablets were stable for at least 12 months during storage at 25 °C/60 % RH and at 40 °C/75 % RH. Statistical comparison of the $AUC_{0\text{-}3h}$-values indicated no significant difference between the dissolution curves obtained before and after storage at the different conditions.

The water uptake during storage (Table 2.5.) was limited.

Table 2.5: Water content (n=3) of porous tablets stored under controlled conditions. A: 25 °C/ 60% RH and B: 40 °C/ 75% RH

Time (months)	Moisture content (%)	
	A	B
0	0.25 ± 0.01	0.25 ± 0.01
3	0.43 ± 0.18	0.55 ± 0.11
6	0.72 ± 0.15	1.05 ± 0.13
9	1.13 ± 0.05	1.31 ± 0.12
12	1.16 ± 0.12	1.81 ± 0.23

2.5. CONCLUSION

Direct compression or modified gelcasting in combination with sintering allowed to manufacture porous tablets, which can be used as an alternative carrier for low-dosed drugs.

The drug was incorporated into the pore network via spiking of the drug solution on the tablet, whereby the drug uptake depended on the pore volume, the presence of interconnecting pores and the drug concentration. As the drug dose per tablet only depended on the volume spiked on each tablet and small volumes of liquid can be dosed with high accuracy, the risk of drug inhomogeneity is minimal. Hence these tablets are an innovative carrier for low dosed drugs. Furthermore, as the drug is incorporated in the porous tablets after compression, this manufacturing technique is also very promising for processing drugs with poor tabletting characteristics.

The drug release from the porous carrier was primarily diffusion controlled, the apparent drug diffusivity depended on the pore size and tortuosity of the porous network.

Furthermore, drug release from these porous tablets was stable for at least 12 months.

2.6. REFERENCES

Barnes, G.T. and Gentle, I.R. (2005). Interfacal Scinece. New york, Oxford Univeristy Press Inc.

Bernache-Assollant, D., Ababou, A., Champion, E. and Heughebaert, M. (2003). Sintering of calcium phosphate hydroxyapatite Ca-10(PO4)(6)(OH)(2) – I. Calcination and particle growth. J. Eur. Ceram. Soc., 23, 229-241.

Cnudde, V., Cnudde, J.P., Dupuis, C. and Jacobs, P.J.S. (2004). X-ray micro-CT used for the localization of water repellents and consolidants inside natural building stones. Materials Characterization, 53, 259-271.

European Pharmacopoeia, Sixth Edition. (2000). The European Department for the Quality of Medicine, Strasbourg, France.

Fell, J. and Newton, J. (1970). Determination of tablet strength by diametral-compression test. J. Pharm. Sci., 59, 688-691.

Ginebra, M.P., Traykova, T. and Planell, J.A. (2006a). Calicium phosphate cements as bone drug delivery systems: A review. J. Control. Release, 113, 102-110.

Ginebra, M.P., Traykova, T. and Planell, J.A. (2006b). Calcium phosphate cements: Competitive drug carriers for the musculoskeletal system? Biomaterials, 27, 2171-2177.

Ishikawa, T. (2000). Metal phosphates and apatites. In: Fine particles. Synthesis, characterization and mechanisms of growth. Sugimoto, T. (Ed.). Marcel Dekker Inc, New York, USA, 350-383.

Jarcho, M. (1986). Biomaterial aspects of calcium phosphates – Properties an applications. Dent. Clin. North Am., 30, 25-47.

Luyten, J. Mullens, S. Cooymans, J. and De Wilde, A.M. (2003). New processing techniques of ceramic foams. Adv. Eng. Mat., 5, 715-718.

Millan, A.J., Nieto, M.I. and Moreno, R. (2001). Aqueous gel-forming of silicon nitride using carrageenans. J. Am. Ceram. Soc., 84, 62-64.

Mouazer, R., Thijs, I., Mullens, S. and Luyten, J. (2004). SiC foams produced by gel casting: Synthesis and characterization. Adv. Eng. Mat., 6, 340-343.

Muralithran, G. and Ramesh, S. (2000). The effects of sintering temperature on the properties of hydroxyapatite. Ceram. Int., 26, 221-230.

Omatete, O.O., Janney, M.A. and Strehlow, R.A. (1991). Gelcasting - A new ceramic forming process. Am. Ceram. Soc. Bul., 70, 1641-1649.

Osaka, A., Miura, Y., Takeuchi, K., Asada, M. and Takahashi, K. (1991). Calcium apatite prepared from calcium hydroxide and orthophosphoric acid. J. Mat. Sci.: materials in medicine, 2, 51-55.

Raynaud, S., Champion, E and Bernache-Assolant, D. (2002). Calcium phosphate apatites with variable Ca/P ratio. II. Calcination and sintering. Biomaterials, 23, 1073-1080.

Raynaud, S., Champion, E., Bernache-Assolant, D. and Thomas, P. (2002). Calcium phosphate apatites with variable Ca/P ratio. I. Synthesis, characterization and thermal stability of powders. Biomaterials, 23, 1073-1080.

Rowe, R., Shesky, P.J. and Weller, P.J. (Ed.) (2003). Handbook of Pharmaceutical Excipients (Fourth Edition). Washington DC, American Pharmaceutical Association and Pharmaceutical Press.

Sepulveda, P and Binner, J.G.P. (1999). Processing cellular ceramics by foaming and in situ polymerization of organic monomers. J. Eur. Ceram. Soc., 19, 2059-2066.

US. Pharmacopeia XXVII & National Formulary 22. (2004). The United States Pharmacopeial Convention, Rockville, MD, USA.

Vallet-Regi, M. and Gonzalez-Calebt, J.M. (2004). Calcium phosphates as substitution of bone tissues. Prog. Sol. St. Chem., 32, 1-31.

Vergnaud, J.M. (1993). Controlled drug release of oral dosage froms. Chichester, Ellis Horwood Limited.

3

In vitro and *in vivo* evaluation of porous tablets

3.1. INTRODUCTION

Chapter 2 demonstrated the development of porous tablets consisting of hydroxyapatite. These tablets are promising drug carriers for low-dosed drugs as they ensure a good content uniformity and furthermore as the drug is spiked onto the tablet surface, drug with poor compaction properties can easily be incorporated in tablet-shaped carriers.

The drug release from the porous tablets in aqueous medium was purely diffusion-controlled, whereby the apparent drug diffusivity depended on the pore size and the tortuosity of the porous network.

As the specific conditions along the gastrointestinal (GI) tract (pH conditions, GI transit time, hydrodynamic flow, mechanical destructive forces) can affect the drug release, an *in vivo* study in dogs was performed to determine the bioavailability of metoprolol tartrate after oral administration of tablets having a different internal pore structure. In addition, the influence of hydrodynamic flow and stress and the effect of physiological relevant dissolution media on the *in vitro* drug release of the porous tablets were evaluated in order to explain the obtained *in vivo* results.

3.2. MATERIALS

For tablets manufactured via direct compression and sintering, hydroxyapatite was obtained from Acros Organics (Geel, Belgium), Avicel PH 200 from FMC Biopolymer (Cork, Ireland) and magnesium stearate from Alpha Pharma (Zwevegem, Belgium).

For tablets manufactured via modified gelcasting and sintering, hydroxyapatite was supplied by Bekaert (Zwevegem, Belgium), Tergitol TMN 10 by Sigma Aldrich (Bornem, Belgium), Targon 1128 by BK Giulini (Ladenburg, Germany), Benecel by Hercules (Beringen-Paal, Belgium) and agar by Fagron (Waregem, Belgium).

Metoprolol tartrate (10 μm) was supplied by Esteve Quimica (Barcelona, Spain).

Pancreatin, bile salts and sodium taurocholate were purchased from Sigma-Aldrich (St-Louis, USA). Egg-phosphatidylcholine (Lipoid E PC) was a gift from Lipoid (Ludwigshafen, Germany). Potassium dihydrogen phosphate, potassium chloride, sodium hydroxide and sodium chloride were obtained from Merck (Darmstadt, Germany).

Hydrochloric acid (37%) was supplied by VWR (Leuven, Belgium). Sodium lauryl sulphate (SLS) was received from Fagron (Uitgeest, The Netherlands).

Lopresor® was obtained from Novartis (Brussels, Belgium). Each tablet contained 100 mg metoprolol tartrate.

3.2.1. Metoprolol tartrate

Metoprolol tartrate (aqueous solubility: > 1 mg/ml) is a Class 1 drug according to the Biopharmaceutics Classification System and is a β1-selective adrenoreceptor antagonist used in the treatment of hypertension and coronary diseases such as angina pectoris. When metoprolol is administered orally it is almost completely absorbed form the gastro-intestinal tract. The absorption from the stomach is minimal, hence metoprolol is primarily absorbed

throughout the small intestine and colon (Godbillon et al., 1985; Jobin et al., 1985; Vidon et al., 1985).

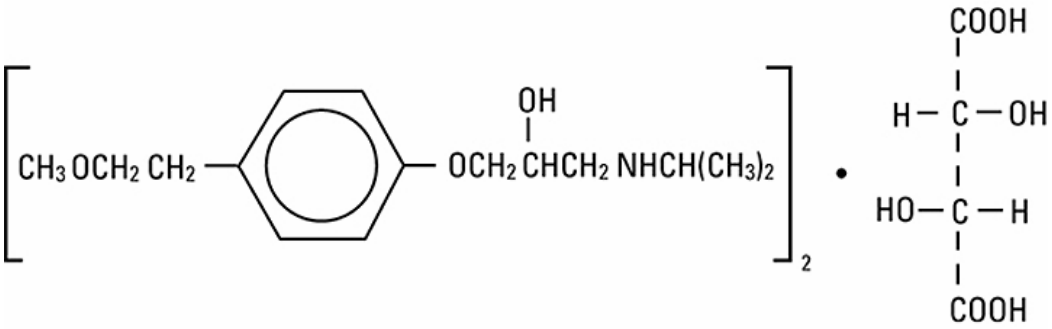

Figure 3.1.: Structure of metoprolol tartrate

3.3. METHODS

3.3.1. Production of the porous tablets

Porous tablets, manufactured via direct compression and sintering, were formulated with Avicel PH 200 as pore forming agent (50%, w/w). The tablets were prepared according to the method described in Chapter 2 (section 2.3.1.).

Porous tablets with a median pore diameter of 100 µm were obtained by modified gelcasting followed by sintering as described in Chapter 2 (section 2.3.1.).

Tablets were spiked (as described in Chapter 2, section 2.3.3.) with 2 x 100 µl of a 15 or 20% (w/v) metoprolol tartrate solution, resulting in a drug content per tablet of 30 and 40 mg, respectively.

3.3.2. *In vivo* study

All procedures were performed in accordance with the guidelines of and after approval by the Ethics Committee of the Institute for Agricultural and Fisheries Research (ILVO) (Merelbeke, Belgium). Male mixed-breed dogs (n=6) (weight 20.5-40.5 kg) were used in this study. A 100 mg MPT dose was administered using the following formulations:

- F-1: 3 porous tablets (median pore diameter: 5 μm) manufactured via direct compression and sintering (equivalent to 100 mg metoprolol tartrate: 2 tablets containing 30 mg metoprolol tartrate per tablet and 1 tablet containing 40 mg metoprolol tartrate per tablet).
- F-2: 3 porous tablets (median pore diameter: 100 μm) manufactured via modified gel casting and sintering (equivalent to 100 mg metoprolol tartrate: 2 tablets containing 30 mg metoprolol tartrate per tablet and 1 tablet containing 40 mg metoprolol tartrate per tablet).
- F-3: Lopresor®, a commercially available immediate release formulation, one tablet containing 100 mg metoprolol tartrate .

The formulations were administered in a cross-over sequence with a wash out of at least 5 days. On the experimental days the dogs were fasted since the previous day at 7 pm, although water was available ad libitum. Before administration of the formulations, an intravenous cannula was placed in the lateral saphenous vein and a blank blood sample was obtained. Each formulation was orally administered with 20 ml water. Blood samples were obtained at 0.5, 1, 1.5, 2, 3, 4, 5, 6, 8, 12 and 24h. The blood samples were collected in dry heparinized tubes and centrifuged for 5 min at 1500*g* within 1 h of sampling. The plasma was stored at -20°C until assay of metoprolol tartrate. No food was administered to the dogs during blood sampling. Water could be taken freely.

3.3.3. Metoprolol tartrate assay

The metoprolol tartarte plasma concentrations were determined by a validated HPLC-fluorescence method (Fang et al., 2004). All chemicals were of analytical or HPLC grade.

Twenty microlitres of an internal standard solution (3.33 µg/ml alprenolol in distilled water), 680 µl phosphate buffered saline (PBS) and 300 µl plasma were transferred into a borosilicate glass tube and mixed. The drug was extracted using a solid phase extraction (SPE) method. The SPE columns were conditioned consecutively with methanol (1 ml), water (1 ml) and phosphate buffer saline (1 ml). Next, the plasma samples were transferred to the SPE columns. The columns were rinsed with water (1 ml) and metoprolol tartrate was eluted with methanol (1 ml). The eluates were evaporated to dryness under a nitrogen flow, the residue was reconstituted in 150 µl water and injected onto the column. The metoprolol tartrate concentrations were determined via a calibration curve. For the standard curve, spiked samples were prepared by mixing 280 µl plasma with 20 µl of a standard solution containing a known concentration of metoprolol tartrate in distilled water. Afterwards 20 µl internal standard solution and 680 µl PBS were added to the spiked plasma samples. These mixtures were extracted as described above.

The HPLC equipment (Merck, Darmstadt, Germany) consisted of a solvent pump (L-7110 pump) set at a constant flow rate of 0.8 ml/min, a variable wavelength fluorescence detector (L-7480) set at 275 nm as excitation wavelength and 300 nm as emission wavelength, a LiChrospher® 100 CN 5 µm column (250 mm x 4 mm) and precolumn (4 mm x 4 mm) an autosampler (Gilson 234 autoinjector, Middleton, Wisconsin, USA) with a 50 µl loop (Valco Instruments, Houston, Texas, USA) and an automatic integration system (L-7000). The SPE equipment consisted of OASIS HLB (1 ml, 30mg) cartridges (Waters, Zellik, Belgium) and a 16-port vacuum manifold (Alltech Europe, Laarne, Belgium). The mobile phase consisted of an acetonitrile/sodium dihydrogen orthophosphate buffer (2M)/water-mixture (5/0.5/94.5 v/v), adjusted to pH 3.0 with phosphoric acid. The injection volume was 20 µl.

3.3.4. Validation of the HPLC method

The HPLC analysis method was validated based on the guidelines of the International Conference on Harmonisation (ICH) for validation of analytical procedures: Text and Methodology (2005). The following characteristics were considered: specificity, linearity, accuracy, precision, recovery, detection and quantification limit.

Specificity

Specificity is the ability to assess unequivocally the analyte in the presence of interfering components (Chan, 2004). It was assessed by comparing the chromatogram of blank plasma, a chromatogram obtained after extraction of blank plasma spiked with metoprolol tartrate and alprenolol (internal standard) and a chromatogram analyzed after administration of an metoprolol tartrate tablet (Fig. 3.1). Since no interfering peaks were observed, it is clear that the method is selective to determine metoprolol tartrate in plasma.

a

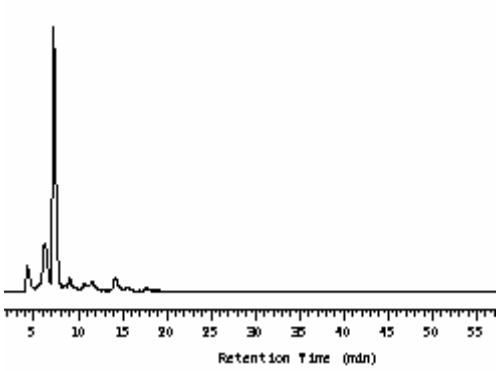

b

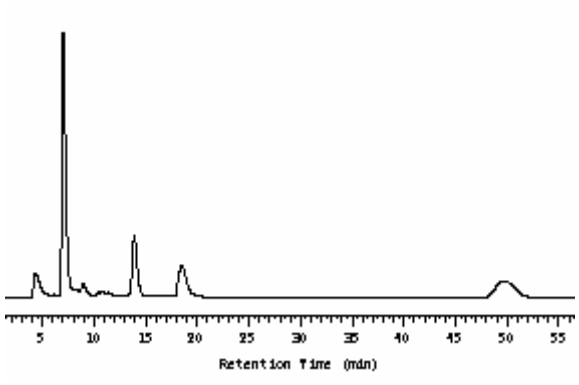

c

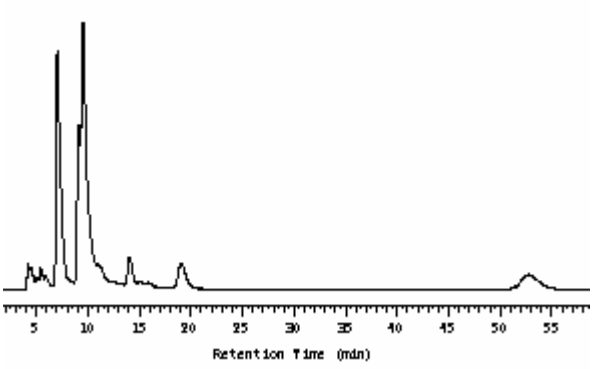

Figure 3.1.: Specificity of the HPLC method. Chromatogram after extraction of (**a**) blank plasma, (**b**) blank plasma spiked with metoprolol tartrate (retention time: 18.45 min) and alprenolol hydrochloride (retention time: 50.10 min), (**c**) dog plasma after intake of a metoprolol tartrate tablet (Lopresor®).

Accuracy

The accuracy of an analytical procedure expresses the closeness of agreement between the true value and the determined value (Chan, 2004) and is expressed as the percent agreement between the mean determined value and the true concentration.

The accuracy was evaluated at three concentration levels on plasma spiked with known amounts of analyte. The accuracy was determined within the same day as well as between different days. The mean accuracies (± S.D.) are listed in Table 3.1.

Table 3.1.: Mean accuracies (± S.D.) of the HPLC method (n=6).

Concentration (ng/ml)	**Accuracy (%)**	
	Within-day	Between-day
37.5	108.1 ± 9.6	110.0 ± 9.2
150	89.8 ± 9.1	91.8 ± 10.3
1500	112.2 ± 6.2	99.4 ± 11.1

Since all mean values were within ± 15% of the actual concentration, this analytical method meets the acceptance criteria for accuracy (Shah et al., 1992).

Precision

The precision expresses the closeness of agreement between repeated determinations and can be determined at three levels: repeatability (intra-assay precision, which is the precision under the same operating conditions over a short time interval), intermediate precision (within laboratory precision, which expresses within-laboratory variations like different days, analysts, equipment, etc.) and reproducibility (between laboratory precision, which is the precision between laboratories). Since the measurements were performed in the same laboratory, by the same person using the same equipment only the repeatability (within-day and between-day) of the measurements was evaluated.

Precision is expressed as the coefficient of variation (%) of a series of measurements of the calibration standards (Lee, 2004) (Table 3.2.). As recommended by Shah et al. (1992), the acceptance criteria are coefficients of variation (CV) less than 15%, except for the lowest concentration, where it should not exceed 20% CV.

Table 3.2.: Precision (expressed as coefficient of variation) of the HPLC method (n=6)

Concentration (ng/ml)	**Precision (%CV)**	
	Within-day	Between-day
37.5	13.3	10.8
75	-	3.5
150	8.5	9.8
300	-	6.7
750	-	5.1
1500	8.5	11.1

Recovery

The amount of analyte in biological samples can be reduced during sample treatment like extraction with organic solvents, etc. The recovery was determined for the calibration standards (at three concentration levels) and the internal standard, and was expressed as the closeness of agreement (in %) between the surface areas of an extracted sample versus a non-extracted sample. The mean recoveries (± S.D.) for the calibration standards and the internal standard are listed in Table 3.3.

Table 3.3.: Mean recoveries (n=6) (± S.D.) for the calibration standards and the internal standard.

	Concentration (ng/ml)	**Recovery (%)**
metoprolol tartrate	37.5	61.8 ± 16.1
	150	65.0 ± 7.1
	1500	81.2 ± 9.2
alprenolol	444	63.3 ± 12.1

Linearity

The linearity of an analytical procedure is its ability - within a given range - to obtain test results which are directly proportional to the analyte concentration in the sample (Chan, 2004).

During validation of the HPLC method and analysis of the samples, several calibration curves were analysed. The linearity of the calibration curves was evaluated by the determination coefficient R^2, its value (n = 7) was 0.9994, indicating that the relationship between response (y) and concentration (x) was linear within the tested concentration range (37.5–1500 ng/ml). The equation of the mean calibration curve was:

$$y = 4.2598x + 0.1128$$

Detection and quantification limit

The detection limit of an analytical procedure is the lowest amount of analyte in a sample which can be detected but not necessarily quantified as an exact value. The quantification limit is the lowest amount of analyte in a sample which can be adequately determined with suitable precision and accuracy. Both values were estimated from the mean calibration curve (International Conference on Harmonisation, 2005):

$DL = 3.3 \times \sigma / S$

$QL = 10 \times \sigma / S$

with DL = detection limit

QL = quantification limit

σ = standard deviation of the Y-intercept of the mean calibration curve

S = slope of the mean calibration curve

The detection and quantification limits of metoprolol tartrate in dog plasma were determined at 40 and 140 ng/ml, respectively.

Since the calculated limit of quantification was higher than the lowest concentration of the calibration curve and the accuracy and precision at the lowest metoprolol tartrate

concentration (37.5 ng/ml) were within the accepted limits (Shah et al., 1992), a concentration of 37.5 ng/ml was considered as limit of quantification.

3.3.5. Data and statistical analysis

The extent of drug absorption ($AUC_{0\text{-}24h}$), the peak plasma concentration (C_{max}) and the time to reach C_{max} (t_{max}) was calculated using the MW-PHARM program version 3.0 (Mediware 1987-1991, Utrecht, The Netherlands). The $AUC_{0\text{-}24h}$ was calculated using logarithm and linear trapezoidal rules. The relative bioavailabilty of the porous tablet formulations (F_{rel}, %) was calculated as the ratio of $AUC_{0\text{-}24h}$ between a porous tablet formulation and Lopresor®. The effect of metoprolol tartrate formulation on the bioavailibility was assessed by repeated-measurements ANOVA (univariate analysis). To further compare the effects of the different formulations, a multiple comparison among pairs of means was performed using Bonferroni post-hoc test with $P < 0.05$ as significance level. The sphericity of covariances was tested with Mauchly's test. SPSS 16 software (SPSS, Chicago, USA) was used to perform the statistical analysis.

3.3.6. *In vitro* evaluation

In order to explain the *in vivo* results after administration of the porous tablets, *in vitro* dissolution testing was performed using conditions that simulate the gastro-intestinal conditions. All dissolution tests (n=6) were performed in a VK 7000 dissolution bath with a VK 8010 autosampler (VanKel Industries, NJ, USA). The system operated at 37±0.5°C using the paddle method (USP 27). Sink conditions were maintained. Samples (5ml) were taken at 5, 10, 15, 20, 30, 45, 60, 90, 120 and 180 min. The drug concentration in the samples was measured at 222 nm with an UV/VIS double beam spectrophotometer (Perkin-Elmer, Zaventem, Belgium).

In order to examine the influence of the hydrodynamic flow and stress in the gastro intestinal tract, different paddle speeds (10, 50 and 150 rpm) were used during dissolution testing, using 900 ml demineralized water as dissolution medium. Furthermore a dissolution test was performed using the reciprocating cylinder method (USP III) (Bio-Dis, Vankel, New Jersey, USA) at a dip speed of 21 dips/min using 250 ml demineralised water as dissolution medium (37±0.5°C) (Katori et al., 1995).

To evaluate the influence of the composition of the dissolution medium, tests were performed in 900 ml Simulated Intestinal Fluid USP 27 (SIF), Simulated Gastric fluid USP 27 (SGF), Fasted State Simulated Intestinal fluid (FaSSIF), Fed State Simulated Intestinal Fluid (FeSSIF) (Table 3.4.) (Dressman et al., 1998; Galia et al., 1998) and an aqueous 4% bile salt solution (consisting of a mixture of sodium cholate and sodium deoxycholate) at a paddle speed of 50 rpm.

Table 3.4.: Composition of Fasted State and Fed State Simulated Intestinal Fluid

Fasted State Simulated Intestinal Fluid (FaSSIF)			**Fed State Simulated Intestinal Fluid (FeSSIF)**		
pH		6.5	pH		5.0
Osmolality		270±10 mOsm	Osmolality		635±10 mOsm
Sodium taurocholate		3 mM	Sodium taurocholate		15 mM
Lecithin		0.75 mM	Lecithin		3.75 mM
KH_2PO_4		3.9 g	KH_2PO_4		8.65g
KCl		7.7g	KCl		15.2 g
NaOH	qs	pH 6.5	NaOH	qs	pH 5.0
Demineralized water	qs	1 L	Demineralized water	qs	1 L

As it was impossible to determine the metoprolol tartrate concentration spectrophotometrically in these media, a validated HPLC-fluorescence method (as described

in section 3.3.4.) was used, whereby the samples were injected directly onto the column after filtration using 0.2 μm Whatman filters (Spartan, regenerated cellulose).

To investigate the influence of surface tension of the dissolution medium, a dissolution was performed in 900 ml $FaSSGF_{SLS}$ (consisting of 0.25% sodium lauryl sulphate, 0.05 M HCl and 0.2% sodium chloride) (Anwar et al., 2005) using a paddle speed of 50 rpm. The metoprolol tartrate concentration in the samples was determined using UV-spectrophotometry.

The $AUC_{0\text{-}3h}$-values of the dissolution test were statistically evaluated with a one-way ANOVA at a significance level of 0.05. The normality of the residuals was checked using the Kolmogorov-Smirnov test and the homogeneity of variance using the Levene's test (significance level=0.05). SPSS version 16.0 was used to perform the statistical analysis.

3.4. RESULTS AND DISCUSSION

3.4.1. *In vivo* study

Fig 3.1. shows the *in vitro* drug release profiles of metoprolol tartrate from Lopresor® and porous tablets with a median pore diameter of 5 and 100 μm. Immediate drug release was obtained from the commercially available reference product and from the porous tablet with a median pore diameter of 100 μm, whereas from the porous tablet with a median pore diameter of 5 μm a slow drug release was obtained.

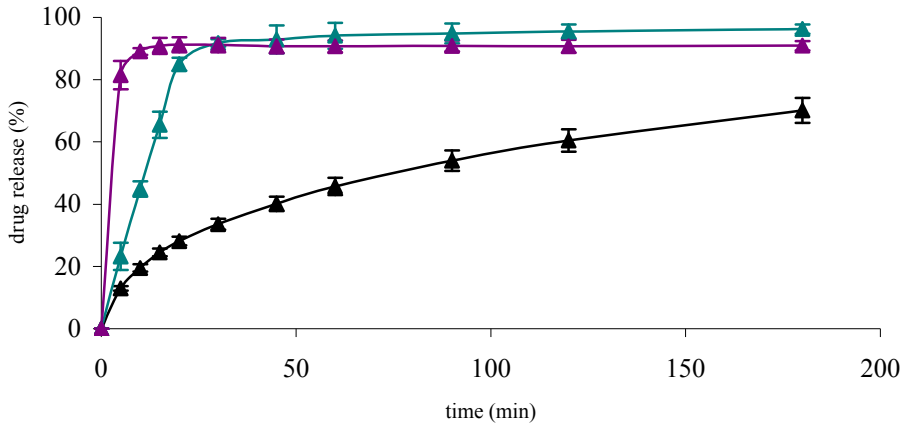

Figure 3.1.: Mean drug release profiles (± S.D.) (n=3) in demineralised water at 50 rpm of metoprolol tartrate from Lopresor® (▲) and porous tablets with a median pore diameter of 5 µm (▲) and 100 µm (▲).

Fig. 3.2. shows the mean plasma concentration-time profiles in dogs after oral administration of 100 mg metoprolol tartrate via porous tablets and Lopresor®-tablets. The pharmacokinetic parameters are given in Table 3.5.

Table 3.5.: Mean pharmacokinetic parameters (± S.D., n=6) in dogs after oral administration of 100 mg metoprolol tartrate as porous tablets with a medium pore diameter of 5 µm (F-1), as porous tablets with a median pore size of 100 µm (F-2) and as Lopresor®-tablets.

	C_{max} (µg/ml)	**t_{max} (h)**	**AUC_{0-24h} (µg.h/ml)**
F-1	9.2 ± 5.7	2.3 ± 0.9	45.6 ± 30.1
F-2	14.4 ± 8.1	1.5 ± 0.4	47.7 ± 26.1
Lopresor®	11.8 ± 5.2	1.3 ± 0.4	38.6 ± 19.7

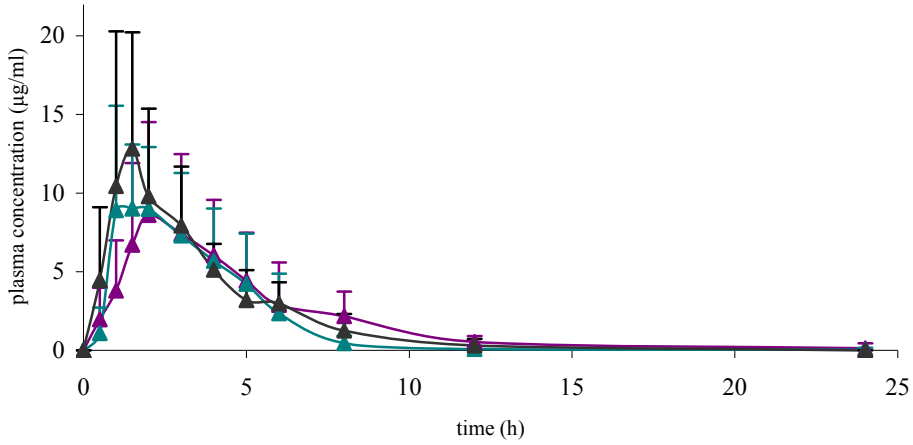

Figure 3.2.: Mean plasma concentration-time profiles ((± S.D., n=6) in dogs after oral administration of 100 mg metoprolol tartrate as porous tablets with a median pore size of 5 µm (▲), as porous tablets with a median pore size of 100 µm (▲) and as Lopresor®- tablets(▲).

The plasma concentration–time profiles of F-1 and F-2 are similar to Lopresor®. The relative bioavailability (F_{rel}) of the porous formulations to Lopresor® was 117.1 ± 35.1% and 120.2 ± 24.4% for the porous tablets with a median pore diameter of 5 µm and of 100 µm, respectively.

Table 3.6.: Results of the statistical analysis of the pharmacokinetic parameters by a multiple comparison among pair of means using Bonferroni post hoc test (P= 0.05).

		Mean difference	95% CI	P value
C_{max} (µg/ml)	F1-F2	2.56	0, 5.096	0.05
	F1-F3	-2.66	-8.87, 3.55	0.57
	F2-F3	-5.22	-10.56, 0.13	0.06
t_{max} (h)	F1-F2	-1.08	-2.33, 0.16	0.08
	F1-F3	-0.17	-1.25, 0.92	1.00
	F2-F3	0.92	-0.48, 2.32	0.21
$AUC_{0\text{-}24h}$(µg.h/ml)	F1-F2	-6.98	-23.90, 9.95	0.62
	F1-F3	-9.06	-21.89, 3.78	0.17
	F2-F3	-2.08	-19.06, 14.91	1.00

No significant mean difference was found for $AUC_{0\text{-}24h}$, C_{max} and t_{max} of these formulations, indicating that similar drug concentrations were available at the absorption site after administration of the porous tablets and an immediate release reference.

The results of the present *in vivo* study showed that the porous formulations have a similar *in vivo drug* release compared with a commercial immediate release formulation (Lopresor®). For the porous tablets with a median pore diameter of 100 μm, this is in agreement with their *in vitro* drug release. However, the *in vitro* drug release from the porous tablets with a median pore diameter of 5 μm was slow and incomplete.

3.4.2. *In vitro* study

In order to explain the discrepancy between *in vitro* and *in vivo* behaviour of the porous tablets with a median pore diameter of 5 μm, dissolution tests were performed using different experimental conditions.

- Influence of hydrodynamic flow and stress

The influence of hydrodynamic stress and flow on the drug release rate of the porous tablets was evaluated via dissolution experiments run at different paddle speeds (10, 50 and 150 rpm) and using the reciprocating cylinder method.

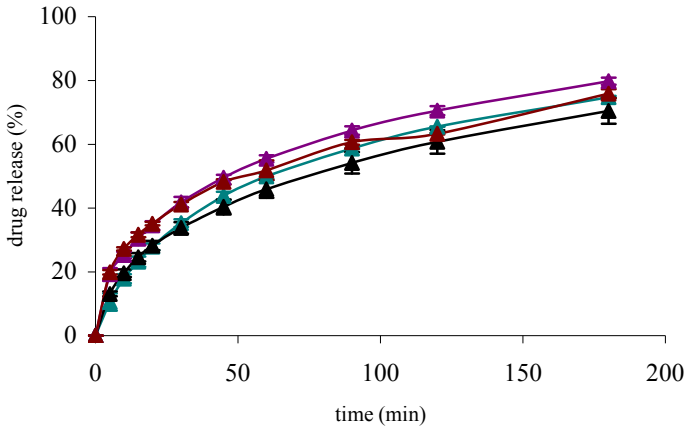

Figure 3.4.: Mean drug release profiles (± S.D.) (n=6) of metoprolol tartrate from the porous tablets using the paddle method at 10 (▲), 50 (▲) and 150 (▲) rpm and using the reciprocating method (▲).

The dissolution profiles (Fig 3.4.) showed that the influence of the hydrodynamic flow of the gastro-intestinal fluids and the hydrodynamic stress in the gastro-intestinal tract was negligible. This indicated that the hydrodynamic flow and stress did not contribute to the immediate *in vivo* drug release, what was confirmed when intact porous tablets were recovered from the dog faeces.

Furthermore, it is known that the influence of hydrodynamic stress on diffusion-controlled drug delivery systems is negligible (Lindner and Lippold, 1995).

➢ Influence of dissolution medium

The effect of six physiologically relevant dissolution media (SGF USP 27, SIF USP 27, FeSSIF, FaSSIF, bile salt solution and $FaSSGF_{SLS}$) on drug release from the porous tablets was investigated. SGF USP 27 and SIF USP 27 contain pepsine and pancreatin, respectively.

Table 3.7.: Influence of physiologically relevant dissolution media on $AUC_{0\text{-}3h}$ (± S.D.) (n=6) of the dissolution profiles of porous tablet with a median pore diameter of 5 µm.

Dissolution medium	$AUC_{0\text{-}3h}$ (± S.D.)
water	151.2 ± 8.5[a]
SGF	218.9 ± 29.5[b]
SIF	163.4 ± 10.0[a]
FaSSIF	175.6 ± 15.4[a]
FeSSIF	222.5 ± 19.9[b]
bile salts	124.4 ± 8.2[a]
$FaSSGF_{SLS}$	225.7 ± 2.6[b]

[a,b]Mean AUC is not significantly different (P>0.05, Scheffé test)

They were selected to investigate the influence of enzymes on drug release. FaSSIF and FeSSIF are dissolution media representing the fasted and fed state in the upper jejunum, containing lecithin and sodium taurocholate to form mixed micelles (Dressman et al., 1998; Galia et al., 1998). An aqueous bile salt solution consisting of a mixture of sodium cholate and sodium deoxycholate was also used. $FaSSGF_{SLS}$ was used as the surface tension of this fluid is similar to the surface tension of stomach fluid during the fasted state (i.e. about 35 mN/m) (Anwar et al., 2005; Aburub et al., 2008).

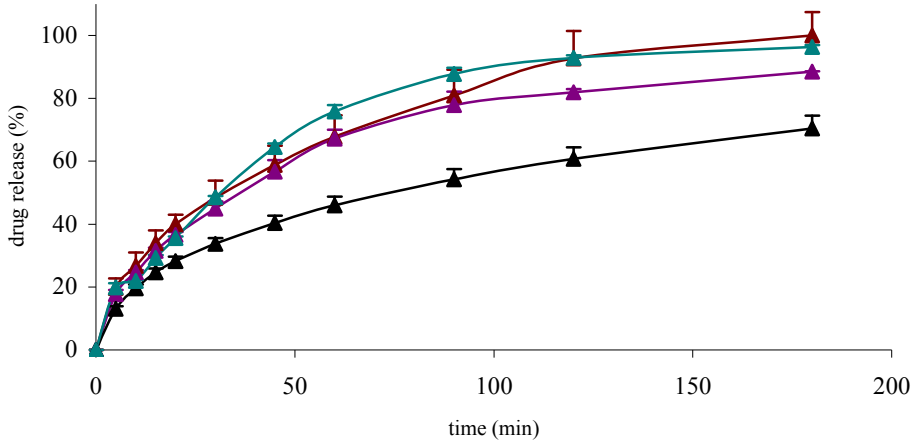

Figure 3.5.: Mean drug release profiles (± S.D.) (n=6) of metoprolol tartrate from a porous tablet (pore diameter 5 µm) in Simulated Gastric Fluid (▲), Fed State Simulated Intestinal Fluid (▲), Fasted State Simulated Gastric Fluid (▲) and demineralised water (▲).

The release from the porous tablet was significantly increased in SGF, FeSSIF and $FaSSGF_{SLS}$ compared to water ($p<0.05$) (Fig 3.5. and Table 3.7.). The other dissolution media had no significant influence on the drug release from the porous tablets (drug release profiles not shown). As the pH of SGF is about 1.2, the tablet was partly dissolved what contributed to a faster *in vitro* drug release. However, the gastric pH in dogs is around 5-7, hence the higher *in vivo* release can not be attributed to a low pH (Lui et al., 1986; Sagara et al., 1992). FeSSIF represents the fed state in the upper jejunum and contains lecithin and sodium taurocholate with tension active properties what can explain the higher *in vitro* drug release in this medium. However, as the dogs were fasted during the *in vivo* experiment the concentration of lecithin and sodium taurocholate in the upper jejunum will have been low, hence this factor will not contribute to the faster *in vivo* drug release.

Table 3.8. shows the surface tension values of some dissolution media used in this study.

Table 3.8.: Surface tension values of dissolution media.

Dissolution medium	Surface tension (mN/m)
water	64.3
SGF	50.8
bile salts	46.5
$FaSSGF_{SLS}$	33.3

The surface tension value of a fasted state stomach (35 mN/m) (Vertzoni et al., 2007) is considerably lower than the surface tension of water and the only dissolution medium having a comparable surface tension as the fasted stomach of a dog is $FaSSGF_{SLS}$.

As the drug release from the porous tablets is pure diffusion-controlled, the initial step of drug release after immersion in the dissolution medium is wetting of the matrix and penetration of the dissolution medium into the porous structure. These processes will be positively influenced by a lower surface tension of the dissolution medium (Luner, 2000), hence a faster drug release from the porous tablets with a median pore diameter of 5 μm was observed in $FaSSGF_{SLS}$. This could explain the faster *in vivo* drug release of these tablets as the low surface tension of the gastric fluid of a fasted dog enhanced drug release.

3.5. CONCLUSION

Although the *in vitro* drug release depended on pore size and pore shape, *in vivo* an immediate drug release was observed from all porous tablets as the bioavailability of these tablets was similar to the *in vivo* behavior of an immediate release formulation.

Dissolution tests simulating the gastro-intestinal conditions showed that the faster drug release was mainly attributed to the low surface tension of the gastric fluid of fasted dog.

3.6. REFERENCES

Aburub, A., Risley, D.S. and Mishra, D. (2008). A critical evaluation of fasted state stimulating gastric fluid (FASSGF) that contains sodium lauryl sulfate and proposal of a modified recipe. Int. J. Pharm., 347, 16-22.

Anwar, S., Fell, J.T. and Dickinson, P.A. (2005). An investigation of the disintegration of tablets in biorelevant media. Int. J. Pharm., 290, 121-127.

Chan, C.C. (2004). Potency method validation. In: Analytical method and instrument performance verification. Chan, C.C., Lam, H., Lee, Y.C. and Zang, X-M. (Eds.) John and Wiley and Sons Inc., Hoboken, New Yersey, USA, 11-26.

Dressman, J., Amidon, G., Reppas, C. and Shah, V. (1998). Dissolution testing as a prognostic tool for oral drug absorption: immediate release dosage forms. Pharm. Res., 15, 11-22.

Fang, J., Semple, H.A. and Song, J. (2004). Determination of metoprolol, and its four metabolites in dog plasma. J. Chrom. B, 809, 9-14.

Galia, E., Nicolaides, E., Hörter, D., Löbenberg, R., Reppas, C. and Dressman, J.B. (1998). Evaluation of various dissolution media for predicting in vivo performance of class I and II drugs. Pharm. Res., 15, 698-705.

Godbillon, J., Evard, D., Vidon, N., Duval, M., Schoeller, J.P., Bernier, J.J. and Hirtz, J. (1985). Investigation of drug absorption from the gastrointestinal tract of man. III. Metoprolol in the colon. Br. J. Clin. Pharmac., 19, 113S-118S.

International Conference on Harmonisation. (2005). ICH Harmonised Tripartite Guideline-Validation of Analytical Procedures: Text and Methodology Q2 (R1) (Parent Guideline, 1994 and Complementary Guideline on Methodology, 1996).

Jobin, G., Cortot, A., Godbillon, Duval, M., Schoeller, J.P., Hirtz, J. and Bernier, J.J. (1985). Investigation of drug absorption from the gastrointestinal tract of man. I. Metoprolol in the stomach, duodenum and jejunum. Br. J. Clin. Pharmac., 19, 97S-105S.

Katori, N. Aoyagi, N. and Terao, T. (1995). Estimation of agitation intensity in the GI tract in humans and dogs based on in Vitro/ in Vivo correlation. Pharm. Res., 12, 237-243.

Lee, Y.C. (2004). Method validation for HPLC analysis of related substance in pharmaceutical drug products. Chan, C.C., Lam, H., Lee, Y.C. and Zang, X-M. (Eds.) John wiley and Sons Inc., Hoboken, New Yersey, USA, 11-26.

Lindner, W.D. and Lippold, B.C. (1995). Drug release from hydrocolloid embeddings with high or low susceptibility to hydrodynamic stress. Pharm. Res., 12, 1781-1785.

Lui, C.Y., Amidon, G.L., Berardi, R.R., Fleisher, D., Youngberg, C. and Dressman, J.B. (1986). Comparison of gastrointestinal pH in dogs and humans: implications on the use of beagle dogs as a model for oral absorption in humans. J. Pharm. Sci., 75, 271-274.

Luner, P. (2000). Wetting properties of bile salt solutions and dissolution media. J. Pharm. Sci., 89, 382-395.

Sagara, K., Nagamatsu, Y., Yamada, I., Kawata, M., Mizuta, H. and Ogawa, K. (1992). Bioavailability study on commercial sustained-release preparations of diclofenac sodium in gastro-intestinal physiology regulated-dogs. Chem. Pharm. Bull., 40, 3303-3306.

Shah, V.P., Midha, K.K., Dighe, S. McGilveray, I.J., Skelly, J.P., Yacobi, A., Layloff, T., Viswanathan, C.T., Cook, C.E., McDowall, R.D., Pittman, K.A. and Spencer, S. (1992). Analytical methods validation: bioavailability, bioequivalence and pharmaceutical studies. J. Pharm. Sci., 81, 309-312.

US. Pharmacopeia XXVII & National Formulary 22. (2004). The United States Pharmacopeial Convention, Rockville, MD, USA.

Vertzoni, M. Pastelli, E., Psachoulias, D., Kalantzi, L. and Reppas, C. (2007). Estimation of intragastric solubility of drugs: In what medium? Pharm.Res., 25, 909-917.

Vidon, N., Evard, D., Godbillon, J., Rongier, M., Duval, M., Schoeller, J.P., Bernier, J.J. and Hirtz, J. (1985). Investigation of drug absorption from the gastrointestinal tract of man. II. Metoprolol in the jejunum and ileum. Br. J. Clin. Pharmac., 19, 107S-112S.

4

Development and evaluation of porous pellets

Accepted for publication in Drug Development and Industrial Pharmacy

4.1. INTRODUCTION

As described in Chapter 1, multiparticulate systems such as pellets are often used as oral solid dosage form since they offer therapeutic as well as technological advantages over single unit dosage forms. They disperse freely in the gastro-intestinal tract, what contributes to maximum drug absorption, reduced peak plasma fluctuations and less side effects. Furthermore, pellets also allow the formulator to modify the drug release by coating the pellets and a mixture of pellets with different release characteristics can be used to obtain the desired release profile (Bechgaard and Hagermann, 1978; Ghebre-Selassie, 1989; Krämer and Blume, 1994). Several methods can be used for pellet preparation whereby extrusion/spheronization is commonly used. This method involves different preparation steps: a wet mass is formed of a uniform powder mixture of drug and excipient(s) by addition of a liquid binder. Next the wet mass is pressed through an extrusion screen to form cylindrical extrudates (extrusion), which are subsequently broken up into smaller cylindrical rods and rounded into spheres by means of fast rotating friction plate (spheronization) followed by drying.

The objective of the study described in this chapter is to develop porous pellets which allow the incorporation of a significant drug fraction (deposited inside the porous structure or layered on the surface of the pellets). To this end pellets consisting of Avicel PH 101 and

sodium chloride were manufactured by extrusion/spheronization and after removal of the NaCl fraction via extraction porous pellets were obtained. Their potential as drug carriers was tested using three techniques to incorporate drugs in the porous pellets: fluid-bed layering, immersing the pellets in a drug solution and supercritical fluid impregnation.

4.2. MATERIALS

Avicel PH 101 (microcrystalline cellulose) (50 μm) was obtained from FMC Biopolymer (Cork, Ireland). Sodium chloride (NaCl) (Alpha Pharma, Zwevegem, Belgium) was used as pore forming agent.

Metoprolol tartrate (Esteve Quimica, Barcelona, Spain) was used as model drug using immersion of the pellet in a drug solution as loading technique. Ibuprofen (BASF, Ludwigshafen, Germany) was used as model drug using supercritical fluid impregnation as drug loading technique. Paracetamol (Alpha Pharma, Zwevegem, Belgium) and hydroxypropylmethylcellulose (HPMC, Methocel E3) (Colorcon, Kent, UK) were used as model drug and binder, respectively, using fluid-bed layering as drug loading technique.

4.3. METHODS

4.3.1. Manufacturing of porous pellets

NaCl was grinded in a ball mill (Pulverisette 6, Fritsch, Idar-Oberstein, Germany) during 10 min and the sieve fraction <125 μm was collected. Avicel PH 101 and NaCl were dry mixed (30/70, w/w) in a planetary mixer (Kenwood Major Classic). Next 42.5 % (w/w) water was added to the mixture and the wet mass was granulated for 10 min. Extrusion was performed using a single screw extruder (Dome extruder lab model DG-L1, Fuji Paudal, Tokyo, Japan) at 50 rpm, equipped with a 1 mm perforated screen. The extrudates were spheronized on a spheronizer (Calvea model 15) with a cross-hatched friction plate, operating at 1000 rpm with

a residence time of 5 min. The pellets were oven-dried at 40°C, followed by sieving whereby the 710-1400 µm pellet fraction was collected. The NaCl fraction was removed from the pellets by aqueous extraction: 30 g pellets were brought onto a 500 ml bottle top filter (0.22 µm) (Corning, New York, USA), the filter was placed on a 2 L flask and connected to a vacuum pump. 2 L water was brought onto the filter in steps of 250 ml to extract the NaCl fraction. Next, the pellets were oven-dried at 40°C.

4.3.2. Pellet evaluation

- Atomic emission spectroscopy

To determine the residual NaCl content after extraction, the amount of Na^+-ions in the porous pellets was determined using atomic emission spectroscopy (AES) (Jenway PEP 7, Essex, England). Porous pellets (1 g) were soaked in 100 ml demineralised water and after disintegration of the pellets (using magnetic stirrer) and centrifugation, the Na^+-concentration in the supernatant was determined (emission λ = 589 nm).

- Pellet friability

The friability was determined by placing 10 g pellets (F_s) in a abrasion wheel (together with 200 glass beads, Ø 4 mm) of a friabilator (PTFE, Hainburg, Germany). The pellets were subjected to falling shocks at a rotational speed of 25 rpm during 10 min. Afterwards the fines were removed by sieving through a 250 µm sieve for 5 min (2 mm amplitude). The fraction above 250 µm (F_a) was used to calculate the friability (Eq.1):

$$\text{Friability (\%)} = [(F_s - F_a)/F_s]*100 \quad (1)$$

➢ Pellet porosity and pore size distribution

The porosity and pore size distribution (0.003-360 μm) of the pellets was determined using mercury intrusion porosimetry (Autopore III, Norcross, GA, USA) and compared with conventional non-porous microcrystalline pellets (Pharmatrans Sanaq, Basel, Switzerland). Sample size (0.6 - 1.4 g) was adjusted in order to use 20-80% of the stem volume. The sample was evacuated to 50 mm Hg, followed by low pressure mercury intrusion in a pressure range from 4.3 kPa to 193 kPa, with a mercury filling pressure of 4.3 kPa, maximal intrusion volume of 0.03 ml/g and equilibration time of 10 s. Next high pressure intrusion was performed in a pressure range from 207 kPa to 41 x 10^4 kPa, maximal intrusion volume of 0.03 ml/g and equilibration time of 10 s.

➢ Pellet sphericity

Pellet size and shape were determined using an image analysis system. Photomicrographs were taken with a digital camera (Camedia C-3030 Zoom, Olympus Optical, Tokyo, Japan). The obtained images were processed by image analysis software (AnalySIS®, Soft Imaging System, Münster, Germany) to characterize each individual pellet by mean Feret diameter (FD) (average of 180 calliper measurements with an angle of rotation of 1°), aspect ratio (AR) (ratio of longest Feret diameter and its longest perpendicular diameter) and two-dimensional shape factor (e_R) (Podczeck and Newton 1994):

$$e_R = \frac{2\pi r}{P_m} - \sqrt{1 - \left(\frac{b}{l}\right)^2} \qquad (2)$$

where r is the radius, P_m the perimeter, l the length (longest Feret diameter) and b the width (longest perpendicular diameter to the longest Feret diameter) of the pellet.

- Atomic force microscopy

The surface roughness of the pellets was evaluated using Atomic Force Microscopy (Autoprobe® CP AFM, Park Scientific Instruments, Sunnyvale, USA). Scanning was performed in contact mode with a cantilever (UL20 B) operating at a scan rate of 1 Hz. The maximum peak-to-valley distance (Rp-V), the average roughness ($R_{ave} = \sum_{n=1}^{N} \frac{|z_n - \bar{z}|}{N}$, i.e. the average deviation of all heights z_n measured in the scanned region from the mean height), the median and mean height (calculated from all heights measured in the scanned region) were determined.

- Scanning electron microscopy

Scanning electron microscopy (SEM) (JSM-5510, JEOL, Tokyo, Japan) was used to visualize the porous structure of the pellets. Pellets were coated with a gold layer using a sputter coater (Autofine Coater, JFC-1300, JEOL, Tokyo, Japan) to assure conductivity.

- Internal pore structure

For the determination of the 3-dimensional internal structure of the samples, the nano-computed tomography (nano-CT) scanner of the UGCT facility (www.ugct.ugent.be) was used (as described in Chapter 2, section 2.3.2.). Combining the data of the maximum inscribed diameter (d_{max}) and the equivalent diameter (d_e) provides information about the structure of the pores.

4.3.3. Drug-loading

Three techniques were evaluated to incorporate drugs into the pellets: immersing the pellets in a drug solution, supercritical fluid impregnation and fluid-bed layering.

➢ Immersion of the pellets in the drug solution

Soaking the pellets in a drug solution is the simplest method to incorporate drugs inside the pellet. The drugs are dissolved in an appropriate solvent and pellets are soaked in solution during a certain time (Byrne and Deasy, 2002).

Porous pellets (1 g) (n=3) were added to 100 ml of a metoprolol tartrate solution (15% and 30%, w/v). After 5 min, 24 and 48h the pellets were separated using a sieve (250 μm) and oven-dried at 40°C.

➢ Supercritical fluid impregnation

Carbon dioxide (CO_2) has many properties that makes it an attractive solvent: low toxicity, nonflammability and an environmentally benign nature. Under supercritical conditions, CO_2 offers mass transfer advantages over conventional organic solvents owing to its gaslike diffusivities, low viscosity and vanishing interfacial tension. Furthermore, supercritical fluids have the additional benefit of "solvent tunability"; a small change in pressure or temperature leads to changes in solvent properties (Panza and Beckman, 2004). Supercritical fluid technology has already proven its applicability to the preparation of pharmaceutical formulations: particle formation (reviewed by Jung and Perrut, 2001), purification of proteins (Yeo et al., 1993), preparation of liposomes (Frederiksen et al., 1997) and submicronization of drugs (Young et al., 2000). Recently, supercritical impregnation was explored for the formulation of drug delivery systems (Kikic and Vecchione, 2003). This technique offers a number of advantages since it avoids organic solvents and heat. Generally, for successful impregnation, the drug should have a sufficient solubility in the supercritical carrier and the partition coefficient should be favorable to enable drug loading in the matrix (Berens et al., 1992; Elvira et al. 2004; Diankov et al., 2007; Duarte et al., 2007). It is important to distinguish two different mechanisms in such impregnation process. The first involves

deposition of a substance soluble in supercritical fluid into the polymer matrix upon depressurizing the cell containing supercritical fluid solution. In this case, even a solute that has low affinity to the polymer matrix can be trapped within the polymer matrix. This approach often results in the formation of re-crystallized substances within the polymer matrix. Another mechanism utilizes the high affinity of the substance dissolved in the supercritical fluid for the polymer matrix. This could result in a high partition coefficient of solute between the polymer and the fluid phases. Furthermore, specific interactions between solute and matrix will result in molecularly dispersed solute within the polymer matrix (Kikic and Vecchione, 2003).

Supercritical fluid ($scCO_2$) was used to impregnate porous pellets with ibuprofen using Separex® equipment (Champigneulles, France).

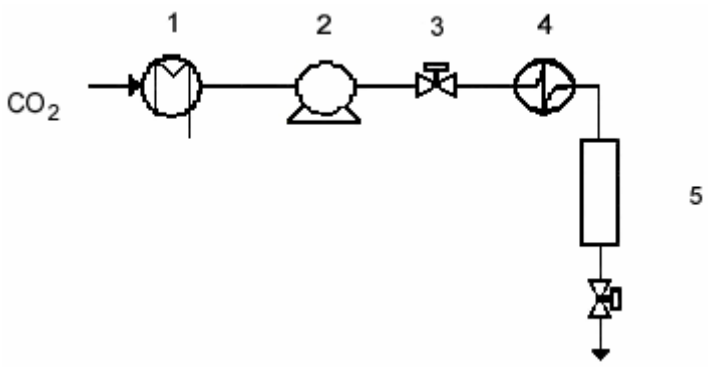

Figure 4.1.: Schematic overview of the SEPAREX® equipment: (1) chiller, (2) pump, (3) valve(s), (4) heater and (5) reactor.

At a pressure between 80 to 220 bar and a temperature from 35 to 45°C the solubility of ibuprofen in $scCO_2$ was found to be in a range from 10^{-5} to 10^{-3} mole fraction (Kazarian and Martirosyan, 2002). During the impregnation experiment $scCO_2$ (in which ibuprofen is dissolved) enters the pores of the pellets under pressure. Following a depressurization step, the drug is deposited in the internal pore structure of the pellet. The impregnation vessel (volume: 17 ml) was filled with 500 mg porous pellets. Ibuprofen was placed on top of the pellets and during 45 min the vessel was pressurized at a constant operating temperature. To

optimize the impregnation process, the influence of the experimental parameters (temperature, pressure and amount of ibuprofen relative to the amount of pellets used) was studied using an experimental design. Preliminary experiments were carried out to establish appropriate ranges for the processing variables. The amount of ibuprofen varied from 50 to 150 % relative to the amount of pellets used, the pressure varied between 150 and 250 bar while the temperature varied from 35 to 45°C. The upper limit of the amount of ibuprofen was limited to avoid overfilling of impregnation vessel. In addition the upper and lower limits of temperature and pressure were selected in order to ensure the solubility of ibuprofen in $scCO_2$. Because interaction between the variables were expected, the following quadratic model was proposed Eq. (3) for modeling the response variable (i.e. the amount of ibuprofen impregnated in the pellets) in function of the process variables:

$$Y = \beta_0 + \sum_{i=1}^{3} \beta_i X_i + \sum_{i=1}^{2} \sum_{j=i+1}^{3} \beta_{ij} X_i X_j + \sum_{i=1}^{3} \beta_{ii} X_{i^2} \qquad (3)$$

where Y is the response, X_i and X_j the set points of the process variables 'i' and 'j', respectively, and β_0, β_i, β_{ij} and β_{ii} the coefficients.

The designs points were chosen by the software (Design-Expert version 6.0.10, Stat-Ease Inc., Minneapolis, USA). Eighteen experiments were carried out using a face-centered central composite statistical design for the study of the three variables, each at three levels (Table 4.1.).

Repeated observations (n=4) at the center point (temperature: 40°C, pressure: 200 bar, ibuprofen concentration: 100% w/w) were used to estimate the experimental error. Manual regression was performed. The highest order significant polynomial (significance threshold: 0.05) was selected, where only significant model terms were included without destroying the model hierarchy. Outlier-t limit was set at 3.5.

Table 4.1.: Process parameters of the face-centered central composite design experiments.

Run	Factors		
	A Temperature (°C)	B Pressure (bar)	C Drug amount (%)
1	35	250	50
2	40	150	100
3	40	200	50
4	40	200	100
5	45	200	100
6	40	200	100
7	45	250	150
8	45	150	150
9	35	200	100
10	35	150	150
11	40	200	100
12	40	200	150
13	45	150	50
14	35	150	50
15	40	200	100
16	45	250	50
17	35	250	150
18	40	250	100

The probability plot of the residuals was performed in order to evaluate the model and to detect outliers. The model provided several comparative measures for model selection: (a) R^2 statistics, which give a correlation between the experimental and predicted response, should be high for a particular model to be significant; (b) adjusted R^2, which gives a similar correlation after ignoring the insignificant model terms, should have a good agreement with predicted R^2 for the model to be fit (Hicks and Turner, 1999); (c) predicted and adjusted R-squares should be within 0.20 of each other. Contour plots for the response were drawn.

➢ Fluid-bed layering

Pellets are fluidized in the fluid-bed system and a drug solution or suspension is sprayed on the pellets. The Wurster fluid-bed is a circulating fluid-bed which differs from conventional fluid-beds by its hydrodynamic features attributed to its grid and tube design. Four zones with distinctly different solid movement patterns can be identified: the up-bed region, the deaccelaration region, the down-bed region and the horizontal transport region. The coating process consists of three phases: the start-up phase, the coating phase and the drying phase. The start-up phase consists of an optional preheating of the equipment and a heating of the substrate. During the coating phase, the coating is applied to the substrate. A spray nozzle in the middle of the grid delivers drops (average diameter: 10-30 μm) of coating solution/suspension on the surface of the particles. The drying of the film starts as the solvent evaporates from the film droplets in the spray mist and continues from the film droplets adhered to the substrate. The space above the inner tube offered to the particles is enlarged, the air velocity decreases and the particles fall down in the annular part. In this region the coating film must be dry enough to avoid sticking and agglomeration. In the lower part, on the grid, the particles form a dense bed from where they are aspirated towards the inner tube for a new cycle (Guignon et al., 2003; Christensen and Bertelsen, 1997).

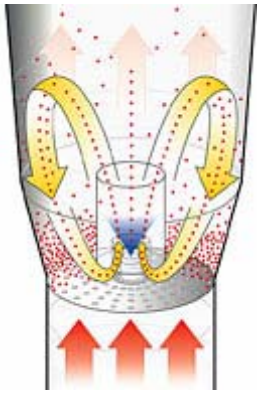

Figure 4.2.: Schematic representation of the substrate motion in a Wurster fluid-bed.

Aqueous coating solutions containing 1% (w/w) paracetamol and 0, 0.5, 1 or 1.5% (w/w) (relative to the amount of pellets used, i.e. 250 g) HPMC (Methocel E3) were prepared. 4L of each coating solution was sprayed on the pellets (batch size: 300 g) in a fluid-bed (GPCG 1, Glatt, Binzen, Germany) using a Wurster setup. The operating conditions during coating were set at 20 g/min spray rate, 1.5 bar atomization pressure, 38°C outlet temperature and 4 h process time. The same procedure was performed using non-porous microcrystalline cellulose pellets (Pharmatrans Sanaq, Basel, Switzerland). Based on the theoretical amount of paracetamol layered on the pellets, the coating efficiency was calculated.

4.3.4. Characterization of the drug-loaded pellets

The distribution of the drug throughout the pellets was evaluated by Raman spectroscopic mapping. A pellet was cut into two halves and the inner surface of the pellet was scanned in point-by-point mapping mode with a step size of 50 µm in both the x and y directions using a long working distance objective lens (spot size laser = 50 µm). The detection system used in this study was a RamanRxn 1 Microprobe (Kaiser Optical Systems, Ann Arbor, USA), equipped with an air cooled CCD detector (back-illuminated deep depletion design). The laser wavelength during the experiments was the 785 nm line from a 785 nm Invictus NIR diode laser. All spectra were recorded at a resolution of 4 cm^{-1} using a laser power of 400 mW and a laser light exposure time of 15 s per collected spectrum. Before data analysis, spectra were baseline corrected. Data collection and data analysis was done using the HoloGRAMS^{TM} data collection software package, the HoloMAP^{TM} data analysis software package and the Matlab® software package (version 6.5).

Furthermore, the Raman spectra of the loaded pellets were compared with the Raman spectra of the raw materials in order to obtain information about the solid state of the drug on the pellet surface as well as inside the pellet.

For the determination of the loading yield (mg drug/g pellets), the pellets were crushed, placed in a solvent (water for metoprolol tartrate and paracetamol, phosphate buffer pH 7.2 for ibuprofen) and stirred during 30 min, followed by centrifugation. The amount of drug in the supernatant was determined by UV spectroscopy.

4.3.5. Drug release

Drug release from the porous pellets was determined using the USP II method (VanKel VK 8000, VanKel Industries, New Jersey, USA) with a paddle speed of 50 rpm and at a temperature of 37±0.5°C. Phosphate buffer pH 7.2 was used as dissolution medium for ibuprofen pellets and water for metoprolol tartrate and paracetamol pellets. Samples were collected at different time points and analysed using a UV/VIS double beam spectrophotometer (Perkin-Elmer, Zaventem, Belgium) at 265, 222 and 243 nm for ibuprofen, metoprolol tartrate and paracetamol, respectively.

The following analytical solution of Fick's second law of diffusion was used to describe metoprolol tartrate and ibuprofen release from the porous pellets (Crank, 1975). This model considers that drug release is purely diffusion-controlled, that the drug is homogeneous distributed within the pellets at t = 0 and that perfect sink conditions are maintained throughout the experiments:

$$\frac{M_\infty - M_t}{M_\infty} = \frac{6}{\pi^2} \cdot \sum_{n=1}^{\infty} \frac{1}{n^2} \cdot \exp\left(- \frac{n^2 \cdot \pi^2}{R^2} \cdot D \cdot t \right) \qquad (4)$$

where M_∞ and M_t denote the absolute cumulative amounts of drug (mg) released at infinite time and time t, respectively; R represents the radius of the pellets and D the apparent diffusion coefficient of the drug within the system.

4.4. RESULTS AND DISCUSSION

4.4.1. Characterization of porous pellets

Preliminary experiments were carried out to determine the maximum concentration of pore forming agent (NaCl) that could be incorporated into the pellet formulation. The results showed that the concentration was limited to 70% (w/w) as at a higher sodium chloride fraction the mass could not be extruded.

Image analysis revealed an AR (n=303, ±SD) of 1.15 ± 0.08, an e_R of 0.94 ± 0.03 and FD of 946 ± 142 μm, indicating that spherical pellets were obtained, and 89.1% of the pellets was found in the 710-1400 μm size range.

Most of the sodium chloride fraction was removed during aqueous extraction as analysis of the porous pellets by AES determined the residual sodium chloride content at 4%.

The porosity and median pore diameter of the porous microcrystalline cellulose pellets were 33.2 ± 0.8% and 0.7 ± 0.2 μm, respectively, whereas the corresponding values of conventional non-porous MCC pellets were 15.1 ± 1.2 % and 0.02 ± 0.01 μm. Although almost 70% NaCl was removed from the porous pellets by extraction, their porosity was only 33.2% due to shrinkage of the pellets during drying. Despite their high porosity, the porous pellets were sufficiently strong to withstand the friction forces during handling as the friability was below 0.1%. Atomic Force Microscopy (AFM) showed that the surface of the porous pellets was more irregular and rough compared with non-porous pellets: all AFM parameters (Rp-V, average roughness, mean and median height) were higher in case of porous MCC pellets (Table 4.2.).

Table 4.2.: Analysis of surface structure via atomic force microscopy of conventional non-porous pellets and porous pellets.

	Rp-V (µm)	R_{ave} (µm)	mean height (µm)	median height (µm)
non-porous pellet	1.33	0.12	0.55	0.28
porous pellets	3.47	0.47	1.86	1.77

Rp-V : maximum peak-to-valley distance
R_{ave} : the average deviation of all heights z_n measured in the scanned region from the mean height

a

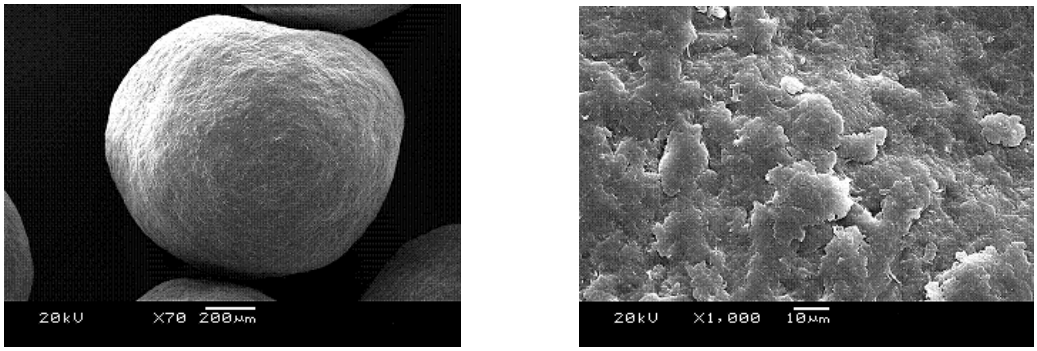

b

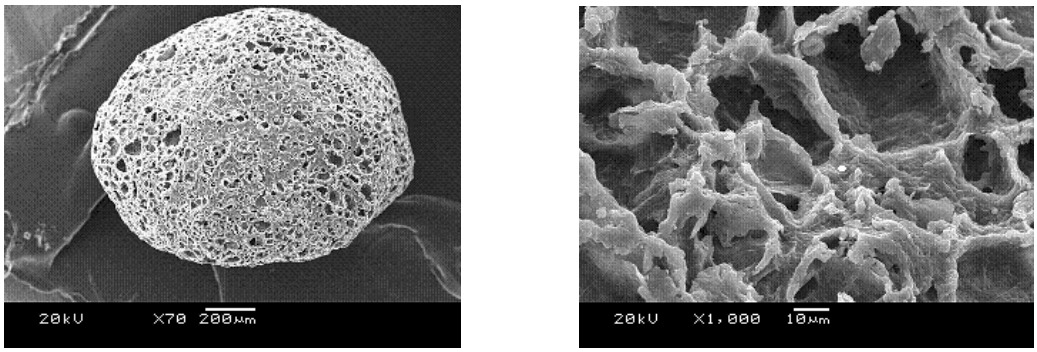

Figure 4.3.: SEM micrographs of the surface of a conventional non-porous pellet (**a**) and a porous pellet (**b**) (manufactured by means of NaCl extraction).

The difference in porosity between the conventional non-porous and porous pellets was visualised by SEM (Fig. 4.3.).

Nano CT-scanning of the porous structure (Fig. 4.4.) detected one pore system with a branched structure (equivalent diameter > maximum inscribed diameter) (Table 4.3.). These

pore system represented 99% of the total porosity volume, indicating that nearly all pores are incorporated in an interconnected network.

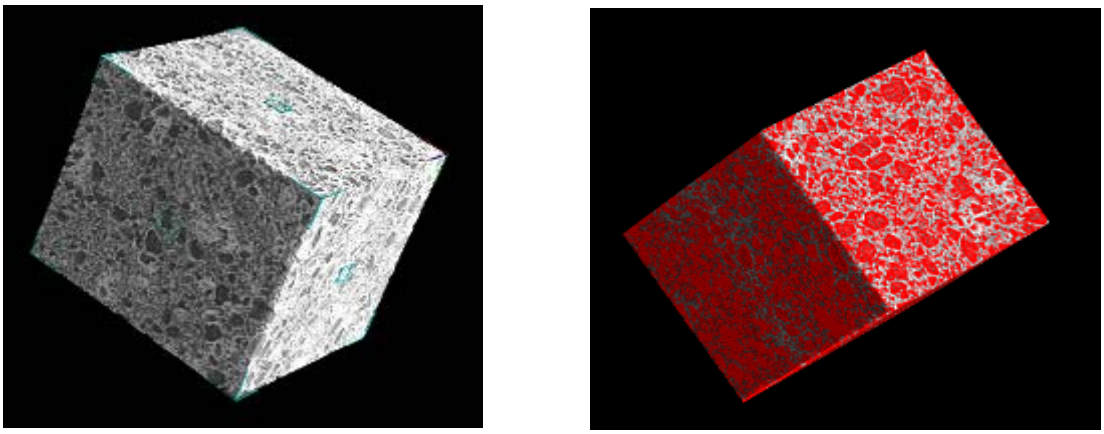

Figure 4.4.: 3-dimensional images of the internal structure of porous pellets.

Table 4.3.: Nano CT-scan analysis of the 3-dimensional internal structure of a porous pellet obtained by NaCl extraction.

maximum inscribed diameter (µm)	equivalent diameter (µm)	porosity represented by pore system (%)
59	340	99

4.4.2. Drug-loading experiments

Several drug loading techniques were tested to maximize drug deposition in the porous structure of the pellets. For each technique a model drug was used that had a good solubility in the solvent used.

- Immersion of the pellets in the drug solution

After soaking the porous pellets during 5 min in a 15 and 30% (w/v) metoprolol tartrate solution (n=3) the drug load was 208 ± 7 and 489 ± 2 mg/g pellets, respectively. A longer soaking time resulted in a higher drug load: 273 ± 13 mg/g pellets and 616 ± 21 mg/g pellets after 24 h in a 15 and 30% (w/v) metoprolol tartrate solution (n=3), respectively. However,

after 48 h soaking the drug load did not further increase. Raman spectroscopy revealed that this technique allowed to deposit drug in the inner pore structure since the solution can easily penetrate inside the porous network and after drying the drug is deposited in the pores. Fig. 4.5. shows that the Raman signal of metoprolol tartrate (encircled peaks in the spectrum, spectral range 627-652 and 806-867 cm^{-1}) was detected at the surface of the pellets as well as inside the pellets, indicating that the drugs was homogeneously distributed after 24 h immersion of the pellets in a 15% metoprolol tartrate solution.

a

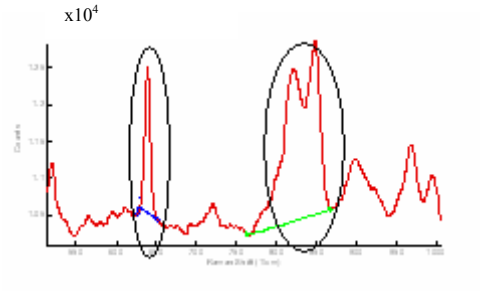

b

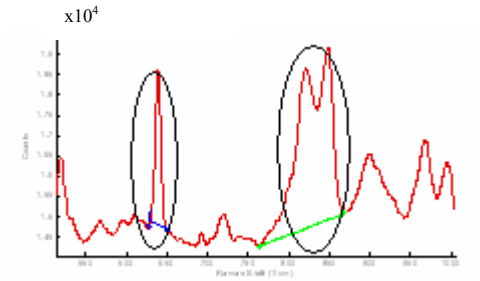

Figure 4.5.: Raman spectra of porous pellets loaded via immersion in a 15% (w/v) metoprololtartrate solution. Spectra recorded at (**a**) surface of the pellet and (**b**) inside the pellet.

Furthermore, the sharp peaks in the spectrum of the drug-containing pellets corresponded with the peaks in the spectrum of crystalline metoprolol tartrate, indicating that metoprolol tartrate in the drug-loaded pellets was crystalline.

All drug-loaded pellets had a friability below 1%.

➢ Supercritical fluid impregnation

Supercritical fluid impregnation was evaluated as a second drug loading technique. Analysis of variance of the response factor (Table 4.4.) indicated that the response surface model developed for drug loading was significant, without significant lack of fit.

The model summary statistics for the selected significant model showed that R^2 (0.9987), predicted R^2 (0.9905) and adjusted R^2 (0.9972) are in good agreement, resulting in a reliable model.

Table 4.4.: ANOVA results of face-centered control composite statistical design for drug loading of porous pellets via supercritical fluid impregnation.

Source	Sum of squares	Mean square	F Value	Prob > F
Model	7.37	0.92	664.48	< 0.0001
A: Temp	5.15	5.15	3716.10	< 0.0001
B: Pressure	0.053	0.053	38.57	0.0004
C: IBU (%)	0.82	0.82	590.29	< 0.0001
A^2	1.57	1.57	1131.00	< 0.0001
B^2	0.053	0.053	37.96	0.0005
C^2	0.043	0.043	30.95	0.0008
AB	0.084	0.084	60.43	0.0001
AC	0.099	0.099	71.32	< 0.0001
Residual	9.700 E-003	1.386 E-003		
Lack of fit	3.458 E-003	8.646 E-004	0.42	0.7922
Pure error	6.241 E-003	2.080 E-003		

Table 4.5.: Response results for process design.

Run	Factors			Response
	A Temperature (°C)	B Pressure (bar)	C Drug amount (%)	Drug Loading (%)
1	35	250	50	2.2
2	40	150	100	23.0
3	40	200	50	15.1
4	40	200	100	18.3
5	45	200	100	17.1
6	40	200	100	17.4
7	45	250	150	23.4
8	45	150	150	34.2
9	35	200	100	17.4(*)
10	35	150	150	5.3
11	40	200	100	17.2
12	40	200	150	27.8
13	45	150	50	23.3
14	35	150	50	8.4(*)
15	40	200	100	19.0
16	45	250	50	15.2
17	35	250	150	5.9
18	40	250	100	18.8

(*): classified as an outlier

The drug loading of runs 9 and 14 was classified as an outlier.

The fitted response surface model in terms of coded factors for the drug loading was:

$$\text{Ln (drug loading)} = 2.89 + 0.94 * A - 0.084 * B + 0.33 * C - 0.98 * A^2 + 0.15 * B^2 + 0.14 * C^2 - 0.12 * A * B - 0.13 * A * C \quad (4)$$

where A is the temperature, B the pressure and C the amount of ibuprofen relative to the amount of pellets used. The contour plot based on Eq. (4) and the 3D surface plots are presented in Fig. 4.6.

a

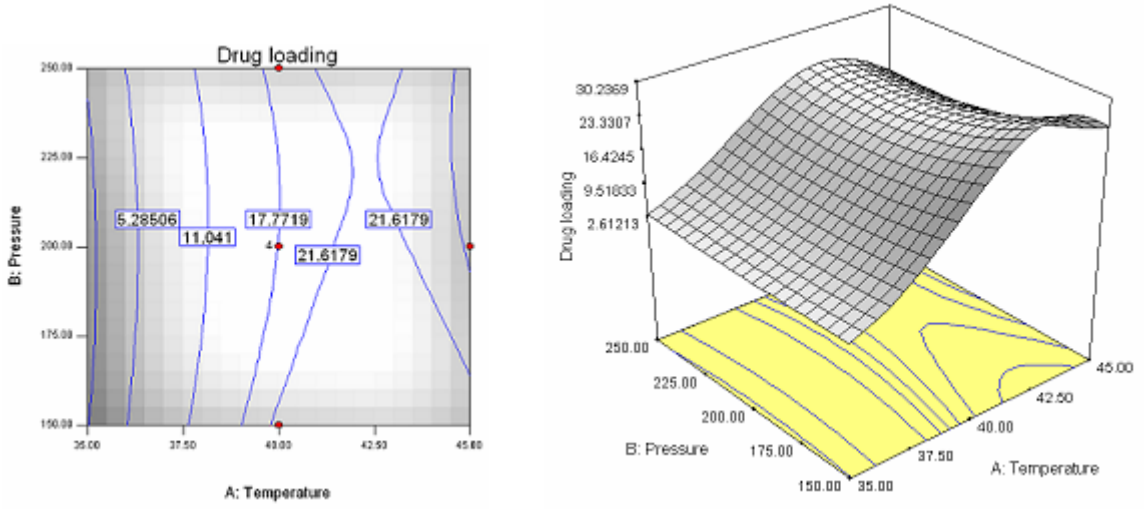

b

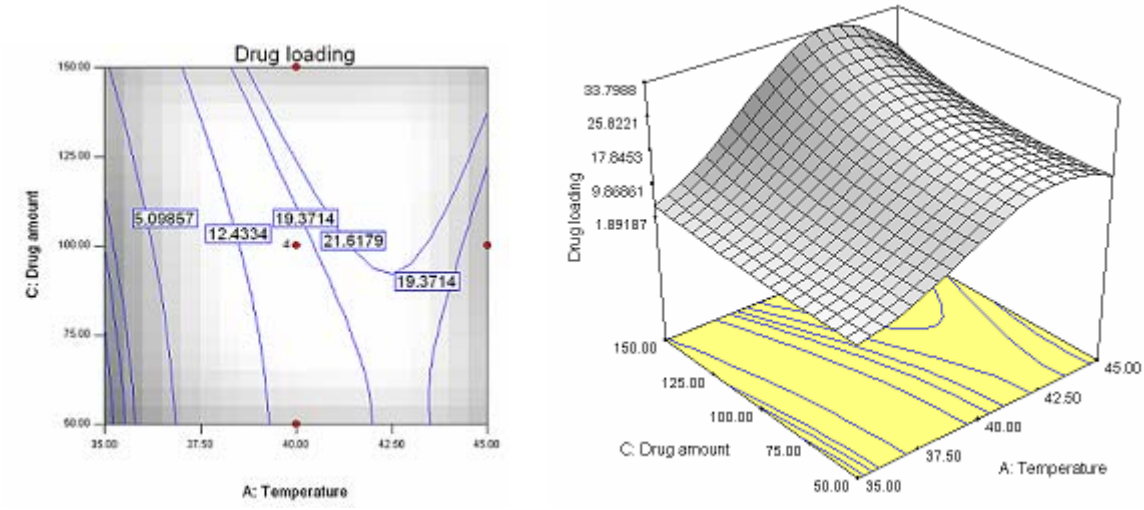

c

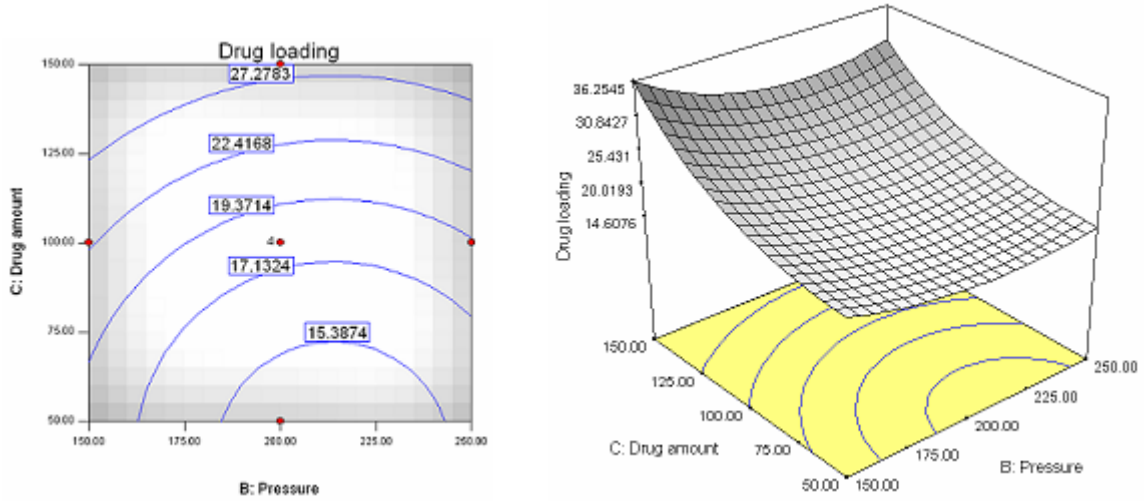

Figure 4.6.: Contour plots and 3D plots for drug loading at **a**) constant ibuprofen amount (100%, relative to the amount of pellets used), **b**) constant pressure (200 bar) and **c**) constant temperature (40°C).

Within the set of parameters tested, the highest ibuprofen concentration (342 mg/g pellets) was achieved when the temperature and pressure were set at 45°C and 150 bar, and when 150% (w/w) ibuprofen (relative to the amount of pellets used) was used (Table 4.5.).

At constant drug amount dissolved in supercritical CO_2 (Fig. 4.6.a), maximum drug load was obtained at low pressure and high temperature. Fig 4.6.b showed that when a constant pressure was applied, a higher drug load was obtained when drug amount and temperature were increased.

The solubility of ibuprofen in supercritical carbon dioxide increased with pressure and temperature (Charoenchaitrakool et al., 2000). In addition, the sorption of carbon dioxide in the matrix also increased with pressure. Hence, more solute uptake was anticipated a higher pressure. However, combining a high temperature and a high pressure did not result in the highest drug load despite the higher solubility of ibuprofen in $scCO_2$ under these conditions. This could be indicative that at high pressure the interaction between ibuprofen and supercritical fluid is stronger compared to the interaction between drug and pellet since a stronger interaction between solute and carbon dioxide is detrimental for the bonding forces between solute and matrix (Duarte et al., 2007).

The loading experiment at the centre point was carried out four times, yielding a mean drug load of 180 ± 8.5 mg ibuprofen/g pellets was found, indicating that this procedure was reproducible.

The friability of pellets after drug loading via $scCO_2$ impregnation was below 0.1%. Raman spectroscopy of the pellets with the highest drug load (342 mg ibuprofen/g pellets) revealed that drug was deposited on the surface as well as inside the porous pellet as for all mapped areas the specific spectrum of ibuprofen (spectral range: 624-645, 731-762 and 808-843 cm^{-1}) was detected (Fig. 4.7.). Raman spectroscopy revealed sharp peaks indicating that most ibuprofen that was deposited at the surface and inside the pellet was crystalline.

a

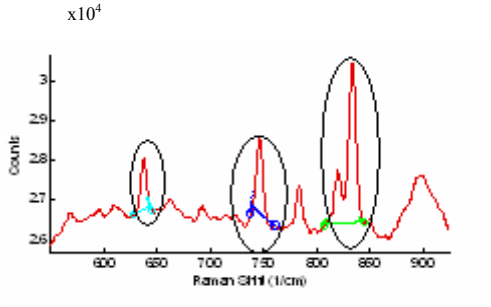

b

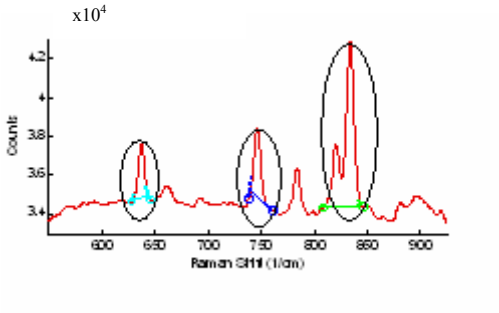

Figure 4.7.: Raman spectra of porous pellets loaded with ibuprofen via supercritical fluid impregnation. Spectra recorded at (**a**) surface of the pellet and (**b**) inside the pellet.

➢ Fluid-bed layering

Layering of porous pellets with a drug solution using fluid-bed coating was also examined for drug loading since this technique is commonly used for loading inert spheres with drugs. The coating efficiency after 4 h layering with a 1% (w/v) paracetamol solution and increasing amounts of binder (Methocel E3) is given in Fig. 4.8.

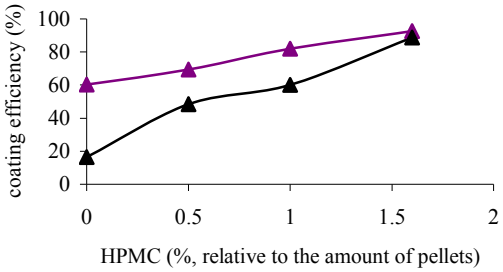

Figure 4.8.: Coating efficiency (%) of paracetamol on non-porous (▲) and porous pellets (▲) in function of Methocel E3 concentration in the coating solution.

The difference in coating efficiency between the non-porous (16.5%) and porous pellets (61.7%) is most pronounced without binder, resulting in a drug load of 97.6 mg paracetamol/g porous pellets. The irregular surface of the porous pellets compared to the non-porous pellets contributed to the difference in drug loading when no binder was used. Furthermore, the irregular surface of the porous pellets facilitated sticking of the drug particles to the surface compared to the smoother surface of conventional non-porous pellets. When a binder was added to the coating solution the drug particles attached to the pellet surface independently of the morphology of their surfaces. The friability of the porous pellets after drug loading was in all cases < 0.1%, whereas for the non-porous pellets the friability was higher (0.9%). Due to the irregular surface of the porous pellets, the drug particles were better protected against friction during friability testing. A layering experiment was performed whereby the spray rate was gradually increased until agglomeration of the pellets occurred, in order to investigate the maximum spray rate that could be obtained. For porous pellets a maximum spray rate of 35 g/min was obtained. In contrast, for non-porous pellets agglomeration already occurred at a spray rate of 20 g/min. The irregular surface of the porous pellets facilitated the evaporation of the coating liquid and its porous structure was able to improve the drainage of water from its surface. Raman spectroscopy (Fig. 4.9.) of the pellets coated with a 1% (w/v) paracetamol / 1% (relative to the amount of pellets used) Methocel E3 solution identified that paracetamol

(spectral range: 1587-1673 cm^{-1}) was only present at the surface of the pellet. The absence of drug inside the pellets was probably due to limited penetration of the drug solution within the pellets as most of the water evaporated once the droplet was distributed on the pellet surface.

a

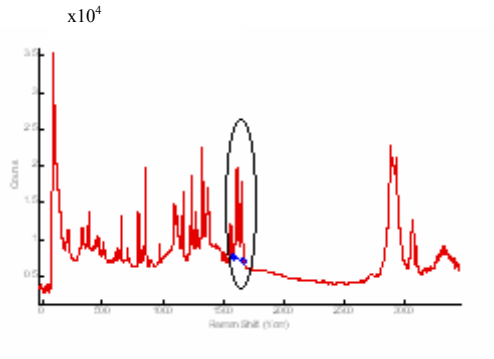

b

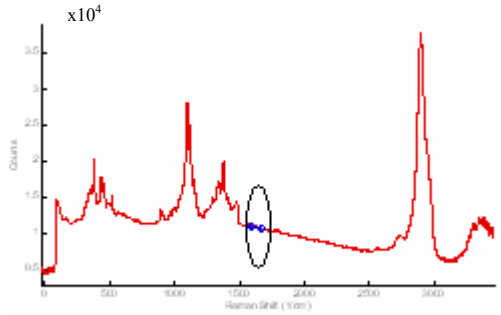

Figure 4.9.: Raman spectra of porous pellets loaded with paracetamol via fluidised bed layering. Spectra recorded at (a) surface of the pellet and (b) inside the pellet.

The sharp peaks presented in the Raman spectrum of the loaded pellets corresponded with the peaks found in the spectrum of pure crystalline paracetamol, indicating that paracetamol was layered on the pellet surface in a crystalline form.

4.4.3. Drug release from porous pellets

Fig. 4.10. shows the *in vitro* release profile of ibuprofen from porous pellets loaded by supercritical fluid impregnation. Clearly, most of the drug was released within less than 10

min. Even higher release rates were observed with metoprolol tartrate-loaded pellets, irrespective of the concentration of the soaking solution (Fig. 4.11.). Fitting of an appropriate analytical solution of Fick's second law of diffusion (considering the given initial and boundary conditions, Eq. 4) to the experimentally determined drug release kinetics, showed a good agreement between theory and experiment.

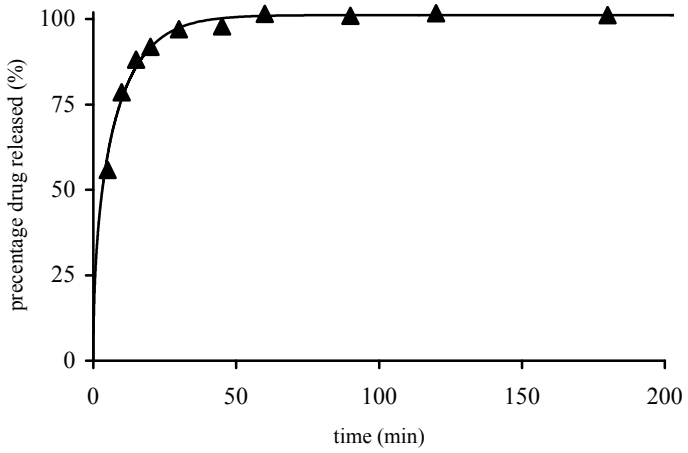

Figure 4.10.: *In vitro* drug release from ibuprofen-loaded, porous pellets: experimental (symbols, n=3) versus theoretical (curve, Eq.1) profiles.

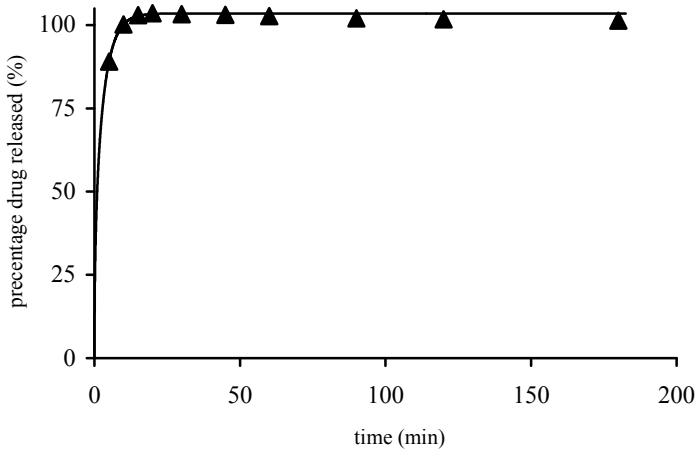

Figure 4.11.: *In vitro* drug release from metoprolol tartrate-loaded, porous pellets: experimental (symbols, n=3) versus theoretical (curve, Eq.1) profiles.

Diffusion was the governing mass transport mechanism in these systems, irrespective of the type of drug and concentration. Based on these calculations the apparent diffusion coefficients of the drugs within the porous pellets could be determined: $4.8 \pm 0.2 \times 10^{-8}$ cm²/s for ibuprofen and $1.5 \pm 0.1 \times 10^{-6}$ cm²/s for metoprolol tartrate.

The paracetamol release from layered porous pellets was immediate (Fig. 4.12.). As paracetamol was only present on the pellet surface, no diffusion mechanisms were involved in drug release.

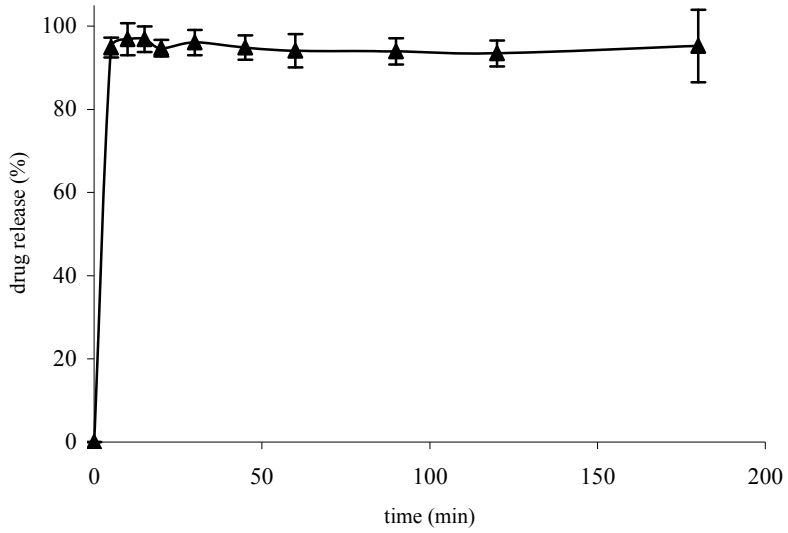

Figure 4.12.: Mean drug release profiles (n=3, ±SD) of from porous pellets loaded with paracetamol via fluid-bed layering.

4.5. CONCLUSION

Porous pellets manufactured by extraction of NaCl from Avicel PH 101-NaCl pellets can be used as drug carriers. The drug loading studies have shown that immersing the pellets in a drug solution and supercritical fluid impregnation are able to deposit drugs inside the porous pellets, whereas after fluid-bed coating drug was only found on the surface of the porous pellets. Drug release from the porous pellets was immediate and primarily controlled by diffusion.

4.6. REFERENCES

Bechgaard, H. and Hagermann, N.G. (1978). Controlled-release multiple units and single unit doses. A literature review. Drug Dev. Ind. Pharm., 4, 53-67.

Berens, A.R., Huvard, G.S., Korsmeyer, R.W. and Kunig, F.W. (1992). Application of compressed carbon dioxide in the incorporation of additives into polymers. J. Appl. Polym. Sci., 46, 231-242.

Byrne, R.A. and Deasy, P.B. (2002). Use of commercial porous ceramic particles for sustained drug delivery. Int. J. Pharm., 246, 61-73.

Charoenchaitrakool, M., Dehghani, F. and Foster, N.R. (2000). Micronization by rapid expansion of supercritical solutions to enhance the dissolution rates of poorly water-soluble pharmaceuticals. Ind. Eng. Chem. Res., 39, 4794-4802.

Christensen, F.N. and Bertelsen, P. (1997). Qualitative description of the Wurster-based fluid-bed coating process. Drug Dev. Ind. Pharm., 23, 451-463.

Crank, J. (1975). The mathematics of diffusion. Oxford, England: Clandendon press.

Diankov, S., Bart, D., Vega-Gonzalez, A., Pentchev, I. and Subra-Paternault, P. (2007). Impregnation isotherms of hydroxybenzoic acid on PMMA in supercritical carbon dioxide. J. Supercr. Fluids, 41, 164-172.

Duarte, A.R., Simplicio, A.L., Vega-Gonzalez, A., Subra-Paternault, P., Coimbra, P., Gil, M.H., de Sousa, H.C. and Duarte, C.M.M. (2007). Supercritical fluid impregnation of a biocompatible polymer for ophthalmic drug delivery. J. Supercr. Fluids, 42, 373-377.

Elvira, C.A., Fernandez, M., Fraile, J., San Roman, J. and Domingo, C. (2004). Evaluation of drug delivery characteristics of microspheres of PMMA-PCL-cholesterol obtained by

supercritical CO_2 impregnation and by dissolution-evaporation techniques. J. Control. Rel., 99, 231-240.

Frederiksen, L., Anton, K. van Hoogevest, P., Keller, H.R. and Leuenberger, H. (1997). Preparation of liposomes encapsulating water-soluble compounds using supercritical carbon dioxide. J. Pharm. Sci., 921-928.

Ghebre-Sellasie, I. (1989). Pellets: A general overview. In: Pharmaceutical pelletilization technology. Ghebre-Sellasie (Ed.), Marcel Dekker Inc., New York, USA, 1-13.

Guignon, B., Regalado, E., Duquenoy, A. and Dumoulin, E. (2003). Helping to choose operating parameters for a coating fluid bed process. Pow. Tech., 130, 193-198.

Hicks, C.R. and Turner, K.V. (1999). Fundamental concepts in the design of experiments. Oxford, England: University Press.

Jung, J and Perrut, M. (2001). Particle design using supercritical fluids: Literature and patent survey. J. Supercr. Fluids, 20, 179-219.

Kazarian, S.G. and Martirosyan, G.G. (2002). Spectroscopy of polymer/drug formulations processed with supercritical fluids: in situ ATR-IR and Raman study of the impregnation of ibuprofen into PVP. Int. J. Pharm., 232, 81-90.

Kikic, I. and Vecchione, F. (2003). Supercritical impregnation of polymers. Curr. Opin. Solid State Mater. Sci., 7, 399-405.

Krämer, J. and Blume H. (1994). Biopharmaceutical aspects of multiparticulats. In: Multiparticulate ral drug delivery. Ghebre-Sellassie, I. (Ed.), Marcel Dekker Inc., New York, USA, 307-332.

Manual Design-Expert version 6.0.10., Stat-Ease Inc., Minneapolis, USA.

Panza, J.L. and Beckman, E.J. (2004). Chemistry and materials design for CO_2 processing. In: Supercritical fluid technology for drug product development. York, P., Kompella; U.B. and Shekunov, B.Y. (Eds.), Marcel Dekker Inc., New York, USA.

Podczeck, F and Newton, J.M. (1994). A shape factor to characterize the quality of spheroids. J. Pharm. Pharmacol., 46, 82-85.

Yeo, S.D., Lim, G.B., Debenedetti, P.G. and Bernstein, H. (1993). Formation of microparticulate protein powders using a supercritical fluid antisolvent. Biotech. Bioeng., 41, 341-346.

Young, T.J., Mawson, S., Johnston, K.P., Henriksen, I.B., Pace, G.W. and Mishara, A.K. (2000). Rapid expansion from supercritical to aqueous solution to produce submicron suspensions of water-insoluble drugs. Biotechnol. Progr., 16, 402-407.

5

In vivo evaluation of porous pellets

5.1. INTRODUCTION

In Chapter 4 the application of porous microcrystalline cellulose pellets as drug carriers was investigated and the *in vitro* drug release from these matrices was characterized as immediate and diffusion-controlled, independent on the model drug.

In this chapter the bioavailability of metoprolol tartrate and ibuprofen in dogs was determined after oral administration of a hard gelatin capsule containing porous microcrystalline cellulose pellets. To examine the influence of the drug solubility on the *in vivo* drug release from porous pellets, metoprolol tartrate and ibuprofen were used as drugs with a high and low aqueous solubility, respectively.

5.2. MATERIALS

To prepare porous pellets, Avicel PH 101 (microcrystalline cellulose) was obtained from FMC Biopolymer (Cork, Ireland) and sodium chloride (NaCl) (Alpha Pharma, Zwevegem, Belgium) was used as pore forming agent. Metoprolol tartrate (Esteve Quimica, Barcelona, Spain) and ibuprofen (BASF, Ludwigshafen, Germany) were used as model drugs.

Commercially available metoprolol tartrate and ibuprofen dosage forms were used as reference formulations during *in vivo* testing: Lopresor® (100 mg metoprolol tartrate per immediate-release tablet; Novartis, Brussels, Belgium), Ibuprofen EG 600 mg (600 mg

ibuprofen per immediate-release tablet; Eurogenerics, Brussels, Belgium) and Ibu-Slow® 600 (600 mg ibuprofen per controlled-release tablet; Therabel, Brussels, Belgium).

5.2.1. Ibuprofen

Ibuprofen (2-(4-isobutylphenyl)propionic acid) is a non-steroidal agent with anti-inflammatory, analgesic and antipyretic properties used to treat rheumatoid arthritis, osteoarthritis and mild to moderate pain. Owing the presence of a single asymmetric carbon atom, the molecule exists as (*S*)-(+) (dextro) or (*R*)-(-) (laevo) isomer. Conventional ibuprofen occurs as a racemic mixture of the two isomers, whereby the (*S*)-(+) isomer possesses the majority of the pharmacological activity, as measured by inhibition of prostaglandin synthesis. The process whereby the (*R*)-(-) isomer is converted into the (*S*)-(+) isomer is chiral inversion, an enzymatic reaction that occurs in a unidirectional manner. The solubility of ibuprofen increases with pH, being largely insoluble at low pH values (pH range 1-4: 0.058 ± 0.004 mg/ml) whereas a rapid and continuous increase in solubility is observed as the pKa is approached and thereafter (Shaw et al., 2005). Ibuprofen is rapidly absorbed, maximum ibuprofen plasma concentrations are achieved 1-2 hours after ingestion of the drug, but due to its short half life (about 2 hours) therapeutic blood concentrations can only be maintained if the drug is administered frequently (Higton, 1999). Ibuprofen displays extensive (99%) binding to plasma proteins (Lin et al., 1987), consequently a relative low distribution volume. Ibuprofen is extensively metabolized to pharmacologically inactive metabolites (Brocks and Jamali, 1999).

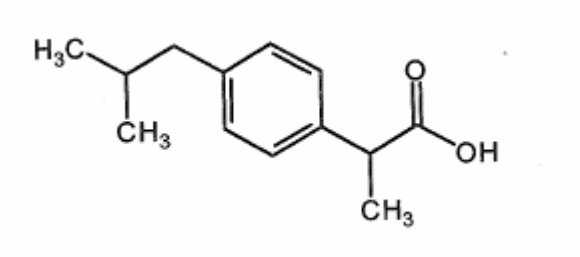

Figure 5.1.: Structure of ibuprofen

5.3. METHODS

5.3.1. Production of porous pellets

The porous pellets were prepared according to the method described in Chapter 4 (section 4.3.1.). Next, the pellets were loaded with metoprolol tartrate by soaking the pellets in a metoprolol tartrate solution (7.5% w/v) or with ibuprofen via supercritical fluid impregnation as described in Chapter 4 (section 4.3.3.).

5.3.2. *In vivo* study

All procedures were performed in accordance with the guidelines and after approval of the Ethics Committee of the Institute for Agricultural and Fisheries Research (ILVO) (Merelbeke, Belgium). Male mixed-breed dogs (weight 20.5-40.5 kg) were used in this study.

5.3.2.1. Metoprolol tartrate

Each dog (n=4) received porous pellets (F-1) (filled into hard gelatine capsules) containing 100 mg metoprolol tartrate. The *in vivo* data obtained after administration of Lopresor® (containing 100 mg metoprolol tartrate) as described in Chapter 3 were used as reference formulation with immediate drug release. Administration of the formulation to dogs and sampling was identical to the methods described in Chapter 3 (section 3.3.3). Sample analysis

was carried out as described in Chapter 3 (section 3.3.3.) using a validated HPLC-fluorescence method (section 3.3.4.).

5.3.2.2. Ibuprofen

The following formulations were administered to each dog (n=6) :

- F-1: porous pellets (filled into hard gelatine capsules) containing 300 mg ibuprofen
- F-2: ½ tablet of Ibuprofen EG® 600 mg (immediate release formulation)
- F-3: ½ tablet of Ibu-Slow® 600 mg (controlled release formulation)

The formulations were administered in a cross-over sequence with a wash-out of at least 8 days. On the experimental days the dogs were fasted for 12 h prior to the study period, water was available ad libitum. Before administration of the formulations a blank sample was obtained from the saphenous vein. The formulations were administered with 10 ml water. Blood samples were obtained at 0.5, 1, 1.5, 2, 3, 4, 5, 6, 8, 12 and 24h. The blood samples were collected in dry heparinized tubes and centrifuged for 10 min at 1450*g* within 1h of sampling. The plasma was stored at -20°C until assay of ibuprofen.

➢ Ibuprofen assay

The ibuprofen plasma concentrations were determined by a validated HPLC-UV method. All chemicals were of analytical HPLC grade.

Fifty microlitres of an internal standard solution (30 µg/ml indomethacin in ethanol), 50 µl ethanol and 500 µl plasma were transferred into a borosilicate glass tube. After 1 min of vortexing, 100 µl HCl (2 N) was added and homogenized by 1 min vortexing. Afterwards, 4ml hexane/ether mixture (4/1, v/v) was added. After 3 min vortexing and 5 min centrifuging at 2500*g*, the upper organic layer was transferred into a new glass tube and evaporated to

dryness under a nitrogen stream. The residue was dissolved in 200 µl mobile phase and 50 µl of this solution was injected onto the column. The ibuprofen plasma concentrations were determined via a calibration curve. The standards for the calibration curve were extracted using the same procedure as described above: 500 µl blank plasma was spiked with 50 µl of the internal standard solution and 50 µl of a standard solution with a known concentration of ibuprofen in ethanol (0, 3, 6, 12, 30, 60, 90, 180 and 240 µg/ml).

The HPLC equipment (Hitachi, Tokyo, Japan) consisted of a solvent pump (L-7100), set at a constant flow-rate of 1.5 ml/min, a variable wavelength UV-detector (L-7400) set at 220 nm, a reversed-phase column and precolumn (LiChroCART® 125-4 and 4-4, LiChrospher® 100 RP-18 (5µm); Merck, Darmstadt, Germany) and an auto-sampler injection system (L-7200) with a 50 µl loop (Valco Instruments Corporation, Houston, Texas, USA) equipped with an automatic integration system (D-7000 Multi-Manager). The mobile phase consisted of 0.1 M KH_2PO_4 (adjusted to pH 7.0 with 2 M NaOH)/acetonitrile (12/3, v/v).

- Validation of the HPLC method

The HPLC method for ibuprofen analysis was validated based on the guidelines of the International Conference on Harmonisation (ICH) for validation of analytical procedures: Text and Methodology (2005). The following characteristics were considered: specificity, linearity, accuracy, precision, recovery, detection and quantification limit (as defined in Chapter 3).

Specificity

The absence of interference between ibuprofen, internal standard and endogenous plasma components was confirmed after comparing the chromatograms of a blank serum sample (a),

a blank serum sample spiked with ibuprofen and indomethacine (b) and a plasma sample obtained after oral administration of ibuprofen to dogs (c) (Fig. 5.1.).

a

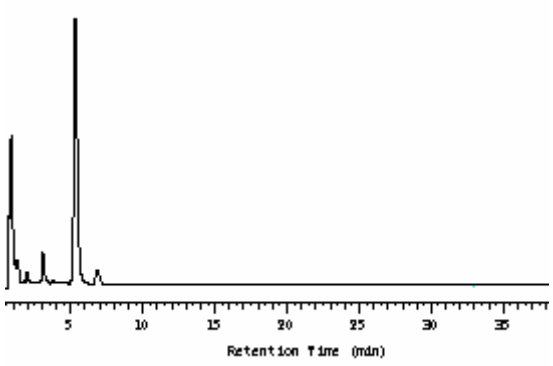

b

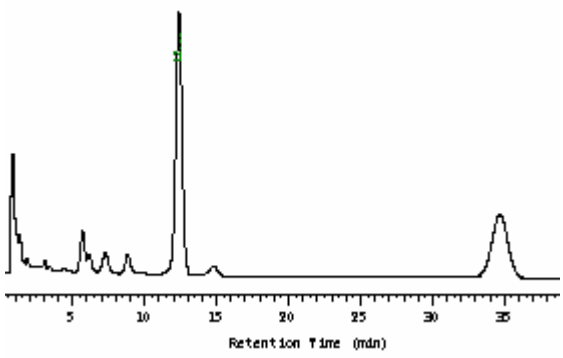

c

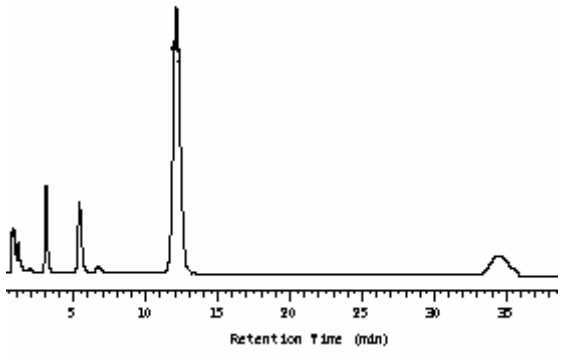

Figure 5.1.: Specificity of the HPLC method. Chromatograms after extraction of (**a**) blank plasma, (**b**) blank plasma spiked with ibuprofen (retention time: 12.4 min) and indomethacine (retention time: 34.7 min) and (**c**) dog plasma after intake of an ibuprofen tablet (½ tablet of Ibu-Slow® 600 mg).

Accuracy

Table 5.1. lists the mean within-day and between-day accuracy of the HPLC method. All values were within ± 15% of the actual concentration (i.e. acceptance criteria recommended by Shah et al., 1992) ,independent of the ibuprofen concentration.

Table 5.1.: Mean accuracy (± S.D.) of the HPLC method (n=6) in function of ibuprofen concentration

Concentration (µg/ml)	**Accuracy (%)**	
	Within-day	Between-day
0.5	104.6 ± 3.7	109.1 ± 4.4
7.5	107.6 ± 4.8	95.5 ± 8.7
40	106.5 ± 7.1	102.6 ± 6.6

Precision

The coefficient of variations used to assess precision are listed in Table 5.2. Since CV values below the limit recommended by Shah et al. (1992) (i.e. CV<15%), the method used for determination of ibuprofen in dog plasma is precise.

Table 5.2.: Precision (expressed as coefficient of variation) of the HPLC method (n=6)

Concentration (µg/ml)	**Precision (%CV)**	
	Within-day	Between-day
0.5	13.1	7.7
1	-	8.5
2.5	-	11.9
5	-	11.2
7.5	10.7	9.1
15	-	14.8
20	-	11.9
40	12.1	10.9

Recovery

Recovery was presented as the mean value of repeated analyses (n=6) of different calibration standards (at three concentration levels) and the internal standard (Table 5.3.).

Table 5.3.: Mean recovery (n=6) (± S.D.) of the calibration standards and the internal standard

	Concentration (µg/ml)	**Recovery (%)**
ibuprofen	0.5	89.2 ± 4.1
	7.5	101.1 ± 8.4
	40	86.2 ± 6.2
indomethacine	2.5	78.3 ± 11.3

Linearity

During validation of the HPLC method and analysis of the samples, several calibration curves were analyzed. The linearity of the calibration curves was evaluated via the determination coefficient R^2: 0.9997 ± 0.0013 (n=7), indicating that a linear relationship between response (y) and concentration (x). The equation of the mean calibration curve was:

$$y = 0.2202x - 0.0075$$

Detection and quantification limits

Detection and quantification limits were calculated from the mean calibration curve based on the equations presented in Chapter 3 (section 3.3.4.). Using this specific HPLC method, the detection limit of ibuprofen in dog plasma was 0.78 µg/ml and the quantification limit was 2.4 µg/ml. Since the calculated quantification limit was higher than the lowest concentration of the calibration curve and the accuracy and precision at a concentration of 0.5 µg/ml were within the accepted limits (Shah et al. 1992), a concentration of 0.5µg/ml was considered as limit of quantification.

5.3.3. Data analysis

The extent of drug absorption ($AUC_{0\text{-}24h}$), the peak plasma concentration (C_{max}) and the time to reach C_{max} (t_{max}) was calculated using the MW-PHARM program version 3.0 (Mediware 1987-1991, Utrecht, The Netherlands). The $AUC_{0\text{-}24h}$ was calculated using logarithm and linear trapezoidal rules. The relative bioavailibility (F_{rel}, %) was calculated as the $AUC_{0\text{-}24h}$ ratio between the porous pellets and a reference formulation.

For the porous pellets loaded with ibuprofen, the sustained-release characteristics were evaluated by the time span during which the plasma concentrations were at least 50% of the C_{max} value ($HVD_{t50\%Cmax}$, the width of the plasma concentration profile at 50% of C_{max}) (Meier et al., 1974; Steinijans, 1990). The $HVD_{t50\%Cmax}$ values were determined from the individual plasma concentration-time profiles. The ratio between the $HVD_{t50\%Cmax}$ values of the test formulation (i.e. porous pellets) and the immediate release reference formulation (i.e. Ibupofen 600 EG) (expressed as R_D) is indicative for the sustained release effect of the porous pellets: a ratio of 1.5, 2 and >3 indicating a low, intermediate and strong sustained release effect, respectively (Meier et al., 1974).

5.3.4. Statistical analysis

The data obtained after administration of metoprolol tartrate were statistically analysed using SPSS 16 software (SPSS, Chicago, USA). A comparison between the pellet and reference formulations was carried out by a paired *t*-test ($P<0.05$). All data were tested for normality using Kolmogorov-Smirnov test.

The effect of ibuprofen formulation on the bioavailibility was assessed by repeated-measurements ANOVA (univariate analysis). To further compare the effects of the different formulations, a multiple comparison among pairs of means was performed using Bonferroni post-hoc testing with $P< 0.05$ as significance level. The sphericity of covariances was tested

with Mauchly's test. SPSS 16 software (SPSS, Chicago, USA) was used to perform the statistical analysis.

5.4. Results and discussion

5.4.1. *In vivo* evaluation of porous pellets containing metoprolol tartrate

The mean plasma concentration-time profiles after oral administration of 100 mg metoprolol tartrate to 4 dogs as a porous pellet formulation and as Lopresor® are presented in Fig. 5.1. The pharmacokinetic parameters are given in Table 5.4.

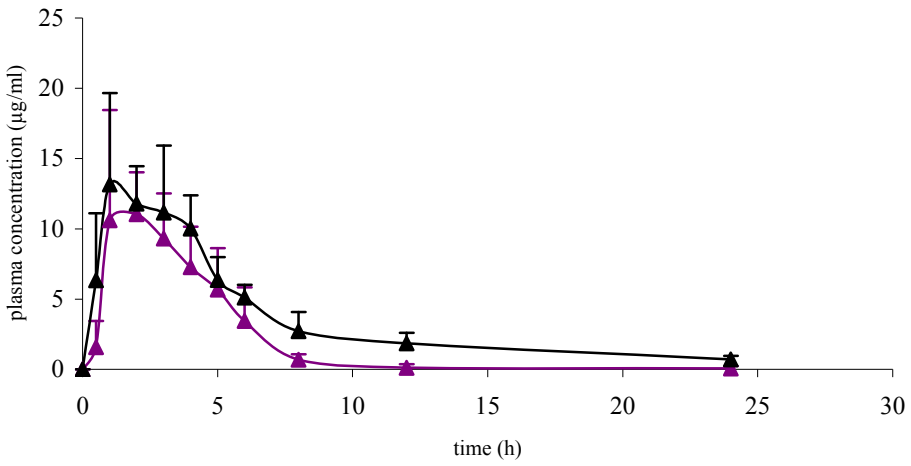

Figure 5.1.: Mean plasma concentration-time profiles (± S.D., n=4) in dogs after oral administration of 100 mg metoprolol tartrate as a porous pellet formulation (F-1) (▲) and as Lopresor® -tablet (▲).

Table 5.4.: Mean pharmacokinetic parameters (± S.D., n=4) in dogs after oral administration of 100 mg metoprolol tartrate as porous pellet formulation (F-1) and as Lopresor®-tablets.

	C_{max} (µg/ml)	t_{max} (h)	AUC_{0-24h} (µg.h/ml)
F-1	15.7 ± 3.3	1.3 ± 0.5	60.1 ± 13.5
Lopresor®	14.7 ± 3.2	1.4 ± 0.5	50.2 ± 10.8

Table 5.5.: Statistical analysis of the pharmacokinetic parameters by paired sample *t*-test (P= 0.05).

		Mean difference	95% CI	P value
C_{max} (µg/ml)	F1- Lopresor®	1.0	-7.8, 9.7	0.7
t_{max} (h)	F1- Lopresor®	-0.1	-1.4, 1.2	0.8
AUC_{0-24h} (µg.h/ml)	F1- Lopresor®	9.9	-3.8, 23.6	0.1

The plasma concentration–time profiles after administration of porous pellets containing 100 mg metoprolol tartrate are similar to Lopresor®. No statistically significant mean differences of AUC_{0-24h}, C_{max} and t_{max} were found between both formulations (Table 5.5.), indicating that similar drug concentrations were available. The relative bioavailability (F_{rel}) of porous pellets compared to Lopresor® was 120.9 ± 21.2%.

5.4.2. *In vivo* evaluation of porous pellets containing ibuprofen

Fig. 5.2. presents the mean plasma concentration-time profiles after oral administration of 300 mg ibuprofen to 6 dogs as a porous pellet formulation, Ibuprofen EG® 600 mg (½ tablet) and Ibu-Slow® 600 mg (½ tablet). The pharmacokinetic parameters are reported in Table 5.6.

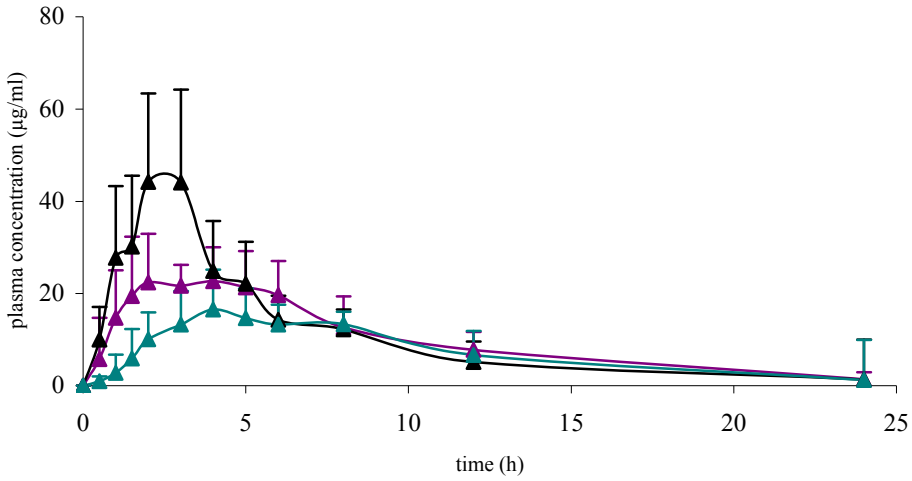

Figure 5.2.: Mean plasma concentration-time profiles (± S.D., n=6) in dogs after oral administration of 300 mg ibuprofen as Ibuprofen EG® 600 mg (½ tablet) (F-1) (▲) and Ibu-Slow® 600 mg (½ tablet) (F-2) (▲) and as a porous pellet formulation (F-3) (▲).

Table 5.6.: Mean pharmacokinetic parameters (± S.D., n=6) in dogs after oral administration of 300 mg ibuprofen as Ibuprofen EG® 600 mg (½ tablet) (F-1) and Ibu-Slow® 600 mg (½ tablet) (F-2) and as a porous pellet formulation (F-3).

	C_{max} (µg/ml)	t_{max} (h)	AUC_{0-24h} (µg.h/ml)	$HVD_{t50\%Cmax}$ (h)	F_{rel}* (%)	R_D
F-1	50.7 ± 9.5	2.4 ± 0.6	256.4 ± 51.3	3.6 ± 0.7	-	-
F-2	19.0 ± 5.3	6.6 ± 3.3	174.8 ± 36.6	10.7 ± 5.0	-	3.0 ± 1.7
F-3	29.0 ± 6.6	3.8 ± 1.7	224.5 ± 82.6	6.8 ± 1.9	136.0 ± 59.6	2.0 ± 0.5

-: not applicable
* Ibu-Slow® 600 (½ tablet)

With regard to the extent of absorption, the mean AUC_{0-24h} of the pellet formulation, Ibuprofen EG® 600 mg and Ibu-Slow® 600 mg was 224.5, 256.4 and 174.8 µg/ml, respectively; yielding a relative bioavailability of the porous pellets versus Ibu-Slow® 600 mg of 136.0%. The statistical analysis of these data is reported in Table 5.7.

Table 5.7.: Statistical analysis of the pharmacokinetic parameters via multiple comparison among pairs of means using the Bonferroni post hoc test (P= 0.05).

		Mean difference	95% CI	P value
C_{max} (µg/ml)	F1-F2	31.7	17.0, 46.4	0.002
	F1-F3	21.8	2.9, 40.6	0.029
	F2-F3	-9.9	-20.4, 0.5	0.060
t_{max} (h)	F1-F2	-4.3	-8.8, 0.3	0.062
	F1-F3	-1.3	-3.9, 1.2	0.378
	F2-F3	2.9	-1.4, 7.2	0.184
AUC_{0-24h}(µg.h/ml)	F1-F2	81.6	-38.9, 202.2	0.186
	F1-F3	28.4	-84.4, 141.3	1.000
	F2-F3	-53.2	-179.7, 73.3	0.592
$HVD_{t50\%Cmax}$ (h)	F1-F2	-7.1	-15.5, 1.3	0.093
	F1-F3	-3.2	-5.4, -0.9	0.013
	F2-F3	3.9	-2.9, 10.7	0.295
R_D	F3-F2	-1.7	-3.0, -0.3	0.026

A significant mean difference of C_{max} was observed between Ibuprofen EG® 600 mg (F-1) and Ibu-Slow® 600 mg (F-2) and between porous pellets (F-3) and Ibuprofen EG® 600 mg (F-1). No significant mean difference between the formulations was found for t_{max} and AUC_{0-24h}. A significant mean difference of $HVD_{t50\%Cmax}$ was detected between Ibuprofen EG® 600 mg (F-1) and the pellets.

The *in vivo* behavior of the pellet formulation was similar to the Ibu-Slow® tablets and its R_D value of 2 indicated that an intermediate sustained release effect was obtained. However the *in vitro* ibuprofen release profile (Chapter 4, section 4.4.3.) in phosphate buffer pH 7.2. was immediate. As the drug release from porous pellets is diffusion–controlled, ibuprofen release from the porous matrix was determined by drug solubility: at pH 7.2 the higher solubility (4.48 ± 0.08 mg/ml, De Brabander et al., 2003) resulted in an immediate release, whereas the lower *in vivo* solubility unexpectedly induced a sustained release effect. Although the residence time of pellets is limited in the stomach, the delay of drug release probably could be

attributed to the gastric fluid. As the pellets absorb the gastric fluid when passing through the stomach, the pores are filled with this acid medium, creating an acid microenvironment which limited the solubility of ibuprofen. Neutralization of the acids during gastro-intestinal passage gradually increased drug solubility, creating a slow and sustained drug release.

The importance of drug solubility on the *in vivo* drug release from porous pellets was confirmed by the plasma concentration-time profiles after administration of porous pellets loaded containing metoprolol tartrate: *in vivo* release of the highly soluble metoprolol tartrate release was immediate.

5.4. Conclusion

The *in vivo* drug release from porous pellets depended on the solubility of the incorporated drug: release of drugs with a high aqueous solubility was immediate, whereas, diffusion from the porous matrix in case of drugs with a low aqueous solubility was slow, yielding plasma concentration similar to a sustained-release tablet.

5.5. References

Brocks, D.R. and Jamali, F. (1999). The Pharmaceutics of ibuprofen. In: Rainsford, K.D. (Ed.), Ibuprofen. A critical bibliographic review. Taylor and Francis, Londen, 87-142.

De Brabander, C., Vervaet, C. and Remon, J.P. (2003). Development and evaluation of sustained release mini-matrices prepared via hot melt extrusion. J. Control. Release, 89, 235-247.

Higton, F. (1999). The Pharmaceutics of ibuprofen. In: Rainsford, K.D. (Ed.), Ibuprofen. A critical bibliographic review. Taylor and Francis, Londen, 53-86.

International Conference on Harmonisation. (2005). ICH Harmonised Tripartite Guideline-Validation of Analytical Procedures: Text and Methodology Q2 (R1) (Parent Guideline, 1994 and Complementary Guideline on Methodology, 1996).

Lin, J.H., Cocchetto, D.M. and Duggan, D.E. (1987). Protein binding as a primary determent of the clinical pharmacokinetic properties of nonsteriodal anti-inflammatory drugs. Clin. Pharmacokin., 12, 402-432.

Meier, J., Nuesch, E. and Schmidt, R. (1974). Pharmacokinetic criteria for evaluation of retard formulations. Eur. J. Clin. Pharmacol., 7, 429-432.

Shaw, L.R., Irwin, W.J., Grattan, T.J. and Conway, B.R. (2005). The effect of selected water-soluble excipients on the dissolution of paracetamol and ibuprofen. Drug Dev. Ind. Pharm., 31, 515-525.

Shah, V.P., Midha, K.K., Dighe, S., McGilveray, I.J., Skelly, J.P., Yacobi, A., Layloff, T., Viswanathan, C.T., Cook, C.E., McDowall, R.D., Pittman, K.A. and Spencer, S. (1992). Analytical methods validation: bioavailability, bioequivalence and pharmaceutical studies. J. Pharm. Sci., 81, 309-312.

Steinijans, V.W. (1990). Pharmacokinetic characterization of controlled-release formulations. Eur. J. Drug Metab. Pharmacokinet., 15, 173-181.

6

Porous pellet formulation of F4 fimbriae for oral vaccination of suckling piglets against *E. coli* infections

6.1. INTRODUCTION

Enterotoxigenic *Escherichia coli* (ETEC) infections are implicated as an important causal agent in diarrhea and mortality in domestic animals and humans. Especially, *E. coli* infections in pigs, immediately after birth or post-weaning, are responsible for significant economic losses in pig farming (Fairbrother et al., 2005). Neonatal infections can be prevented by passive colostral and lactogenic immunity (Deprez et al., 1986; Rutter and Jones, 1973), but active intestinal immunization is needed for protection of newly weaned piglets since they are deprived of passive lactogenic immunity. Active intestinal immunization can occur following oral infection but is not obtained by parenteral immunization, which tends to stimulate the systemic rather than the mucosal immune system (Moon and Blum, 1993). Therefore vaccination of piglets against post-weaning infections is still an important challenge; there is clearly a need for competent oral vaccines to induce mucosal protection.

Some of the ETEC strains bear F4 fimbriae, a surface antigen which enables the bacteria to adhere to F4-specific receptors (F4R) present on the brush borders of the villous enterocytes

and subsequently to colonize the small intestine. The presence or absence of F4R is genetically determined, whereby it is known that piglets without the F4 receptor are resistant to $F4^+$ *E. coli* infections, indicating that F4-mediated adhesion is a prerequisite for infection (Rutter et al., 1975; Gibbons et al., 1977). Antibodies against these fimbriae prevent ETEC adhesion in a direct or indirect manner (van Zijderveld et al., 1998). Consequently these fimbriae are possible antigens to induce a protective mucosal immune response. It has been demonstrated that newly weaned F4R-positive piglets can be orally immunized with purified F4 fimbriae in solution (Van den Broeck et al., 1999a). However, to prevent post-weaning diarrhea, an active mucosal immunity is needed at the moment of weaning. Therefore, the piglets have to be immunized during the suckling period using a vaccine formulation that can be mixed with creep food to facilitate administration. Previously, enteric coated pellets have been used for oral administration of vaccines, as they protect F4 fimbriae against the detrimental effects in stomach and duodenum. However, incompatibility between the protein and the enteric coating polymer was noticed (Huyghebaert et al., 2005).

In the study described in this chapter, the use of porous pellets for oral vaccination of suckling piglets with F4 fimbriae was evaluated *in vitro* and *in vivo*. As the pellets consisted of an interconnected pore network, the F4 fimbriae can penetrate in the porous matrix of the pellets which can offer protection to against acids, bile, enzymes, antibodies etc. during gastro-intestinal transit, thus ensuring release of the protein at the target site (major inductive sites; jejunal Peyer's patches) in an immunizing conformation (Snoeck et al., 2006). Since binding of F4 to the F4 receptor on the villous enterocytes is a prerequisite for the induction of a protective intestinal immune response, the correct F4 confirmation is of crucial importance to ensure this binding. The application of this system to obtain mucosal immunization after oral administration is investigated.

6.2. MATERIALS

To manufacture porous pellets, microcrystalline cellulose (Avicel PH 101) was obtained from FMC Biopolymer (Cork, Ireland) and sodium chloride (NaCl) (Alpha Pharma, Zwevegem, Belgium) was used as pore forming agent.

To prepare the F4 stock solution, F4 fimbriae of enterotoxigenic *E. coli* bacteria were isolated as described by Van den Broeck et al. (1999b). The protein concentration of the isolated solution was determined using the Bicinchoninic Acid Protein Assay kit (Sigma-Aldrich, Bornem, Belgium). The purity was assessed by electrophoresis on SDS-12% polyacrylamide slab gels.

6.3. METHODS

6.3.1. Production and loading of the porous pellets

The porous pellets were prepared according to the method described in Chapter 4 (section 4.3.1.).

In order to load the pellets with F4 fimbriae, vials (15ml) were filled with 500 mg pellets (glass type 1, Gaash Packaging, Mollem, Belgium) and spiked with 500 µl F4 solution (3.35 mg/ml). As the solution was completely absorbed by the porous pellets, each vial contained 1.68 mg F4. The pellets were dried by freeze-drying (Amsco-Finn Aqua GT4, Amsco, Germany). The samples were frozen to -45°C within 175 min. Primary drying was performed during 13 h at -15°C and at a pressure varying between 0.8 and 1 mbar, followed by secondary drying for 7 h at elevated temperature (10°C) without changing the pressure. After freeze-drying the vials were closed and kept on ice until analysis or administration.

6.3.2. Evaluation of the pellets

➢ F4 biological activity

In order to investigate if F4 fimbriae retained their activity during the manufacturing process, 500 mg freeze-dried pellets (n=3) were soaked in 100 ml PBS. After crushing the pellets (using a magnetic stirrer) and centrifugation at 2500*g*, the supernatant was collected and stored at -20°C until analysis.

The amount of biologically active F4 was determined via ELISA, as described by Verdonck et al. (2004). Briefly, the wells of a 96-well microtiter plate (NUNC® Brand Products, Polysorp Immuno Plates, Life Technologies, Merelbeke, Belgium) were coated with F4-specific swine polyclonal antiserum in PBS. This polyclonal antiserum was able to bind native as well as denaturated F4 fimbrial FaeG. After 2 h incubation at 37°C, the remaining binding sites were blocked overnight with PBS + 0.2% Tween® 80. Subsequently the F4 stock solution and the samples (previously diluted until the same concentration as the stock solution was obtained, taking a complete release from the porous pellets in consideration) were added in series of two-fold dilutions (1-0.001 µg/ml) in ELISA buffer (PBS, pH 7.4 with 0.2% Tween® 20 and 3% BSA). The dilution of the stock solution started at a concentration of 1µg/ml. Thereafter, an optimal dilution of the FaeG-specific monoclonal antibody IMM01 (MAb) was added to the wells for 1 h at 37°C. Subsequently, rabbit anti-mouse horseradish peroxidase (HRP) conjugated serum (Dakon, Denmark) diluted in ELISA buffer and supplemented with 2% (v/v) pig serum was brought onto the plates for 1 h at 37°C. An ABTS (2,2'-azinobis 3-ethylbenzthiazoline-6-sulfonic acid) solution containing H_2O_2 was added, resulting in a colorimetric reaction (eq.1):

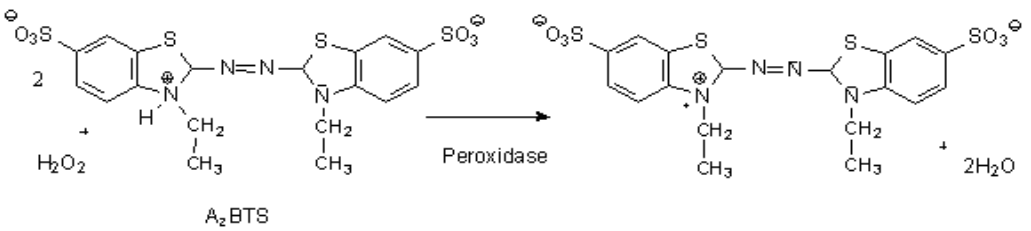

(eq.1.)

The optical density was measured spectrophotometrically at 405 nm.

➢ Distribution of F4 in the porous pellet

Pellets were fixed in formol. A cassette containing the pellets was placed overnight in a Tissue-Tek-VIP machine and consecutively soaked in different media (formol-ethanol-methanol) in order to dehydrate the pellets. Next, the pellets were rinsed in xyleen, followed by embedding in paraffin (Medite TBS 88 paraffin embedding system, Klinipath). Slices (4 µm) were made and dried during 10 min at 60°C.

To visualize the F4 fimbriae, the slices were immunostained by incubating them with anti-F4 rabbit antiserum followed by adding anti-rabbit IgG (whole molecule)/FITC antiserum (Sigma-Aldrich, Schneldorf, Germany). In order to ensure that no background fluorescence was detected, slices incubated in PBS followed by adding anti-rabbit IgG/FITC antiserum were used as control. The slices were examined using a fluorescence microscope.

6.3.3. *In vitro* F4 release from the porous pellets

➢ *In vitro* dissolution testing

To simulate feed preparation 500 mg pellets (containing 1.675 mg F4) were immersed for 5 min in a pH 7.4 phosphate buffer saline (PBS) solution. The amount of F4 released after 5 min was determined via ELISA.

Secondly, after removing the pellets from PBS, a dissolution test was performed using the reciprocating cylinder method (USP apparatus 3) (Bio-Dis, Vankel, NJ, USA) at a dip rate of 21 dpm with two consecutive media (250 ml): during 2 h in simulated gastric fluid (SGF, pH 3.0) (USP 27) and during 5 h in PBS pH 7.4 (Snoeck et al., 2004a) to simulate the gastric and intestinal passage, respectively. Samples were taken after 1 and 2 h in SGF and 1, 3 and 5 h

dissolution in PBS. As positive control, the same test was performed without pellets, but by adding 1 ml F4 solution (1.67 mg/ml) to the dissolution media.

The amount of F4 in the samples was determined using ELISA.

- *In vitro* assay for competitive inhibition of villous adhesion

An *in vitro* villous adhesion/inhibition test was carried out to determine if the released F4 had the capacity to bind to the F4 receptor (Cox and Houvenaghel, 1993). Wells were coated with intestinal villi of an $F4R^+$ pig. Supernatants after dissolution of the F4 pellets in PBS, F4 solution (+ control) and PBS (- control) were added to the wells followed by incubation. Afterwards, F4 *E. coli* (GIS 26) was added followed by incubation. Villi were examined by phase contrast microscopy at 600x magnification and the adhesion of the bacteria was evaluated quantitatively by counting the number of bacteria adhering along a 50 µm villous brush border at 20 different places, after which the mean bacterial adhesion per 250 µm villous length was calculated. Adhesion of more than 30 bacteria per 250 µm villous length was noted as strong adhesion, less than 30 bacteria per 250 µm villous length was classified as weak adhesion.

6.3.4. *In vivo* F4 release from the porous pellets: an oral immunization experiment

For the *in vivo* study 17 $F4R^+$ pigs were selected using a PCR-RFLP assay (Rasschaert et al., 2007) what was confirmed after slaughter by a villous adhesion/inhibition test (Cox and Houvenaghel, 1993). At the age of 9 weeks (63 days), 5 animals received an oral dose of 1 mg F4 fimbriae in 5 ml PBS on three successive days (orally administered using a syringe) (solution group). Seven animals received a similar immunization with F4 fimbriae (1.675 mg) formulated in porous pellets. The pellets were orally administered with 15 ml PBS (pellet group). Another 5 animals were not immunized (control group). Both vaccinated groups

received a booster vaccination at day 15. Finally, at day 30, all animals were infected with a virulent $F4^+$ETEC strain as described by Cox et al. (1991). Briefly, piglets were treated with florfenicol in PBS (20mg/kg/day) (Nuflor, Schering-Phough, Brussels, Belgium) at day 3 and 2 pre-infection. They were fasted overnight and were deprived of water 3 h pre-infection. Subsequently, they were orally infected with 10^{10} $F4^+$ETEC, 15-30 min after neutralizing the acidic gastric pH with 60 ml of $NaHCO_3$ (1.4% (w/v) in distilled water).

- F4-specific serum antibody response

Blood was sampled on a weekly basis (during 7 weeks) from the jugular vein for determining the total antibody titer in serum. Serum was collected and inactivated at 56°C and subsequently treated with kaolin (Sigma-Aldrich, Bornem, Belgium) to decrease the background reading in ELISA.

The wells of a 96-well microtiter plate were coated with a F4ac-specific MAb at a concentration of 1 µg/ml in coating buffer (PBS). After 2 h of incubation at 37°C, the remaining binding sites were blocked for 30 minutes at room temperature with PBS supplemented with 0.2% (v/v) Tween 80. Subsequently F4 antigen was added to the wells at a concentration of 50 µg/ml in ELISA dilution buffer and incubated for 1 h at 37°C. Then, treated sera were added in series of twofold dilution (1/10, 1/20,…), and the plates were incubated for 1 h at 37°C. Thereafter, the wells were treated for 1 h at 37°C with optimal dilutions of anti-swine IgG (H+L) (Bethyl Laboratories, Montgomery, Texas). Conjugates had been prepared by coupling anti-swine IgG (H+L) specific MAb to peroxidase with a peroxidase labeling kit (Boehringer Mannheim, Brussels, Belgium). The substrate, ABTS, was added, and the OD_{405} was spectrophotometrically measured after 15 min incubation at 37°C (Van den Broeck et al., 1999b).

The obtained ODs of all sera (dilutions 1/10) at day 0 were averaged, and the standard deviation was calculated. The mean, increased by twice the standard deviation, was considered as cut-off value. The antibody titer was the inverse of the highest dilution which still had an OD_{405} higher than the calculated cutoff value.

➢ Mucosal immune response

• Isolation of monomorphonuclear cells (MC) in lymph nodes

At the moment of slaughter (age 22 weeks), mesenteric lymph nodes were aseptically dissected. After removing surrounding fat from the tissue, MC were isolated by tearing the tissue apart, followed by lysis of the red blood cells with ammonium chloride. After centrifugation (270*g* at 4°C for 10 min), the pelleted cells were washed and resuspended at 10^7 cells/ml in leukocyte medium (RPMI-1640 (GIBCO BRL, Life Technologies, Merelbeke, Belgium) containing foetal calf serum (5 %), 2-mercaptoethanol (5 x 10^{-5} M), nonessential amino acids, Na-pyruvate (100 µg/ml), L-glutamine (292 µg/ml), penicillin (100 IU/ml), streptomycin (100 µg/ml) and kanamycin (100 µg/ml)).

• Preparing Peyer's patches MC

To isolate MC from Peyer's patches, small intestine pieces (from ileum and jejunum) were washed and incubated in CMF/EDTA/DDT medium at 37°C for 30 minutes followed by collagenase and DNAse incubation (RPMI + 5% FCS + 20 mM HEPES + 0.015% collagenase (SERVA, polylab, Antwerp, Belgium) + 0.010% DNAse I (Boehringer, Mannheim, Brussels, Belgium)) at 37°C for 45 min. Subsequently, Peyer's patches MC were collected by scrapping the Peyer's patches, washing and resuspending in leukocyte medium at 10^7 cells/ml.

• Elispot assay for F4-specific IgM- and IgA-secreting cells

The wells of a 96-well microtiter plate were coated with F4-specific polyclonal antiserum in PBS. After 2 h incubation at 37°C, the remaining binding sites were blocked for 30 min at room temperature with PBS supplemented with 0.2% (v/v) Tween 80. Next, F4 antigen was added to the wells at a concentration of 10 µg/ml in ELISA dilution buffer and incubated for 1 h at 37°C. Subsequently, MC suspensions at a concentration of 10^7 cells/ml leukocyte medium were added to 10 wells (100 µl/well) and plates were incubated for 3 h at 37°C in a humidified 5% CO_2 atmosphere. After removing cells by three subsequent washes with PBS-T, plates were treated with anti-swine IgM- and IgA-peroxidase conjugates for 1 h. Unbound conjugates were removed by three washes and the substrate solution, consisting of 4 volumes of 3-amino-9-ethylcarbazole (AEC) working solution (0.67 ml AEC stock solution (0.4% in dimethylformamide) in 10 ml sodium acetate (0.1 M, pH 5.2) + 10 µl 30% H_2O_2) and 1 volume of 3% low melting agarose (BIOzym, Landgraaf, The Netherlands), was added. Brown spots were counted with an inverted microscope after plates had been incubated in the dark at least overnight at room temperature. For each MC suspension, spots in 10 wells (10^6 MC/well) were counted, so that finally the amount of antigen-secreting cells (ASC) per 10^7 MC was determined.

6.4. RESULTS AND DISCUSSION

6.4.1. F4 biological activity

As in our study F4 fimbriae were incorporated in the pellets after extrusion/sferonization, the only process that could influence the stability of the antigen during manufacturing of the formulation was freeze-drying. The ELISA results of the supernatant of crushed freeze-dried pellets and of a F4 solution (standard, 100% activity) were compared: 79.8 ± 3.8 % of the F4 activity was recovered in the porous pellets.

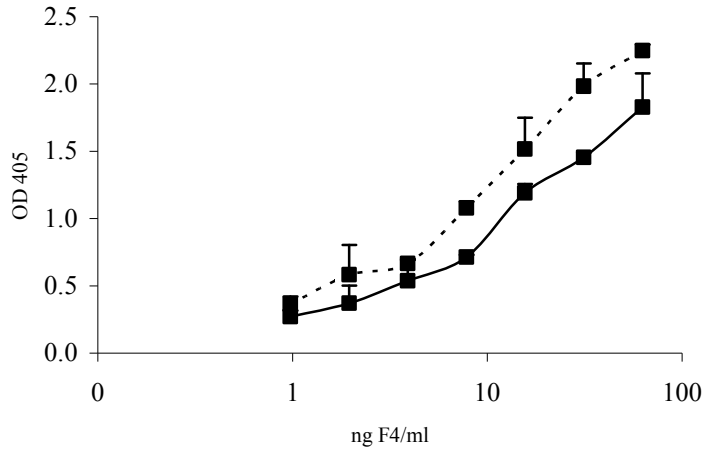

Figure 6.1.: Influence of manufacturing process on stability of the F4 fimbriae (n=3): standard solution (----) and supernatant of crushed pellets (—).

For both the standard solution and the pellets, sigmoid OD_{405} curves with a steep linear phase were found (Fig. 6.1., only linear part of the curve is shown). The slope of both curves was similar. A more shallow curve for the pellets would indicate a lower affinity of MAb for F4 fimbriae, most likely due to a conformational change in the epitope recognized by MAb, resulting in a lower activity (Verdonck et al., 2004). As this was not observed, the decrease in F4 activity in the pellet formulation is mainly contributed to an incomplete release of F4 from the pellets.

6.4.2. Distribution of F4 in the porous pellets

To visualize the distribution of F4 in the porous pellets, slices were made from pellets which were incubated with a F4-specific antibody followed by adding a FITC-labeled anti-rabbit IgG antiserum. Fig. 6.2. shows that F4 was not only present on the surface of the pellets but was found in the entire pellet. After spiking the pellets with the F4 solution, the pellets absorbed the solution and due to the presence of an interconnected pore network, the solution

passes trough the entire pellet whereby F4 fimbriae becomes distributed throughout the entire pellet.

a **b**

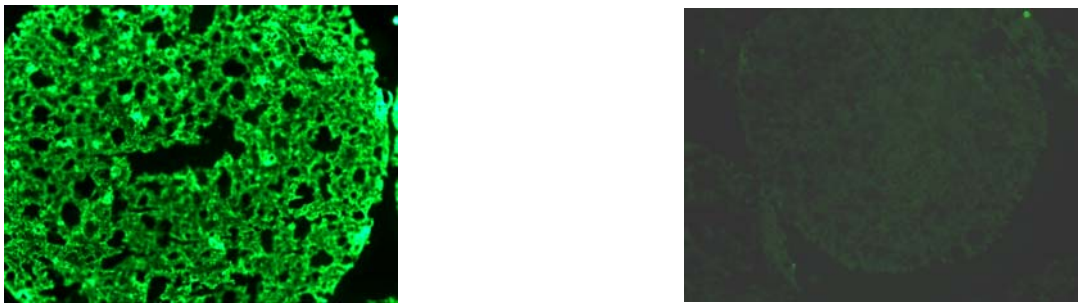

Figure 6.2.: Image obtained by fluorescence microscopy of a cross section of a porous pellet loaded with F4 fimbriae after incubation with (**a**) anti-F4 rabbit antiserum and (**b**) PBS, both followed by the addition of anti-rabbit IgG/FITC antiserum

6.4.3. *In vitro* study: release of F4 fimbriae from the porous pellets

During real-life use the pellets will be added to a solution before administration to the piglets. To simulate this procedure, pellets were immersed in a PBS solution during 5 min. During this procedure only a small amount (19 ± 5%) of F4 was released, indicating that F4 loss from the pellets during feed preparation is limited.

To investigate the release of F4 in the stomach and the gut, a reciprocating dissolution test was performed on the pellets after immersing them for 5 min in PBS.

The diffusion-controlled release during 2 h in SGF was slow (22 ± 8 %) whereas during 5 h in PBS 68 ±14 % of the F4 fraction was released. This indicated that most of F4, absorbed in the internal pellet structure will be protected during gastric passage as most of the F4 dose is only released in the intestine. Hence a large fraction of F4 fimbriae will be available for interaction with the mucosa at the jejunal Peyer's patches, which are the major inductive site of the F4-specific immune response (Snoeck et al., 2006).

As previous studies have shown that F4 fimbriae retain their antigenicity during at least 4 h at pH 3.0 as demonstrated by recognition with an F4 specific Mab (Snoeck et al., 2004b), the limited amount of F4 detected in SGF is only attributed to the slow release of F4 from the pellets and not to inactivation of F4 in SGF. Furthermore, pellets have a limited residence time in the stomach as their gastric emptying is similar to that of fluids.

The slow release of F4 from the porous pellets can be attributed to the size of F4 fimbriae: 27.5 kDa (0.1-1 μm length and 2.1 nm diameter) whereas the size of conventional drugs is in the Angstrom range (0.1 nm).

A villous adhesion/inhibition assay was done on the supernatant of the porous pellets after 5 h dissolution in PBS to ascertain if the released F4 were able to adhere to F4 receptors. The mean number of bacterial adhesion per 250 μm villous length was 8.3 (weak adherence) and 86 (strong adherence) for the F4 (positive control) and PBS solution (negative control), respectively. After dissolution of pellets in PBS the mean number adhered bacteria was determined at 8.5 (weak adherence), indicating that the F4 receptor on the brush borders were occupied by F4 fimbriae present in the sample. This indicated that F4 fimbriae released from the pellets in PBS solution retained their binding capacity (even after residence in an acid medium).

6.4.4. *In vivo* study: oral immunization of piglets with F4 loaded porous pellets

- Systemic F4-specific antibody response

The solution as well as the pellet group were orally vaccinated at day 1, 2 and 3 (age of 63, 64 and 65 days) and again at day 15 (age 78 days). The control group was not immunized. At day 30 (age 93 days) all animals were inoculated with the virulent $F4^+$ ETEC strain. The F4-specific serum antibody response was analyzed till day 45 (age of 108 days).

Fig. 6.3. shows that following primary vaccination a similar increase in F4-specific antibody response was detected in the solution as well as pellet group, but not in the control group.

The second vaccination resulted in a further increase in antibody titer for the pellet group whereas in the solution group no increase was observed. After challenge, all groups displayed an antibody response whereas the increase in antibody titer was most pronounced in the control group. From day 40 (age 103 days) the antibody titer in the control group further increased whereas in the solution and pellet group the antibody tended to stabilize.

The results of this immunization experiment provided evidence that F4 fimbriae in solution and pellets were able to induce an immune response upon oral administration to suckling piglets, with the serum antibody response in the pellet group being higher than in the solution group. The boost response upon challenge was lower than in the control group suggesting a certain decrease in colonization and multiplication of $F4^{+}$E.coli.

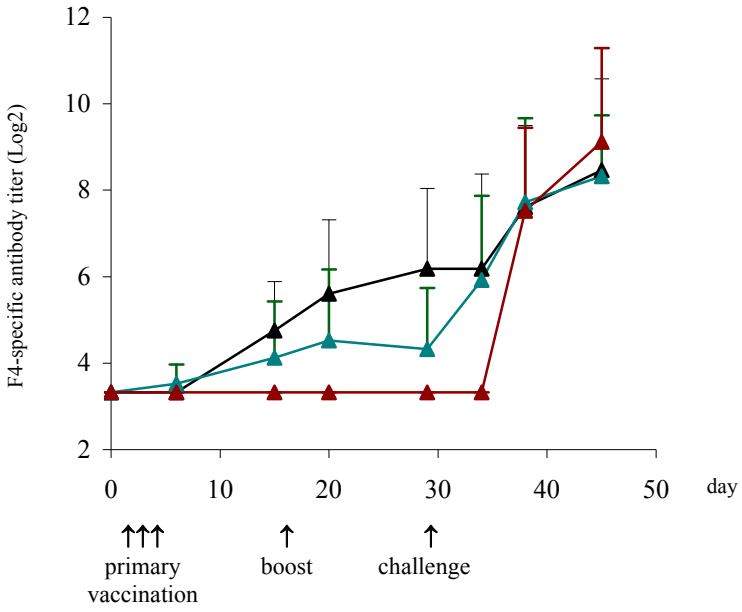

Figure 6.3.: Kinetics of the total antibody titer in the control group (▲), the pellet group (▲) and the solution group (▲). Primary vaccination on day 1, 2 and 3, second vaccination on day 15 and challenge with virulent $F4^{+}$ ETEC on day 30.

➢ Mucosal immune response

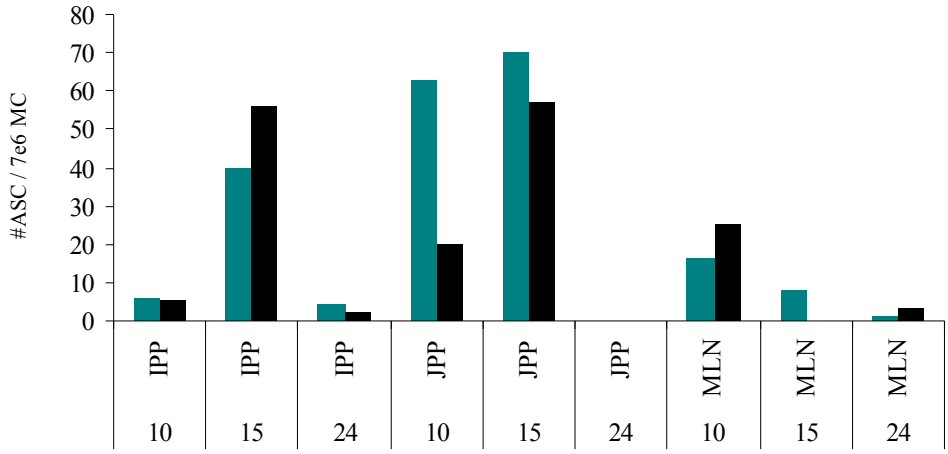

Figure 6.4.: F4-specific IgA (■) and IgM (■) ASC in the ileal Peyer's patches (IPP), the jejunal Peyer's patches (JPP) and the mesenteric lymph nodes (MLN) after vaccination with F4 pellets (15), vaccination with F4 solution (10) and without vaccination (24).

The piglet of the pellet group had high numbers of F4-specific IgM and IgA ASC in the ileal and jejunal Peyer's patches and low numbers in the mesenteric lymph nodes, whereas the piglet receiving an F4 solution showed only a high response in jejunal Peyer's patches suggesting a less pronounced priming compared to the F4 pellets. The control piglet only showed a weak response in the inductive sites, with mainly IgM in the mesenteric lymph nodes and very few IgA response. In contrast, both vaccination procedure had an IgA response, demonstrating a primary response in the control pig and a secondary response in immunized piglets.

6.5. CONCLUSION

Since *in vitro* F4 release in simulated gastric fluid was limited and most of the F4 dose was released in PBS, this indicated that F4 fimbriae formulated in porous microcrystalline pellets are protected during gastric passage and that the antigens are available at the jejunal Peyer's patches, the main target site for an F4 specific immune response.

Systemic immune response after oral vaccination of piglets with F4-containing porous pellets was higher compared to oral vaccination via an F4 solution, suggesting that more active F4 was released from the porous pellets at the inductive site.

The high amount of IgA and IgM antigen-presenting cells found at the jejunal Peyer's patches of the piglet vaccinated with F4 pellets indicated the efficiency of this procedure. However, the shedding of *E. coli* bacteria in the faeces has to be evaluated to determine which procedure is the most efficient to induce mucosal protection.

6.6. REFERENCES

Cox, E., Schrauwen, E., Cools, V. and Houvenaghel, A. (1991). Experimental induction of diarrhea in newly-weaned piglets. J. Vet. Med., 38, 418-426.

Cox, E. and Houvenaghel, A. (1993). Comparison of the in vitro adhesion of K88, K99, F41 and P987 positive *Escherichia coli* to intestinal villi of 4-week-old to 5-week-old pigs. Vet. Microbiol., 34, 7-18.

Deprez, P., Van Den Hende, C., Muylle, E. and Oyaert, W. (1986). The influence of the administration of sow's milk on the postweaning excretion of hemolytic *Escherichia coli* in piglets. Vet. Res. Commun., 10, 469-478.

Fairbrother, J.M., Nadeau, E. and Gyles, C.L. (2005). Escherichia coli in postweaning diarrhea in pigs: an update on bacterial types, pathogenesis, and prevention strategies. Anim. Health Res. Rev., 6, 17-39.

Gibbons, R.A., Sellwood, R., Burrows, M. and Hunter, P.A. (1977). Inheritance of resistance to neonatal *Escherichia coli* diarrhea in pigs. Theor. Appl. Genet., 51, 65.

Huyghebaert, N., Snoeck, V., Vermeire, A., Cox, E., Goddeeris, B.M. and Remon, J.P. (2005). Development of an enteric-coated pellet formulation of F4 fimbriae for oral vaccination of suckling piglets against enterotoxigenic *Escherichia coli* infections. Eur. J. Pharm. Biopharm., 59, 273-281.

Moon, H.W. and Bunn, T.O. (1993). Vaccines for preventing enterotoxigenic *Escherichia coli* infections in farm animals. Vaccine, 11, 213-220.

Rasschaert, K., Verdonck, F., Goddeeris, B.M., Duchateau, L. and Cox, E. (2007). Screening of pigs resistant to F4 enterotoxigenic *Escherichia coli* (ETEC) infection. Vet. Microbiol., 123, 249-253.

Rutter, J.M. and Jones, G.M. (1973). Protection against enteric disease caused by *Escherichia coli*: A model for vaccination with a virulent determinant? Nature, 242, 531-532.

Rutter, J.M., Burrows, M.R., Sellwood, R. and Gibbons, R.A. (1975). A genetic basis for resistance to enteric disease cause by *E. coli*. Nature, 257, 135-136.

Snoeck, V., Huyghebaert, N., Cox, E., Vermeire, A., Saunders, J., Remon, J.P., Verschooten, F. and Goddeeris, B.M. (2004a). Gastrointestinal transit time of nondisintegrating radio-opaque pellets in suckling and recently weaned piglets. J. Control. Rel., 94, 143-153.

Snoeck, V., Cox, E., Verdonck, F., Joensuu, J.J., Goddeeris, B.M. (2004b). Influence of porcine intestinal pH and gastric digestion on antigenicity of F4 fimbriae for oral immunization. Vet. Microbiol., 98, 45-53.

Snoeck, V., Verfaillie, T., Verdonck, F., Goddeeris, B.M. and Cox, E. (2006). The jejunal Peyer's patches are the major inductive sites of F4-specific immune response following intestinal immunisation of pigs with F4 (K88) fimbriae. Vaccine, 24, 3812-3820.

Van den Broeck, W., Cox, E. and Goddeeris, B.M. (1999a). Induction of immune responses in pigs following oral administration of purified F4 fimbriae. Vaccine, 17, 2020-2029.

Van den Broeck, W., Cox, E. and Goddeeris, B.M. (1999b). Receptor-dependent immune responses inpigs after oral immunization with F4 fimbriae. Infect. Immun., 67, 520-526.

van Zijderveld, F.G., van Zijderveld-van Bemmel, A.M. and Bakker, D. (1998). The F41 adhesin of enterotoxigenic *Escherichia coli*: inhibition of adhesion by monoclonal antibodies. Vet. Quart., 20, S73-S78.

Verdonck, F., Snoeck, V., Goddeeris, B.M., and Cox, E. (2004). Binding of a monoclonal antibody positively correlates with bioactivity of the F4 fimbrial adhesion FaeG associated with post-weaning diarrhea in piglets. J. Immunol. Methods, 294, 81-88.

General conclusion and future perspectives

The first part of this research work described the development and evaluation of porous tablets and evaluated the application of this porous dosage form for oral drug delivery. Direct compression of a powder mixture of a ceramic powder (hydroxyapatite) and space holding material (pore forming agent) yielded tablets which were transformed into a porous structure via a heat treatment (calcination-sintering). Modified gelcasting of a hydroxyapatite slurry followed by a heat treatment also resulted in a porous tablet structure. Drug loading of the porous tablets occurred by spiking a drug solution on the tablet surface, where drug absorption depended on pore size, pore volume, presence of an interconnected pore network and drug concentration of the solution. As small liquid volumes can be dosed with high accuracy, these porous tablets can be used as innovative carriers for low-dosed drugs with limited risk of drug inhomogeneity. Furthermore as the drug is incorporated in the porous tablets after compression, this technique is also promising for processing drugs with poor tabletting characteristics. Drug release from the porous tablets is diffusion-controlled whereby the apparent drug diffusivity depended on the pore size and tortuosity of the porous network. Larger and more regular shaped pores resulted in a faster drug release. The bioavailibility of metoprolol tartrate after oral administration of porous tablets to dogs was similar to the *in vivo* behavior of an immediate release metoprolol tartrate tablet.

The second part of this research work described the development of porous pellets and evaluated the use of these porous pellets for oral delivery of conventional drugs and vaccines. Pellets were prepared by extrusion/spheronization of a microcrystalline cellulose/sodium chloride mixture, followed by aqueous extraction of the sodium chloride fraction to obtain porous pellets. Drug loading via supercritical fluid impregnation and immersion of the pellets in a drug solution resulted in drug being distributed in the entire pellet. In vitro drug release of ibuprofen and metoprolol tartrate from porous pellets was immediate, whereas an *in vivo* study in dogs showed that drug release in the gastro-intestinal tract depended on the drug solubility: release of drugs with a high aqueous solubility was immediate, whereas diffusion from the porous matrix in case of drugs with a low aqueous solubility was slow, yielding plasma concentrations similar to a sustained-release tablet formulation.

In addition porous pellets can be used as carriers for oral vaccination purposes. Spiking a solution of F4 fimbriae onto the porous pellets, followed by freeze-drying was a suitable technique for the production of a multi-particulate formulation of biologically active F4. This opened interesting perspectives for the large-scale production of oral vaccines. The *in vitro* F4 release in simulated *in vivo* conditions revealed a promising release profile: a limited loss of F4 in simulated gastric fluid (about 20% after 2 h), while the largest fraction (± 68%) was only released in phosphate buffer pH 7.4, indicating that most of the F4 fraction will be available at the site of infection (i.e. jejunal Peyer's patches) to induce a mucosal immune response. An *in vivo* study in piglets demonstrated that after oral vaccination with F4-containing pellets a mucosal immune response was elicited.

Although some interesting applications of porous scaffolds for oral drug and vaccine delivery have been identified in this research project, some additional major hurdles can be identified before large scale application of these dosage forms becomes feasible:

- scale-up of the production process of porous tablets and pellets
- scale-up and automatization of the drug loading process
- confirmation of the mucosal immunization study by determining the shedding of *E Coli* in the faeces
- applicability of porous pellets for oral vaccination using other antigens

Summary

1 As porous materials (polymers, metals and ceramics) have many interesting physical and chemical properties, they have widespread applications in nearly every technology sector. Chapter 1 described the main biomedical application of cellular materials: the use of porous ceramics, polymers and/or metals as bone implants for structural purposes as well as for local drug delivery. Several manufacturing techniques for porous ceramics are reviewed and the drug release from these porous devices is described. Chapter 1 also summarizes the most important aspects of the manufacturing and formulation of conventional tablets and pellets since the overall aim of this research project was to evaluate the possible applications of porous tablets and pellets for oral drug delivery. More specifically the application of porous tablets for the manufacturing of tablets containing low-dosed drugs or drugs with limited compression properties were investigated as well as the possibilities offered by porous pellets for oral delivery of conventional drugs as well as vaccines.

2 The development of porous tablets as possible drug carrier for oral drug delivery was described in Chapter 2. To manufacture porous hydroxyapatite matrices which can be used as drug carrier two techniques were used: direct compression and modified gelcasting, both in combination with sintering to obtain a porous matrix. The influence of formulation (type and concentration of pore forming agent) and process parameters (temperature and duration of the sinter process) on the quality and porosity of the hydroxyapatite tablets was evaluated. Highly porous tablets were obtained via direct compression and sintering, where the porosity was determined by the type (microcrystalline cellulose, starch, sorbitol) and concentration of the pore forming agent as well as by the sinter temperature. These experiments also showed that direct compression of a mixture of microcrystalline cellulose (Avicel PH 200, pore forming agent) and hydroxyapatite (50/50, w/w) in combination with sintering at 1250°C resulted in porous tablets with suitable

characteristics for its application as oral drug delivery system: a low friability and high tensile strength, a median pore of 5 µm and an interconnected pore network. Modified gelcasting of hydroxyapatite slurry in combination with sintering at 1350°C also resulted in tablets having suitable properties for oral drug delivery: spherical pores with a median pore diameter that could be varied from 20 to 100 µm, all incorporated in an interconnected pore network, an acceptable friability and tensile strength. Furthermore, all tablets were able to easily absorb the drug solution whereby an acceptable content uniformity was obtained.

To incorporate a drug in the porous tablet structure a limited volume of drug solution was spiked on the tablet surface (using metoprolol tartrate as model drug). The drug load in the tablet was determined by the drug concentration in the solution spiked on the porous matrix and by the number of loading steps, but this application was limited to the formulation of low-dosed drugs. Absorption of the liquid in the internal pore structure was rapid due to the interconnected pore network in the tablets manufactured via direct compression and gelcasting. Drug release from the porous tablets was primarily diffusion controlled whereby the apparent drug diffusivity depended on the pore size and tortuosity of the porous network. A slow drug release was obtained from porous pellets manufactured via direct compression (median pore diameter: 5 µm) whereas the porous tablets prepared via modified gelcasting have larger and more regular shaped pores with a median pore diameter of 100 µm yielded a faster drug release. The porous tablets were at least 12 months stable when stored at 25°C/60 % relative humidity (RH) and at 40°C/75 % RH.

This study identified porous tablets as innovative carriers for oral delivery of low dosed drugs. Furthermore, as the drug is incorporated in the porous tablets after compression, this manufacturing technique is also promising for processing drugs with poor tabletting characteristics.

3 Chapter 3 describes the bioavailibility of metoprolol tartrate after oral administration of porous tablets with a median pore diameter of 5 and 100 µm. During the *in vivo* experiment an oral dose of 100 mg metoprolol tartrate was administered to dogs in a cross-over sequence. Porous tablets with a median pore diameter of 5 µm (manufactured by direct compression of microcrystalline cellulose/hydroxyapatite (50/50, w/w) and sintering at 1250°C) and 100 µm (manufactured via modified gelcasting and sintering at 1350°C) were selected as test formulations. The tablets were loaded with metoprolol tartrate via spiking of a metroprolol tartrate solution and after drying a formulation containing 100 mg metoprolol

tartrate was obtained. The bioavailibility of the test formulations was compared to a commercial immediate release formulation (Lopresor®, 100 mg metoprolol tartrate). Metoprolol tartrate plasma concentrations were determined with a validated HPLC-fluorescence method.

Oral administration of the porous tablets with a median pore diameter of 5 and 100 µm resulted in both cases in immediate drug release. Statistical analysis of the pharmacokinetic parameters showed no significant difference between the test and reference formulations, indicating that although the *in vitro* drug release depended on pore size (Chapter 2), *in vivo* an immediate drug release was obtained from all porous tablets.

To explain the discrepancy between *in vitro* and *in vivo* drug release from the porous tablets after administration of the porous tablets, additional dissolution tests were performed using conditions that simulate the gastro-intestinal conditions. The influence of hydrodynamic flow and stress in the gastro-intestinal tract was examined using different paddle speeds as well as the reciprocating cylinder method. Furthermore, the effect of several physiological relevant dissolution media (SGF, SIF, 4% bile salts solution, FaSSIF, FeSSIF and $FASSGF_{SLS}$) on the *in vitro* drug release was investigated. The resulting drug release profiles showed that the faster *in vivo* drug release from the porous tablets with a median pore diameter of 5 µm in comparison to its *in vitro* drug release was mainly due to the low surface tension of the gastric fluid in fasted dogs.

4 The development of porous pellets as potential drug carriers for oral drug delivery was described in Chapter 4. Pellets were manufactured via extrusion/spheronization of a mixture consisting of microcrystalline cellulose and NaCl (30/70, w/w). Afterwards the NaCl fraction was removed from the pellets by aqueous extraction and the pellets were dried to obtain porous drug carriers. Via this technique spherical pellets (aspect ratio < 1.2) with an acceptable friability (< 0.1%) and a porosity of 33.2% with a median pore diameter of 0.7 µm were obtained. X-ray tomography showed that the pores formed an interconnected pore network. Drugs were incorporated in the porous pellets via three different drug loading techniques: immersion of the pellets in a drug solution (using metoprolol tartrate as model drug), supercritical fluid impregnation (using ibuprofen as model drug) and fluid-bed layering (using paracetamol as model drug). Raman spectroscopy showed that the drug was homogeneously distributed throughout the pellets (i.e. drug was deposited inside the porous pellets) after immersion of pellets in a drug solution or supercritical fluid impregnation,

whereas after fluid-bed layering drug was only present on the pellet surface. Drug release from the porous pellets was immediately and in case of pellets with drug deposited in its internal pore structure drug release was primarily diffusion-controlled.

5 Chapter 5 evaluated the bioavailability of drugs after oral administration of drug-loaded porous pellets to dogs. Metoprolol tartrate and ibuprofen were used as model drugs with a high and low aqueous solubility, respectively. Metoprolol tartrate (100 mg) was administered to dogs in a cross-over study. As test formulation a hard gelatin capsule containing porous microcrystalline cellulose pellets loaded with 100 mg metoprolol tartrate was selected and the bioavailibility of this test formulation was compared to a commercial immediate release formulation (Lopresor®, 100 mg metoprolol tartrate). Ibuprofen (300 mg) was administered to dogs in a cross-over sequence. As test formulation a hard gelatin capsule containing porous microcrystalline cellulose pellets loaded with 300 mg ibuprofen was selected. The bioavailibilty of the ibuprofen test formulation was compared to a commercial immediate release formulation (½ tablet of Ibuprofen EG® 600 mg) and a commercial controlled-release formulation (½ tablet of Ibu-Slow® 600 mg). Metoprolol tartrate and ibuprofen plasma concentrations were determined with a validated HPLC-fluorescence method and a validated HPLC-UV method, respectively. Statistical analysis of the pharmacokinetic parameters after administration of metoprolol tartrate revealed no significant difference between the test and reference formulation, indicating that drug release in the gastro-intestinal tract was immediate. In contrast, ibuprofen release from the porous pellets was sustained as indicated by the pharmacokinetic parameters. These observations indicated that the *in vivo* drug release from porous pellets depended on the solubility of the incorporated drug: release of highly soluble drugs was immediate, whereas diffusion from the porous matrix in case of drugs with a low aqueous solubility was slow, yielding plasma concentration similar to a sustained-release tablet.

6 Chapter 6 described the development of a porous pellet formulation containing F4 fimbriae. It was shown that incorporation of F4 fimbriae in porous microcrystalline pellets (via spiking of a F4 solution on porous pellets in combination with freeze drying) resulted in a remaining F4 bioactivity of 79.8 ± 3.8%, whereby F4 fimbriae were

distributed in the entire pellet. An *in vitro* study was performed to determine F4 release from the pellets under setting simulating *in vivo* conditions: pellets were initially immersed during 5 min in a pH 7.4 phosphate buffer solution (PBS) to simulate the feed preparation, next the pellets were transferred for 2 h to simulated gastric fluid (SGF) and for 5 h to PBS pH 7.4 to simulate gastric and intestinal passage, respectively. The dissolution profile revealed that about 19% of F4 was lost during feed preparation and that 20% was released in SGF. However, the largest fraction (about 68%) was released in PBS and would be available at the intended site of action in the gastro-intestinal tract. Furthermore, a villous adhesion inhibition test showed that F4 released in PBS retained there antigenicity, indicating that F4 were protected during gastric passage. F4-loaded porous pellets were orally administered to piglets and the elicited immune response after oral vaccination with F4 pellets was compared with the immune response obtained after oral vaccination with an F4 solution and a placebo formulation (control group, non-vaccinated piglets). The F4-specific antibody titer was determined in blood samples, and the F4-specific IgM- and IgA-secreting cells (ASC) were determined in the ileal and jejunal Peyer's patches and in the mesenteric lymph nodes. Oral vaccination of piglets with F4-containing porous pellets resulted in the highest systemic immune response, suggesting that more active F4 was released from the porous pellets at the site of infection, compared with the F4 solution. A high number IgA and IgM ASC were found at the major site of infection (jejunal Peyer's patches) in the piglets vaccinated with F4 pellets and F4 solution. However, in order to investigate if oral vaccination of piglets using the porous pellets is the most efficient procedure, shedding of *E. coli* bacteria in the faeces should be monitored.

Samenvatting

1 Poreuze materialen (polymeren, metalen en ceramische materialen) kennen omwille van hun interessante chemische en fysische eigenschappen verschillende toepassingen. De belangrijkste biomedische toepassing van poreuze materialen wordt beschreven in Hoofdstuk 1: het gebruik van poreuze ceramische materialen, polymeren en/of metalen als botimplantaat bij structurele chirurgie enerzijds en als drager van geneesmiddelen voor een lokale geneesmiddelvrijstelling anderzijds. Verschillende productietechnieken voor poreuze ceramische materialen alsook de geneesmiddelvrijstelling uit de poreuze materialen worden beschreven. Eveneens wordt in Hoofdstuk 1 een kort overzicht gegeven van de belangrijkste aspecten bij de productie van conventionele tabletten en pellets omdat deze doctoraatsthesis de mogelijke toepassingen van poreuze tabletten en pellets voor orale geneesmiddeltoediening evalueert. Meer bepaald wordt het gebruik onderzocht van poreuze tabletten bij de ontwikkeling van laaggedoseerde geneesmiddelen of bij de aanmaak van tabletten die geneesmiddelen bevatten met beperkte compressie-eigenschappen, alsook de mogelijke toepassingen van poreuze pellets bij orale toediening van conventionele geneesmiddelen en vaccins.

2 Hoofdstuk 2 beschrijft de ontwikkeling van poreuze hydroxyapatiet tabletten waarbij twee technieken werden aangewend: directe compressie en gelgieten, beide in combinatie met sinteren ten einde een poreuze matrix te bekomen. De invloed van formulatie- (type en concentratie porievormer) en procesparameters (temperatuur en duur van het sinterproces) op de kwaliteit en de porositeit van poreuze hydroxyapatiet tabletten werd onderzocht. Via directe compressie en sinteren werden poreuze tabletten bekomen waarbij de porositeit afhankelijk is van het type (microkristallijne cellulose, zetmeel of sorbitol) en de concentratie van de porievormer en de sintertemperatuur. Directe compressie van een mengsel bestaande uit microkristallijne cellulose (Avicel PH 200, porievormer) en hydroxyapatiet

(50/50 g/g) in combinatie met sinteren bij 1250°C resulteerde in poreuze tabletten met een lage friabiliteit, hoge tabletsterkte, een mediaan poriëndiameter van 5 µm en bestaande uit een poriënnetwerk waarin de verschillende poriën met elkaar verbonden zijn.

Gelgieten van een hydroxyapatiet-suspensie in combinatie met een sintertemperatuur van 1350°C resulteerde eveneens in poreuze tabletten met geschikte eigenschappen om als geneesmiddeldrager aangewend te worden: sferische poriën met een mediaan poriëndiameter van 20 tot 100 µm allen deel uitmakend van een poriënnetwerk, een lage friabiliteit en hoge tabletsterkte. Het opladen van de poreuze tabletten met geneesmiddel gebeurde door een beperkt volume geneesmiddeloplossing (gebruik makend van metoprolol tartraat als modelgeneesmiddel) op het tabletoppervlak aan te brengen waarbij de oplossing snel en volledig geabsorbeerd werd door de aanwezigheid van een poriënnetwerk. De maximale geneesmiddelopname in de tablet werd bepaald door de geneesmiddelconcentratie van de oplossing en door het aantal opladingstappen. De geneesmiddelvrijstelling was diffusie-gecontroleerd waarbij de diffusiesnelheid afhankelijk was van de poriëngrootte en de tortuositeit van het poriënnetwork. De geneesmiddelvrijstelling uit de poreuze tabletten, aangemaakt via directe compressie (mediane poriëndiameter: 5 µm) was traag. Daarentegen werd onmiddellijke geneesmiddelvrijstelling bekomen uit poreuze tabletten geproduceerd via gelgieten (mediane poriëndiameter: 100 µm). Dit toonde aan dat grotere en sferische poriën resulteerden in een snellere geneesmiddelvrijstelling. De poreuze tabletten waren stabiel gedurende 12 maanden bewaring bij 25°C en 60% relatieve vochtigheid (RV), evenals bij 40°C en 75% RV.

Deze studie toonde aan dat poreuze tabletten mogelijkheden bieden voor de orale toediening van laaggedoseerde geneesmiddelen, bovendien kunnen deze poreuze tabletten ook een oplossing bieden voor het produceren van tabletten met geneesmiddelen met slechte compressie-eigenschappen aangezien de poreuze matrix pas na compressie wordt opgeladen met geneesmiddel.

3

De biologische beschikbaarheid van metoprolol tartraat na orale toediening van poreuze tabletten (mediane poriëndiameter: 5 en 100 µm) werd behandeld in Hoofdstuk 3. Hierbij werd 100 mg metoprolol tartraat toegediend aan honden in een ‘cross-over’ studie. Poreuze tabletten met een mediane poriëndiameter van 5 en 100 µm, respectievelijk geproduceerd via directe compressie en sinteren van een hydroxyapatiet/microkristallijne cellulose mengsel (50/50, g/g) en via gelgieten en sinteren

van een hydroxyapatiet-suspensie, werden geselecteerd als testformulaties. De tabletten werden opgeladen met een metoprolol tartraat-oplossing. De biologische beschikbaarheid van de testformulaties werd vergeleken met een commercieel beschikbaar preparaat met onmiddellijke geneesmiddelvrijstelling (Lopresor®, bevat 100 mg metoprolol tartraat). De metoprolol plasmaconcentraties werden bepaald met een gevalideerde HPLC-fluorescentie methode. Orale toediening van poreuze tabletten met een mediane poriëndiameter van 5 en 100 µm resulteerde in beide gevallen in een onmiddellijke geneesmiddelvrijstelling. Statistische evaluatie van de farmacokinetische parameters toonde geen significant verschillen aan tussen de test- en referentie-formulaties. Ondanks het feit dat de *in vitro* geneesmiddelvrijstelling afhankelijk was van de poriëngrootte (Hoofdstuk 2), wijzen de resultaten van de *in vivo* experimenten op een onmiddellijke vrijstelling onafhankelijk van de poriëngrootte.

Om deze verschillen tussen de *in vitro* en *in vivo* resultaten te verklaren, werden bijkomende dissolutietesten uitgevoerd onder omstandigheden die de *in vivo* condities nabootsen. De invloed van hydrodynamiek en stress in het gastro-intestinaal kanaal werd nagegaan via dissoluties met verschillende mengintensiteit en door gebruik te maken van de Biodis methode. Bovendien werd de invloed van verschillende ‘fysiologisch relevante‘ dissolutiemedia uitgetest. Uit deze dissolutietesten werd besloten dat de snellere *in vivo* vrijstelling uit de poreuze tabletten met een mediaan poriediameter van 5 µm voornamelijk te wijten was aan een lagere oppervlaktespanning van het dissolutiemedium. Dit correleerde met *in vivo* data gelet op de lage oppervlaktespanning van het maagsap bij de hond in nuchtere toestand.

4 De productie van poreuze pellets werd beschreven in Hoofdstuk 4, waarbij als productietechniek werd geopteerd voor extrusie/sferonistie van een mengsel bestaande uit microkristallijne cellulose en NaCl (30/70, g/g). Vervolgens werd de NaCl fractie verwijderd via een waterige extractie en na drogen werden poreuze pellets bekomen. Via deze techniek werden sferische pellets (aspect ratio: 1.2) bekomen met een lage friabiliteit (< 0.1%), een hoge porositeit (33.2%) en een mediane poriëndiameter van 0.7 µm. X-straal tomografie toonde aan dat de poriën deel uitmaken van één groot poriënnetwerk. De pellets werden opgeladen met geneesmiddel via 3 verschillende methodes: het onderdompelen van de pellets in een geneesmiddeloplossing (gebruik makend van metoprolol tartraat als modelgeneesmiddel), met behulp van superkritische vloeistoffen (ibuprofen als

modelgeneesmiddel) en via het omhullen van de pellets met een geneesmiddeloplossing (paracetamol als modelgeneesmiddel). Via Raman-spectroscopie werd aangetoond dat het geneesmiddel homogeen verdeeld was in de poriënstructuur van de pellet indien gebruik gemaakt werd van de onderdompelingsmethode en superkritische vloeistoffen om de pellets met geneesmiddel op te laden. Het gebruik van de omhullingtechniek resulteerde enkel in geneesmiddelafzetting aan het oppervlak van de pellet. Geneesmiddelvrijstelling uit de poreuze pellets was onmiddellijk en indien het geneesmiddel aanwezig was in de poriënstructuur van de pellets was de vrijstelling diffusie-gecontroleerd

5 De biologische beschikbaarheid van geneesmiddelen na orale toediening van poreuze pellets aan de hond werd behandeld in Hoofdstuk 5. Metoprolol tartraat en ibuprofen werden gebruikt als modelgeneesmiddelen met respectievelijk een hoge en lage wateroplosbaarheid. Metoprolol tartraat (100 mg) werd toegediend aan honden in een 'cross-over' studie. Hiervoor werd een harde gelatinecapsule gevuld met poreuze pellets (equivalent met 100 mg metoprolol tartraat) en de biologische beschikbaarheid van deze testformulatie werd vergeleken met een commercieel beschikbaar preparaat met onmiddellijke geneesmiddelvrijstelling (Lopresor®, 100 mg metoprolol tartraat). Ibuprofen (300 mg) werd eveneens toegediend aan de honden in een 'cross-over' studie. De testformulatie was een harde gelatinecapsule gevuld met poreuze pellets (equivalent met 300 mg ibuprofen). De biologische beschikbaarheid van deze testformulatie werd vergeleken met de biologische beschikbaarheid na toediening van commercieel beschikbare ibuprofen-preparaten met een onmiddellijke en gecontroleerde vrijgave: respectievelijk ½ tablet Ibuprofen EG® 600 mg en ½ tablet Ibu-Slow® 600 mg. De metoprolol tartraat en ibuprofen plasmaconcentraties werden bepaald via respectievelijk een gevalideerde HPLC-fluorescentie en HPLC-UV methode. Na orale toediening van metoprolol tartraat pellets werd een onmiddellijke geneesmiddelvrijstelling bekomen aangezien er geen significant verschillen waren tussen de test- en referentie-formulaties. Dit in tegenstelling tot de *in vivo* vrijstelling van ibuprofen uit de poreuze pellets, waarvoor een vertraagde vrijstelling werd vastgesteld. Deze observaties tonen aan dat de *in vivo* geneesmiddelvrijstelling uit de poreuze pellets afhankelijk was van de oplosbaarheid van het geneesmiddel: een onmiddellijke vrijstelling voor een goed wateroplosbaar geneesmiddel, terwijl de diffusie van een geneesmiddel met een lage

wateroplosbaarheid uit de poreuze matrix traag verloopt, wat resulteert in een vertraagde geneesmiddelvrijstelling.

6 Hoofdstuk 6 beschreef de ontwikkeling van een poreuze pellet formulatie van F4 fimbriae. Het bevochtigen van poreuze microkristallijne pellets met een F4-oplossing, gecombineerd met vriesdrogen was een geschikte techniek om F4 fimbriae over de gehele pellets te verdelen, waarbij na productie 79.8 ± 3.8% van de biologische activiteit van F4 bewaard bleef. *In vitro* experimenten werden uitgevoerd om de vrijstelling van F4 uit de poreuze pellets te bepalen onder omstandigheden die de *in vivo* condities nabootsen: F4 pellets werden gedurende 5 min ondergedompeld in een fosfaatbuffer-oplossing (PBS, pH 7.4) om het verlies van F4 tijdens voedselbereiding te simuleren. Vervolgens werd een dissolutietest uitgevoerd gedurende 2u in kunstmatig maagsap (pH 3) en gedurende 5u in PBS pH 7.4 om respectievelijk de passage van de pellets doorheen de maag en de darm te simuleren. Tijdens de voedselbereiding werd ongeveer 19% van de F4-dosis verloren, terwijl 20% F4 werd vrijgesteld in kunstmatig maagsap. De grootste fractie (68%) werd echter vrijgesteld gedurende de 5u dissolutietest in fosfaatbuffer en is dus beschikbaar ter hoogte van de target. Bovendien werd met een villus adhesie inhibitietest bewezen dat F4 fimbriae vrijgesteld in PBS hun antigeniciteit behielden, wat wijst op een protectie van F4 gedurende de maagtransit. Na toediening van F4 pellets aan biggen werd de immuunrespons vergeleken met de immuunrespons na orale toediening van een F4 oplossing en een placebo-formulatie (controle-groep, niet-gevaccineerd). Naast de F4-specifieke antilichaamtiter in het bloed werden ook de F4-specifieke IgM en IgA secreterende cellen in de ileale en jejunale Peyerse platen alsook in de messentherische lymfeknopen, bepaald. Orale vaccinatie van de biggen met F4 pellets resulteerde in de hoogste systemische immuunrespons, wat aantoont dat ter hoogte van de inductieve plaatsen (jejunale Peyerse platen) meer actief F4 werd vrijgesteld in vergelijking met orale vaccinatie via een F4 oplossing.

Het hoogste aantal antigen-secreterende cellen werd teruggevonden ter hoogte van de belangrijkste inductieve plaatsen (jejunale Peyerse platen) zowel bij biggen gevaccineerd met F4 pellets als bij biggen gevaccineerd met een F4 oplossing. Teneinde definitief te bepalen welke vaccinatie-procedure het meest efficiënt is, moet de uitscheiding van E. coli bacteriën via de faeces worden bepaald.